1 BLOCK CONSTITUTIVE MODELS

1.1 Introduction

Numerical solution schemes face several difficulties when implementing constitutive models to represent geomechanical material behavior. There are three characteristics of geo-materials that cause particular problems. One is physical instability. Physical instability can occur in a material if there is the potential for softening behavior when the material fails. When physical instability occurs, part of the material accelerates and stored energy is released as kinetic energy. Numerical solution schemes often have difficulties at this stage because the solution may fail to converge when a physical instability arises.

A second characteristic is the path dependency of nonlinear materials. In most geomechanical systems, there are an infinite number of solutions that satisfy the equilibrium, compatibility and constitutive relations that describe the system. A path must be specified in order for a "correct" solution to be found. For example, if an excavation is made suddenly (e.g., by explosion), then the solution may be influenced by inertial effects that introduce additional failure of the material. This may not be seen if the excavation is made gradually. The numerical solution scheme should be able to accommodate different loading paths in order to apply the constitutive model properly.

A third characteristic is the nonlinearity of the stress-strain response. This includes the nonlinear dependence of both the elastic stiffness and the strength envelope on the confining stress. This can also include behavior after ultimate failure that changes character according to the stress level (e.g., different post-failure response in the tensile, unconfined and confined regimes). The numerical scheme needs to be able to accommodate these various forms of nonlinearity.

The difficulties faced in numerical simulations in geomechanics – physical instability, path dependence, and implementation of extremely nonlinear constitutive models – can all be addressed by using the *explicit, dynamic solution* scheme provided in *UDEC*. This scheme allows the numerical analysis to follow the evolution of a geologic system in a realistic manner, without concerns about numerical instability problems. In the explicit, dynamic solution scheme, the full dynamic equations of motion are included in the formulation. By using this approach, the numerical solution is stable even when the physical system being modeled is unstable. With nonlinear materials, there is always the possibility of physical instability (e.g., the sudden collapse of a slope). In real life, some of the strain energy in the system is converted into kinetic energy, which then radiates away from the source and dissipates. The explicit, dynamic solution approach models this process directly, because inertial terms are included – kinetic energy is generated and dissipated.

In contrast, schemes that do not include inertial terms must use some numerical procedure to treat physical instabilities. Even if the procedure is successful at preventing numerical instability, the path taken may not be a realistic one. The numerical scheme should not be viewed as a black box that will give "the solution." The way the system evolves physically can affect the solution. The explicit, dynamic solution scheme can follow the physical path. By including the full law of motion, this scheme can evaluate the effect of the loading path on the constitutive response.

The explicit, dynamic solution scheme also allows the implementation of strongly nonlinear constitutive models because the general calculation sequence allows the field quantities (forces/stresses and velocities/displacements) at each element in the model to be physically isolated from one another during one calculation step. The general calculation sequence of *UDEC* is described in Section 1.2.1 in **Theory and Background**. The implementation of elastic/plastic constitutive models within the framework of this scheme is discussed in Section 1.3.

The constitutive models available in *UDEC* range from linearly elastic models to highly nonlinear plastic models. The basic constitutive models are listed below. A short discussion of the theoretical background and simple example tests for each model follow this listing.*

---

* The data files in this section are all created using a text editor, the built in test editor may be used. The files are stored in a folder in user documents selected by the user following initial startup. The files may also be found in the folder "ITASCA\UDEC700\datafiles\Models\BlockModel" with the extension ".DAT." A project file is also provided for each example. In order to run an example and compare the results to plots in this section, open a project file in the *GIIC* or *GUI* by clicking on the FILE/OPEN PROJECT menu item and selecting the project file name (with extension ".PRJ" for the *GIIC* or ".UDPRJ" for the *GUI*). In the *GIIC* Click on the *Project Options* icon at the top of the *Project Tree Record*, select *Rebuild unsaved states*, and the example data file will be run, and plots created. In the *GUI*, click on the green circle.

1.2 Constitutive Models in *UDEC*

The constitutive models provided in *UDEC* Version 7.0 are arranged into null, elastic and plastic model groups:

Null model group

(1) *null* model

A null material model is used to represent material that is removed or excavated. (See Section 1.4.1.)

Elastic model group

(2) *elastic, isotropic* model

The elastic, isotropic model provides the simplest representation of material behavior. This model is valid for homogeneous, isotropic, continuous materials that exhibit linear stress-strain behavior with no hysteresis on unloading. (See Section 1.5.1.)

(3) *elastic, transversely isotropic* model

The elastic, transversely isotropic model gives the ability to simulate layered elastic media in which there are distinctly different elastic moduli in directions normal and parallel to the layers. (See Section 1.5.2.)

Plastic model group

(4) *Drucker-Prager* model

The Drucker-Prager plasticity model may be useful to model soft clays with low friction angles. However, this model is not generally recommended for application to geologic materials. It is included here mainly to permit comparison with other numerical program results. (See Section 1.6.1.)

(5) *Mohr-Coulomb* model

The Mohr-Coulomb model is the conventional model used to represent shear failure in soils and rocks. Vermeer and deBorst (1984), for example, report laboratory test results for sand and concrete that match well with the Mohr-Coulomb criterion. (See Section 1.6.2.)

(6) *ubiquitous-joint* model

The ubiquitous-joint model is an anisotropic plasticity model that includes weak planes of specific orientation embedded in a Mohr-Coulomb solid. (See Section 1.6.3.)

(7) *strain-softening* model

The strain-softening model allows representation of nonlinear material softening and hardening behavior based on prescribed variations of the Mohr-Coulomb model properties (cohesion, friction, dilation and tensile strength) as functions of the deviatoric plastic strain. (See Section 1.6.4.)

(8) *softening-ubiquitous-joint* model

The bilinear strain-hardening/softening ubiquitous-joint model allows representation of material softening and hardening behavior for the matrix and the weak plane based on prescribed variations of the ubiquitous-joint model properties (cohesion, friction, dilation and tensile strength) as functions of deviatoric and tensile plastic strain. The variation of material strength properties with mean stress can also be taken into account by using the bilinear option. (See Section 1.6.5.)

(9) *double-yield* model

The double-yield model is intended to represent materials in which there may be significant irreversible compaction in addition to shear yielding, such as hydraulically placed backfill or lightly cemented granular material. (See Section 1.6.6.)

(10) *modified Cam-clay* model

The modified Cam-clay model may be used to represent materials when the influence of volume change on bulk property and resistance to shear need to be taken into consideration, as in the case of soft clay. (See Section 1.6.7.)

(11) *Hoek-Brown-PAC* model

The Hoek-Brown failure criterion characterizes the stress conditions that lead to failure in intact rock and rock masses. The failure surface is nonlinear, and is based on the relation between the major and minor principal stresses. The model incorporates a plasticity flow rule that varies as a function of the confining stress level. (See Section 1.6.8.)

(12) *Hoek-Brown* model

The Hoek-Brown model provides an alternative to the Hoek-Brown-PAC model with a stress-dependent plastic flow rule, described above. The model characterizes post-failure plastic flow by simple flow rule choices given in terms of a user-specified dilation angle. This model also contains a tensile strength limit similar to that used by the Mohr-Coulomb model. In addition, a factor-of-safety calculation based on the shear-strength reduction method can be run with the Hoek-Brown model. (See Section 1.6.9.)

(13) *cap-yield* model

The cap-yield soil model provides a comprehensive representation of the non-linear behavior of soils. The model includes frictional strain-hardening and softening shear behavior, an elliptic volumetric cap with strain-hardening behavior, and an elastic modulus function of plastic volumetric strain. The model allows a more realistic representation of the loading/unloading response of soils. (See Section 1.6.10.)

(14) *cap-yield-simplified* model

A simplified version of the cap-yield model offers built-in features including a friction-hardening law that uses hyperbolic model parameters as direct input, and a Mohr-Coulomb failure envelope with two built-in dilation laws. (See Section 1.6.11.)

There are also several time-dependent (creep) material models available in the creep model option for *UDEC* (see Section 1 in **Creep Material Models**).

Input parameters to all of these built-in models can be controlled via *FISH* to modify the behavior of the models.

In addition, the C++ source codes for all of the models are provided in the directory folder "\UDEC700\PLUGINFILES\MODELS." Users can modify these models or create their own constitutive models as *dynamic link libraries* (DLLs) by following the procedures given in writing new constitutive models in Section 4.

1.3 Incremental Formulation

All constitutive models share the same incremental numerical algorithm. Given the stress state at time, t, and the total strain increment for the current timestep, Δt, the purpose is to determine the corresponding stress increment and the new stress state at time $t + \Delta t$. When plastic deformations are involved, only the elastic part of the strain increment will contribute to the stress increment. In this case, a correction must be made to the elastic stress increment as computed from the total strain increment, in order to obtain the actual stress state at the new timestep.

Note that all models operate on effective stresses only; pore pressures are used to convert total stresses to effective stresses before the constitutive model is called. The reverse process occurs after the model calculations are complete.

1.3.1 Incremental Equations of the Theory of Plastic Flow

In order to describe the implementation of elastic/plastic constitutive laws in the framework of the explicit dynamic-solution scheme, we consider the implementation algorithm for the case when the incremental elastic stress-strain relations are linear functions of strain increment, and the yield relation is a linear function of the generalized stress components.

We note that all stress increments described in this section are corotational stress increments. The stresses at time $t + \Delta t$ are computed as "new stress values." However, in large-strain mode, these values must be incremented by the stress-rotation correction.

The description of plastic flow rests on several relations:

(1) *the failure criterion*

$$f(\underline{\sigma}_n) = 0 \tag{1.1}$$

where f, the yield function, is a known function that specifies the limiting stress combination for which plastic flow takes place. (This function is represented by a surface in the generalized stress space, and all stress points below the surface are characterized by elastic behavior.) $[\underline{\sigma}]$ is the generalized stress vector of dimension n with components $\underline{\sigma}_i, i = 1, n$.

(2) *the relation expressing the decomposition of strain increments into the sum of elastic and plastic parts*

$$\Delta\underline{\epsilon}_i = \Delta\underline{\epsilon}_i^e + \underline{\epsilon}_i^p \tag{1.2}$$

$\Delta[\underline{\epsilon}]$ is the generalized strain-increment vector with components $\Delta\underline{\epsilon}_i, i = 1, n$.

(3) *the elastic relations between elastic strain increments and stress increments*

$$\Delta\underline{\sigma}_i = S_i(\Delta\underline{\epsilon}_n^e) \quad \text{i=1,}n \tag{1.3}$$

where S_i is a linear function of the elastic strain increments, $\Delta\underline{\epsilon}_n^e$.

(4) *the flow rule specifying the direction of the plastic-strain increment vector as that normal to the potential surface* $g(\underline{\sigma}_n) = constant$

$$\Delta\underline{\epsilon}_i^p = \lambda\frac{\partial g}{\partial\underline{\sigma}_i} \tag{1.4}$$

where λ is a constant. (The flow rule is said to be associated if $g \equiv f$, and nonassociated otherwise.)

(5) *the requirement for the new stress-vector components to satisfy the yield function*

$$f(\underline{\sigma}_n + \Delta\underline{\sigma}_n) = 0 \tag{1.5}$$

This equation provides a relation for evaluation of the magnitude of the plastic-strain increment vector.

Substitution of the expression for the elastic-strain increment derived from Eq. (1.2) into the elastic relation Eq. (1.3) yields, taking into consideration the linear property of the function S_i,

$$\Delta\underline{\sigma}_i = S_i(\Delta\underline{\epsilon}_n) - S_i(\Delta\underline{\epsilon}_n^p) \tag{1.6}$$

In further expressing the plastic strain increment by means of the flow rule Eq. (1.4), this equation becomes

$$\Delta\underline{\sigma}_i = S_i(\Delta\underline{\epsilon}_n) - \lambda S_i\left(\frac{\partial g}{\partial\underline{\sigma}_n}\right) \tag{1.7}$$

where use has been made of the linear property of S_i.

In the special case where $f(\underline{\sigma}_n)$ is a linear function of the components $\underline{\sigma}_i$, $i = 1, n$, Eq. (1.5) may be expressed as

$$f(\underline{\sigma}_n) + f^*(\Delta\underline{\sigma}_n) = 0 \tag{1.8}$$

where, as a notation convention, f^* represents the function f minus its constant term,

$$f^*(.) = f(.) - f(\underline{0}_n) \tag{1.9}$$

For a stress point $\underline{\sigma}_n$ on the yield surface, $f(\underline{\sigma}_n) = 0$, and Eq. (1.8) becomes, after substitution of the expression Eq. (1.7) for the stress increment, and further using the linear property of f^*,

$$f^*\left[S_n(\Delta\underline{\epsilon}_n)\right] - \lambda f^*\left[S_n\left(\frac{\partial g}{\partial \underline{\sigma}_n}\right)\right] = 0 \tag{1.10}$$

We now define *new* stress components $\underline{\sigma}_i{}^N$ and *elastic guesses* $\underline{\sigma}_i^I$ as

$$\underline{\sigma}_i^N = \underline{\sigma}_i + \Delta\underline{\sigma}_i \tag{1.11}$$

$$\underline{\sigma}_i^I = \underline{\sigma}_i + S_i(\Delta\underline{\epsilon}_n) \tag{1.12}$$

Note that the term $S_i(\Delta\underline{\epsilon}_n)$ in Eq. (1.12) is the component i of the stress increment induced by the total-strain increment $\Delta\underline{\epsilon}_n$, in case no increment of plastic deformation takes place. This justifies the name of "elastic guess" for $\underline{\sigma}_i^I$.

From the definition Eq. (1.12), it follows, using the same arguments as above, that

$$f(\underline{\sigma}_n^I) = f^*\left[S_n(\Delta\underline{\epsilon}_n)\right] \tag{1.13}$$

Hence, an expression for λ may be derived from Eqs. (1.9), (1.10) and (1.13):

$$\lambda = \frac{f(\underline{\sigma}_n^I)}{f\left[S_n(\partial g/\partial\underline{\sigma}_n)\right] - f(\underline{0}_n)} \tag{1.14}$$

Using the expression of the stress increment Eq. (1.7), and the definition of the elastic guess Eq. (1.12), the new stress may be expressed from Eq. (1.11) as

$$\underline{\sigma}_i^N = \underline{\sigma}_i^I - \lambda S_i\left(\frac{\partial g}{\partial \underline{\sigma}_n}\right) \tag{1.15}$$

For clarity, recall that, in these last two expressions, $S_i(\partial g/\partial\underline{\sigma}_n)$ is the stress increment obtained from the incremental elastic law, where $\partial g/\partial\underline{\sigma}_i$ is substituted for $\Delta\underline{\epsilon}_i$, $i = 1, n$.

1.3.2 Implementation

An elastic guess $\underline{\sigma}_i^I$, $i = 1, n$ for the stress state at time $t + \Delta t$ is first evaluated by adding to the stress components at time, t, increments computed from the total-strain increment for the step, using an incremental elastic stress-strain law (see Eq. (1.12)). If the elastic guess violates the yield function, Eq. (1.15) is used to place the new stress exactly on the yield curve. Otherwise, the elastic guess gives the new stress state at time $t + \Delta t$.

If the stress point $\underline{\sigma}_i^I$, $i = 1, n$ is located above the yield surface in the generalized stress space, the coefficient λ in Eq. (1.15) is given by Eq. (1.14), provided the yield function is a linear function of the generalized stress vector components. Eq. (1.15) is still valid, but λ is set to zero in case $\underline{\sigma}_i^I$, $i = 1, n$ is located below the yield surface (elastic loading or unloading).

The implementation of each of the constitutive models is described separately in the following sections. All models except the null and elastic models potentially involve plastic deformations. Note that a wide range of material behavior may be obtained from these fourteen models by assigning appropriate values to the model parameters.

1.4 Null Model Group

1.4.1 Null Model

The stresses within null blocks (**block change model = 0**) or null zones (**block zone cmodel assign null**) are are not transfered to adjacent blocks. The null material may be changed to a different material model at a later stage of the simulation. In this way, backfilling an excavation, for example, can be simulated. It is not allowed to mix null zones with other models within a single block. Any number of null zones in a block will mark that block as null. To prevent collapse of the null zones under gravity and to allow the null zones to displace evenly in response to displacement of the opening, material properties must be assigned to the null zones. The recomended properties are the same as for other blocks.

1.4.1.1 **block zone cmodel** *Command and Property Keywords*

null – **block zone cmodel assign null**

(1)	**bu**lk	elastic bulk modulus, K
(2)	**dens**ity	material density, ρ
(3)	**sh**ear	elastic shear modulus, G

1.5 Elastic Model Group

The models in this group are characterized by reversible deformations upon unloading; the stress-strain laws are linear and path-independent.

1.5.1 Elastic, Isotropic Model

In this model, the relation of stress to strain in incremental form is expressed by Hooke's law in *plane strain* as

$$\begin{aligned} \Delta\sigma_{11} &= \alpha_1\ \Delta e_{11} + \alpha_2\ \Delta e_{22} \\ \Delta\sigma_{22} &= \alpha_2\ \Delta e_{11} + \alpha_1\ \Delta e_{22} \\ \Delta\sigma_{12} &= 2G\ \Delta e_{12} \qquad\qquad (\Delta\sigma_{21} = \Delta\sigma_{12}) \\ \Delta\sigma_{33} &= \alpha_2\ (\Delta e_{11} + \Delta e_{22}) \end{aligned} \tag{1.16}$$

where α_1 = $K + (4/3)G$;
α_2 = $K - (2/3)G$;
K = bulk modulus; and
G = shear modulus.

$$\Delta e_{ij} = \frac{1}{2}\left[\frac{\partial \dot{u}_i}{\partial x_j} + \frac{\partial \dot{u}_j}{\partial x_i}\right]\Delta t \tag{1.17}$$

where Δe_{ij} = incremental strain tensor;
$\dot{u}_i$ = displacement rate; and
Δt = timestep.

In *plane stress*, these equations become

$$\begin{aligned} \Delta\sigma_{11} &= \beta_1\ \Delta e_{11} + \beta_2\ \Delta e_{22} \\ \Delta\sigma_{22} &= \beta_2\ \Delta e_{11} + \beta_1\ \Delta e_{22} \\ \Delta\sigma_{12} &= 2G\ \Delta e_{12} \qquad\qquad (\Delta\sigma_{21} = \Delta\sigma_{12}) \\ \Delta\sigma_{33} &= 0 \end{aligned} \tag{1.18}$$

where β_1 = $\alpha_1 - (\alpha_2^2/\alpha_1)$; and
β_2 = $\alpha_2 - (\alpha_2^2/\alpha_1)$.

For *axisymmetric* geometry:

$$\begin{aligned}
\Delta\sigma_{11} &= \alpha_1\ \Delta e_{11} + \alpha_2\ (\Delta e_{22} + \Delta e_{33}) \\
\Delta\sigma_{22} &= \alpha_1\ \Delta e_{22} + \alpha_2\ (\Delta e_{11} + \Delta e_{33}) \\
\Delta\sigma_{12} &= 2G\ \Delta e_{12} \qquad\qquad (\Delta\sigma_{21} = \Delta\sigma_{12}) \\
\Delta\sigma_{33} &= \alpha_1\ \Delta e_{33} + \alpha_2\ (\Delta e_{11} + \Delta e_{22})
\end{aligned} \tag{1.19}$$

1.5.1.1 **block zone cmodel** *Command and Property Keywords*

Isotropic Elastic – **block zone cmodel assign elastic**

(1) **bu**lk elastic bulk modulus, K
(2) **dens**ity material density, ρ
(3) **sh**ear elastic shear modulus, G

1.5.2 Elastic, Transversely Isotropic Model

A transversely isotropic body has a plane of elastic symmetry (and all directions in such a plane are elastically equivalent) at each point, and these planes are parallel at all points. The model deforms as a two-dimensional slice of a transversely isotropic elastic material subjected to plane-strain or plane-stress boundary conditions in the global xy plane, and oriented such that the global z-axis is parallel with the planes of isotropy (see Figure 1.1).

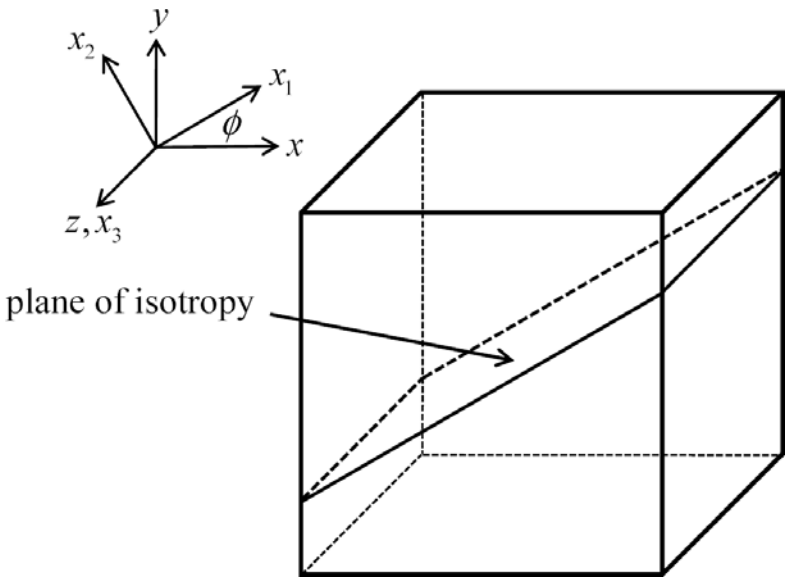

Figure 1.1 Transverse isotropy coordinate axes convention (x_1x_3-axes are in the plane of isotropy)

There are five independent constants in the elastic, transversely isotropic model. The constants are specified in terms of an orthogonal material coordinate system, x_1, x_2, x_3, in which the x_2 axis is normal to a plane of symmetry, with the x_1 and x_3 axes directed arbitrarily in this plane. The material coordinate system is oriented by specifying the angle ϕ (measured positive counterclockwise from the global x-axis) and noting that the x_3 axis is parallel with the global z-axis (see Figure 1.1). A bedded material can be well approximated as a transversely isotropic body with the x_1x_3 plane coinciding with the bedding plane.

There are five elastic constants:

E_1	modulus of elasticity in plane of isotropy
E_2	modulus of elasticity in plane perpendicular to plane of isotropy
G_{12}	cross-shear modulus between plane of isotropy and perpendicular plane (i.e., x_1x_2- or x_2x_3-plane)

ν_{21} Poisson's ratio for the normal strain in the x_1-direction (in the plane of isotropy) related to the normal strain in the x_2-direction (in the perpendicular plane) due to uniaxial stress in the x_2-direction

ν_{31} Poisson's ratio for the normal strain in the x_1-direction (in the plane of isotropy) related to the normal strain in the x_3-direction due to uniaxial stress in the x_3-direction

For a transversely isotropic body whose plane of isotropy lies within the x_1x_3-plane, the following relations apply.

$$E_3 = E_1$$

$$\nu_{31} = \nu_{13}$$

$$\nu_{23} = \nu_{21}$$

$$G_{23} = G_{12}$$

$$G_{13} = \frac{E_1}{2(1+\nu_{31})}$$

$$\nu_{12} = \nu_{21}\,\frac{E_1}{E_2}$$

There are limitations on the variations in elastic properties (Amadei 1982). The following restrictions apply.

$$\begin{aligned} \mathrm{E}_1 &> 0 \\ \mathrm{E}_2 &> 0 \\ \mathrm{G}_{12} &> 0 \\ \nu_{12}^2 &\le 1 \\ \nu_{13}^2 &\le 1 \\ (1-\nu_{13}) - \frac{2\,\mathrm{E}_1\,\nu_{21}^2}{\mathrm{E}_2} &\ge 0 \end{aligned} \tag{1.20}$$

The stress-strain equations are given by Lekhnitskii (1981, p. 34) for a general orthotropic body. When written in terms of the global x, y, z coordinate system, the equations are

$$\begin{aligned}
\Delta e_{xx} &= S_{11}\ \Delta\sigma_{xx} + S_{12}\ \Delta\sigma_{yy} + S_{13}\ \Delta\sigma_{zz}\ +\ S_{16}\ \Delta\sigma_{xy} \\
\Delta e_{yy} &= S_{12}\ \Delta\sigma_{xx} + S_{22}\ \Delta\sigma_{zz} + S_{23}\ \Delta\sigma_{zz}\ +\ S_{26}\ \Delta\sigma_{xy} \\
\Delta e_{zz} &= S_{13}\ \Delta\sigma_{xy} + S_{23}\ \Delta\sigma_{yy} + S_{33}\ \Delta\sigma_{zz}\ +\ S_{36}\ \Delta\sigma_{xy} \\
\Delta e_{yz} &= \frac{1}{2}\left[(S_{44}\ \Delta\sigma_{yz})\ +\ (S_{45}\ \Delta\sigma_{xz})\right] \\
\Delta e_{xz} &= \frac{1}{2}\left[(S_{45}\ \Delta\sigma_{yz})\ +\ (S_{55}\ \Delta\sigma_{xz})\right] \\
\Delta e_{xy} &= \frac{1}{2}\left[(S_{16}\ \Delta\sigma_{xx})\ +\ (S_{26}\ \Delta\sigma_{yy})\ +\ (S_{36}\ \Delta\sigma_{zz})\ +\ (S_{66}\ \Delta\sigma_{xy})\right]
\end{aligned} \tag{1.21}$$

where

$$S_{11} = \frac{\cos^4\phi}{E_1} + (\frac{1}{G_{12}} - \frac{2\nu_{12}}{E_1})\ \sin^2\phi\ \cos^2\phi + \frac{\sin^4\phi}{E_2}$$

$$S_{22} = \frac{\sin^4\phi}{E_1} + (\frac{1}{G_{12}} - \frac{2\nu_{12}}{E_1})\ \sin^2\phi\ \cos^2\phi + \frac{\cos^4\phi}{E_2}$$

$$S_{12} = (\frac{1}{E_1} + \frac{1}{E_2} + \frac{2\nu_{12}}{E_1} - \frac{1}{G_{12}})\ \sin^2\phi\ \cos^2\phi - \frac{\nu_{12}}{E_1}$$

$$S_{13} = -(\frac{\nu_{23}}{E_2})\sin^2\phi - (\frac{\nu_{13}}{E_1})\ \cos^2\phi$$

$$S_{23} = -(\frac{\nu_{23}}{E_2})\cos^2\phi - (\frac{\nu_{13}}{E_1})\ \sin^2\phi$$

$$S_{33} = \frac{1}{E_3}$$

$$S_{44} = \frac{\cos^2\phi}{G_{23}} + \frac{\sin^2\phi}{G_{13}}$$

$$S_{45} = \left(\frac{1}{G_{23}} - \frac{1}{G_{13}}\right) \sin\phi \cos\phi$$

$$S_{55} = \frac{\sin^2\phi}{G_{23}} + \frac{\cos^2\phi}{G_{13}}$$

$$S_{16} = -\left[2\left(\frac{\sin^2\phi}{E_2} - \frac{\cos^2\phi}{E_1}\right) + \left(\frac{1}{G_{12}} - \frac{2\nu_{12}}{E_1}\right)(\cos^2\phi - \sin^2\phi)\right] \sin\phi \cos\phi$$

$$S_{26} = -\left[2\left(\frac{\cos^2\phi}{E_2} - \frac{\sin^2\phi}{E_1}\right) - \left(\frac{1}{G_{12}} - \frac{2\nu_{12}}{E_1}\right)(\cos^2\phi - \sin^2\phi)\right] \sin\phi \cos\phi$$

$$S_{36} = -2\left(\frac{\nu_{13}}{E_1} - \frac{\nu_{23}}{E_2}\right) \sin\phi \cos\phi$$

$$S_{66} = 4\left(\frac{1}{E_1} + \frac{1}{E_2} + \frac{2\nu_{12}}{E_1} - \frac{1}{G_{12}}\right) \sin^2\phi \cos^2\phi + \frac{1}{G_{12}}$$

ϕ = angle of anisotropy measured counterclockwise from the x-axis (see Figure 1.1).

A state of *plane stress* with respect to the xy-plane is obtained by setting

$$\Delta\sigma_{zz} = \Delta\sigma_{xz} = \Delta\sigma_{yz} = 0$$

in Eq. (1.21). This gives

$$\begin{aligned}
\Delta e_{xx} &= S_{11}\,\Delta\sigma_{xx} + S_{12}\,\Delta\sigma_{yy} + S_{16}\,\Delta\sigma_{xy} \\
\Delta e_{yy} &= S_{12}\,\Delta\sigma_{xx} + S_{22}\,\Delta\sigma_{yy} + S_{26}\,\Delta\sigma_{xy} \\
\Delta e_{xy} &= \frac{1}{2}\left(S_{16}\,\Delta\sigma_{xx} + S_{26}\,\Delta\sigma_{yy} + S_{66}\,\Delta\sigma_{xy}\right)
\end{aligned} \tag{1.22}$$

which can be written as

$$\begin{bmatrix} \Delta e_{xx} \\ \Delta e_{yy} \\ 2\Delta e_{xy} \end{bmatrix} = \begin{bmatrix} s_{11} & s_{12} & s_{16} \\ s_{12} & s_{22} & s_{26} \\ s_{16} & s_{26} & s_{66} \end{bmatrix} \begin{bmatrix} \Delta\sigma_{xx} \\ \Delta\sigma_{yy} \\ \Delta\sigma_{xy} \end{bmatrix} \tag{1.23}$$

The stress-strain relations can easily be found by inverting the matrix.

A state of *plane strain* in the xy-plane is obtained from Eq. (1.21) by setting

$$\Delta e_{zz} = \Delta e_{xz} = \Delta e_{yz} = 0$$

This results in

$$\begin{aligned}
\Delta e_{xx} &= s_{11}\Delta\sigma_{xx} + s_{12}\Delta\sigma_{yy} + s_{13}\Delta\sigma_{zz} + s_{16}\Delta\sigma_{xy} \\
\Delta e_{yy} &= s_{12}\Delta\sigma_{xx} + s_{22}\Delta\sigma_{yy} + s_{23}\Delta\sigma_{zz} + s_{26}\Delta\sigma_{xy} \\
0 &= s_{xz}\Delta\sigma_{xx} + s_{23}\Delta\sigma_{yy} + s_{33}\Delta\sigma_{zz} + s_{36}\Delta\sigma_{xy} \\
0 &= s_{44}\Delta\sigma_{yz} + s_{45}\Delta\sigma_{xz} \\
0 &= s_{55}\Delta\sigma_{xz} + s_{45}\Delta\sigma_{yz} \\
\Delta e_{xy} &= \frac{1}{2}(s_{16}\Delta\sigma_{xx} + s_{26}\Delta\sigma_{yy} + s_{36}\Delta\sigma_{zz} + s_{66}\Delta\sigma_{xy})
\end{aligned} \tag{1.24}$$

which can be written as

$$\begin{bmatrix} \Delta e_{xx} \\ \Delta e_{yy} \\ 0 \\ 2\Delta e_{xy} \end{bmatrix} = \begin{bmatrix} s_{11} & s_{12} & s_{13} & s_{16} \\ s_{12} & s_{22} & s_{23} & s_{26} \\ s_{13} & s_{23} & s_{33} & s_{36} \\ s_{16} & s_{26} & s_{36} & s_{66} \end{bmatrix} \begin{bmatrix} \Delta\sigma_{xx} \\ \Delta\sigma_{yy} \\ \Delta\sigma_{zz} \\ \Delta\sigma_{xy} \end{bmatrix} \tag{1.25}$$

The stress-strain relations can be obtained by inverting the matrix.

1.5.2.1 **block zone cmodel** *Command and Property Keywords*

Transversely Isotropic Elastic – **block zone cmodel assign anisotropic**

(1)	**ang**le	angle of anisotropy, taken counterclockwise from the x-axis, ϕ
(2)	**dens**ity	mass density, ρ
(3)	**yo**ung-**pl**ane	elastic Young's modulus in the plane of isotropy, E_1
(4)	**yo**ung-**no**rmal	elastic Young's modulus in the plane perpendicular to the plane of isotropy, E_2
(5)	**po**isson-**pl**ane	Poisson's ratio for the normal strain in the x_1-direction (in the plane of isotropy) related to the normal strain in the x_2-direction (in the perpendicular plane) due to uniaxial stress in the x_2-direction, ν_{21}
(6)	**po**isson-**no**rmal	Poisson's ratio for the normal strain in the x_1-direction (in the plane of isotropy) related to the normal strain in the x_3-direction due to uniaxial stress in the x_3-direction, ν_{31}
(7)	**sh**earV-normal	elastic cross-shear modulus between plane of isotropy and perpendicular plane (i.e., x_1x_2- or x_2x_3-plane), G_{12} *

---

* The cross-shear modulus, **shear-normal**, for anisotropic elasticity must be determined. Lekhnittskii (1981) suggests the following equation based on laboratory testing of rock.

$$shear - normal = \frac{E_1 E_2}{E_1(1 + 2\nu_{12}) + E_2}$$

assuming the x_1x_3-plane is the plane of isotropy.

1.6 Plastic Model Group

All plastic models potentially involve some degree of permanent, path-dependent deformation (failure) – a consequence of the nonlinearity of the stress-strain relations. The different models are characterized by their yield function, hardening/softening functions and plastic flow. These functions or criteria are represented by one or more limiting surfaces in a generalized stress space with points below or on the surface being characterized by an incremental elastic or plastic behavior, respectively. The plastic flow formulation rests on basic assumptions from plasticity theory that the total strain increment may be decomposed into elastic and plastic parts, with only the elastic part contributing to the stress increment by means of an elastic law. In addition, both plastic and elastic strain increments are taken to be coaxial with the current principal axes of the stresses. (This is only valid if elastic strains are small compared to plastic strains during plastic flow.) The flow rule specifies the direction of the plastic strain increment vector as that normal to the potential surface; it is called associated if the potential and yield functions coincide, and nonassociated otherwise. A detailed description of the plastic flow calculation is given in Section 1.3.1. See Vermeer and deBorst (1984) for further discussion on the theory of plasticity.

For Drucker-Prager, Mohr-Coulomb, ubiquitous-joint, strain-softening and softening-ubiquitous models, a shear yield function and a nonassociated shear flow rule are used. For the double-yield and cap-yield models, shear and volumetric yield functions, nonassociated shear flow and associated volumetric flow rules are included. The simplified cap-yield model is a version of the cap-yield model that provides built-in friction hardening and dilation hardening/softening laws, and does not include a volumetric cap. In addition, the failure envelope for each of the above models is characterized by a tensile yield function with associated flow rule.

The modified Cam-clay model formulation rests on a combined shear and volumetric yield function and associated flow rule.

The two types of Hoek-Brown model provide different formulations to represent yielding. For the Hoek-Brown model, plastic flow is handled in a manner similar to that in the Mohr-Coulomb model, in which a dilation angle is specified. Also, a tensile yield function similar to that used with the Mohr-Coulomb model is included with the Hoek-Brown model. The Hoek-Brown-PAC model uses a nonlinear shear-yield function and a plasticity flow rule that varies as a function of the stress level.

The out-of-plane stress is taken into consideration in the formulation that is expressed in three-dimensional terms. All models are based on plane-strain conditions, with the exception of the strain-softening model, which is also available in a plane-stress option. Also note that all plasticity models are formulated in terms of *effective* stresses, *not* total stresses.

The plasticity models can produce localization (i.e., the development of families of discontinuities such as shear bands in a material that starts as a continuum). Note that localization is grid-dependent since there is no intrinsic length scale incorporated in the formulations. This is an important consideration when creating a grid for a plasticity analysis.

As discussed in Section 1.3.2, in the numerical implementation of the models, an *elastic trial* (or elastic guess) for the stress increment is first computed from the total strain increment using the incremental form of Hooke's law. The corresponding stresses are then evaluated. If they violate

the yield criteria (i.e., the stress point representation lies above the yield function in the generalized stress space), plastic deformations take place. In this case, only the elastic part of the strain increment can contribute to the stress increment; the latter is corrected by using the plastic flow rule to ensure that the stresses lie on the composite yield function. This section describes the yield and potential functions, flow rules and stress corrections for the different plasticity models.

1.6.1 Drucker-Prager Model

The failure envelope for this model consists of a Drucker-Prager criterion with tension cutoff. The shear flow rule is nonassociated, and the tensile flow rule is associated. For a detailed description of the model, see Chen and Han (1988), for example.

1.6.1.1 Incremental Elastic Law

The Drucker-Prager model is expressed in terms of two generalized stress components: the tangential stress, τ, and mean normal stress, σ, defined as

$$\begin{aligned} \tau &= \sqrt{J_2} \\ \sigma &= \frac{1}{3}(\sigma_{11} + \sigma_{22} + \sigma_{33}) \end{aligned} \tag{1.26}$$

where J_2 is the second invariant of the stress deviator tensor. This quantity may be expressed as

$$J_2 = \frac{1}{6}\left[(\sigma_{11} - \sigma_{22})^2 + (\sigma_{22} - \sigma_{33})^2 + (\sigma_{11} - \sigma_{33})^2\right] + {\sigma_{12}}^2 \tag{1.27}$$

The shear strain increment, $\Delta\gamma$, and volumetric strain increment, Δe, associated with τ and σ have the form

$$\begin{aligned} \Delta\gamma &= 2\sqrt{\Delta J_2'} \\ \Delta e &= \Delta e_{11} + \Delta e_{22} + \Delta e_{33} \end{aligned} \tag{1.28}$$

where $\Delta J_2'$, the second invariant of the incremental strain deviator tensor, is given by

$$\Delta J_2' = \frac{1}{6}\left[(\Delta e_{11} - \Delta e_{22})^2 + (\Delta e_{22} - \Delta e_{33})^2 + (\Delta e_{11} - \Delta e_{33})^2\right] + {\Delta e_{12}}^2 \tag{1.29}$$

The strain increments are decomposed:

$$\begin{aligned} \Delta\gamma &= \Delta\gamma^e + \Delta\gamma^p \\ \Delta e &= \Delta e^e + \Delta e^p \end{aligned} \tag{1.30}$$

where the superscripts ^{e} and ^{p} refer to elastic and plastic parts, respectively, and the plastic components are nonzero during plastic flow only. The incremental expression of Hooke's law in terms of generalized stresses and strains is

$$\begin{aligned} \Delta\tau &= G\Delta\gamma^e \\ \Delta\sigma &= K\Delta e^e \end{aligned} \tag{1.31}$$

where G and K are the shear and bulk modulus, respectively.

1.6.1.2 Yield and Potential Functions

The representation of the failure criterion in the (σ, τ) plane is sketched in Figure 1.2. The failure envelope is defined from point A to B by the Drucker-Prager yield function,

$$f^s = \tau + q_\phi\sigma - k_\phi \tag{1.32}$$

and from B to C by the tension yield function,

$$f^t = \sigma - \sigma^t \tag{1.33}$$

where q_ϕ and k_ϕ are constant material properties, and σ^t is the tensile strength for the Drucker-Prager model. Note that this strength is defined as the maximum value of the *mean normal stress* for the material under consideration. For a material whose property q_ϕ is not equal to zero, the tensile strength cannot exceed the value σ^t_{max} given by

$$\sigma^t_{max} = \frac{k_\phi}{q_\phi} \tag{1.34}$$

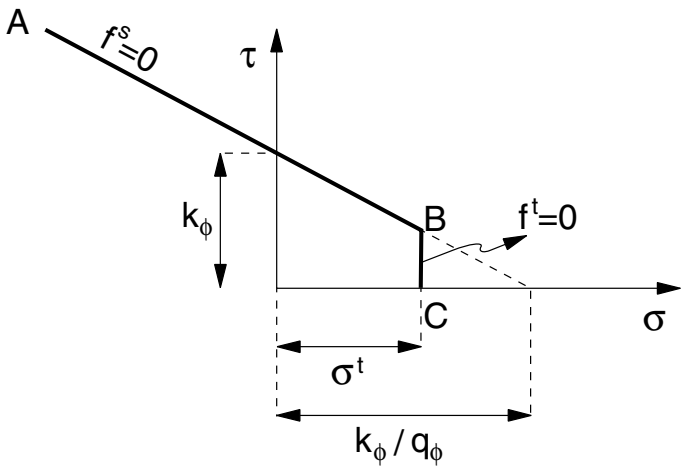

Figure 1.2 Drucker-Prager failure criterion in UDEC

The shear potential function g^s corresponds in general to a nonassociated flow rule, and has the form

$$g^s = \tau + q_\psi \sigma \tag{1.35}$$

where q_ψ is a material constant equal to q_ϕ if the flow rule is associated.

The flow rule for tensile failure is associated. It is derived from the potential function g^t given by

$$g^t = \sigma \tag{1.36}$$

The flow rules are given a unique definition in the vicinity of an edge of the composite yield function by application of the following technique. A function, $h(\sigma, \tau) = 0$, which is represented by the diagonal between the representation of $f^s = 0$ and $f^t = 0$ in the (σ, τ) plane, is defined (see Figure 1.3). This function may be written as

$$h = \tau - \tau^P - \alpha^P(\sigma - \sigma^t) \tag{1.37}$$

where τ^P and α^P are two constants defined as

$$\begin{aligned} \tau^P &= k_\phi - q_\phi \sigma^t \\ \alpha^P &= \sqrt{1 + {q_\phi}^2} - q_\phi \end{aligned} \tag{1.38}$$

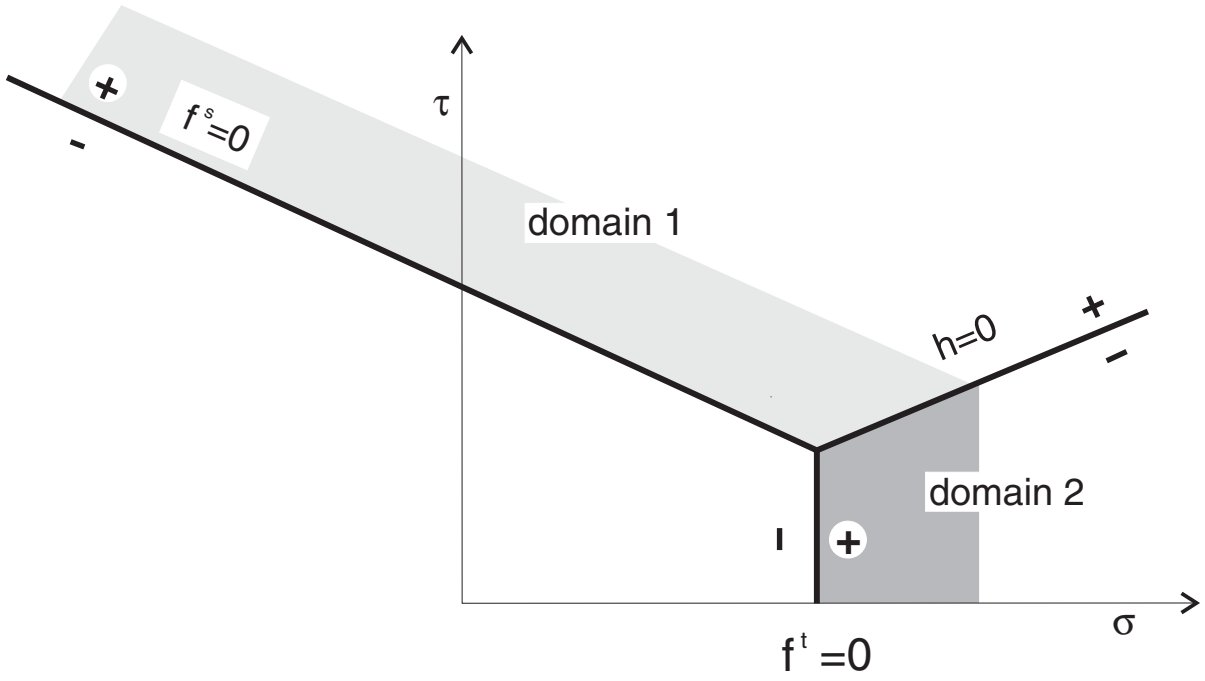

Figure 1.3 Drucker-Prager model: domains used in the definition of the flow rule

An elastic guess violating the failure criterion is represented by a point in the (σ, τ) plane, located either in domain 1 or 2, corresponding to positive or negative domains of $h = 0$, respectively. If in domain 1, shear failure is declared, and the stress point is brought back to the curve $f^s = 0$ using a flow rule derived using the potential function g^s. If in domain 2, tensile failure takes place, and the stress point is brought back to $f^t = 0$ using a flow rule derived using g^t. Further comments on this technique may be found in the Mohr-Coulomb model section.

1.6.1.3 Plastic Corrections

First consider shear failure. The flow rule has the form

$$\Delta\gamma^p = \lambda^s \frac{\partial g^s}{\partial \tau}$$
$$\Delta e^p = \lambda^s \frac{\partial g^s}{\partial \sigma} \tag{1.39}$$

where the magnitude of the parameter λ^s remains to be defined. Using Eq. (1.35) for g^s, these expressions give, after partial differentiation,

$$\begin{aligned} \Delta\gamma^p &= \lambda^s \\ \Delta e^p &= \lambda^s q_\psi \end{aligned} \tag{1.40}$$

The elastic strain increments may be expressed from Eq. (1.30) as total increments minus plastic increments. In further using Eq. (1.40), the elastic laws in Eq. (1.31) may be expressed:

$$\begin{aligned} \Delta\tau &= G\Delta\gamma - G\lambda^s \\ \Delta\sigma &= K\Delta e - Kq_\psi\lambda^s \end{aligned} \tag{1.41}$$

Let the new and old stress states be referred to by the superscripts ^{N} and ^{O}, respectively. Then, by definition:

$$\begin{aligned} \tau^N &= \tau^O + \Delta\tau \\ \sigma^N &= \sigma^O + \Delta\sigma \end{aligned} \tag{1.42}$$

Substitution of Eq. (1.41) gives

$$\begin{aligned} \tau^N &= \tau^I - G\lambda^s \\ \sigma^N &= \sigma^I - Kq_\psi\lambda^s \end{aligned} \tag{1.43}$$

where the superscript ^{I} is used to represent the elastic guess obtained, by adding to the old stresses, elastic increments computed using the total strain increments – i.e.,

$$\begin{aligned} \tau^I &= \tau^O + G\Delta\gamma \\ \sigma^I &= \sigma^O + K\Delta e \end{aligned} \tag{1.44}$$

The parameter λ^s may now be defined by requiring that the new stress point be located on the shear yield surface. Substitution of τ^N and σ^N for τ and σ in $f^s = 0$ gives, after some manipulations (see Eqs. (1.32) and (1.43)),

$$\lambda^s = \frac{f^s(\sigma^I, \tau^I)}{G + Kq_\phi q_\psi} \tag{1.45}$$

Noting that the new deviatoric stresses may be obtained by multiplying the corresponding deviatoric elastic guesses with the ratio τ^N/τ^I, the new stresses may be written as

$$\sigma_{ij}^N = (\sigma_{ij}^I - \sigma^I \delta_{ij})\frac{\tau^N}{\tau^I} + \sigma^N \delta_{ij} \tag{1.46}$$

where δ_{ij} is the Kronecker delta symbol.

We now consider tensile failure. The flow rule has the form

$$\begin{aligned} \Delta\gamma^p &= \lambda^t \frac{\partial g^t}{\partial \tau} \\ \Delta e^p &= \lambda^t \frac{\partial g^t}{\partial \sigma} \end{aligned} \tag{1.47}$$

where the magnitude of the parameter λ^t must be determined. Using the Eq. (1.36) for g^t, these expressions give, after partial differentiation,

$$\begin{aligned} \Delta\gamma^p &= 0 \\ \Delta e^p &= \lambda^t \end{aligned} \tag{1.48}$$

Applying a reasoning similar to that described above, we obtain

$$\begin{aligned} \tau^N &= \tau^I \\ \sigma^N &= \sigma^I - K\lambda^t \end{aligned} \tag{1.49}$$

and

$$\lambda^t = \frac{\sigma^I - \sigma^t}{K} \tag{1.50}$$

As expected, substitution of this expression in Eq. (1.49) yields

$$\begin{aligned} \tau^N &= \tau^I \\ \sigma^N &= \sigma^t \end{aligned} \tag{1.51}$$

In this mode of failure, the new deviatoric stresses correspond to the elastic guess and we may write

$$\sigma_{ij}^N = \sigma_{ij}^I + (\sigma^t - \sigma^I)\delta_{ij} \tag{1.52}$$

1.6.1.4 Implementation Procedure

In the implementation of the Drucker-Prager model in *UDEC*, an elastic guess σ_{ij}^{I} is first computed, by adding to the old stress components, increments calculated by application of Hooke's law to the total strain increment for the step. The generalized stress components (σ^I, τ^I) are then derived from σ_{ij}^{I} using Eqs. (1.26) and (1.27).

If these stresses violate the composite yield criterion, a correction must be applied to the generalized stress components to give the new stress state. In this situation, we have that either $h(\sigma^I, \tau^I) > 0$ or $h(\sigma^I, \tau^I) \leq 0$ (see Eq. (1.37)). In the first case, shear failure is declared. New, generalized stresses are evaluated from Eq. (1.43) using Eq. (1.45) for λ^s. In the second case, tensile failure takes place and new stresses are calculated from Eq. (1.51). The stress tensor components in the system of reference axes are then calculated from the generalized stresses, using Eq. (1.46) in the case of shear failure, and Eq. (1.52) when tensile failure takes place.

In *UDEC*, the default value for the tensile strength is zero if the material property q_ϕ is zero, and is σ_{max}^{t} otherwise (see Eq. (1.34)). This last value is also retained if the value assigned to the tensile strength exceeds σ_{max}^{t}. There is no tensile softening in this model.

1.6.1.5 Note on Material Parameters

The Drucker-Prager shear criterion $f^s = 0$ is represented in the principal stress space $(\sigma_1, \sigma_2, \sigma_3)$ by a cone with axis along $\sigma_1 = \sigma_2 = \sigma_3$, and apex at $(\sigma_1, \sigma_2, \sigma_3) = (a, a, a)$ with $a = k_\phi / q_\phi$ (see Figure 1.4). The Mohr-Coulomb shear criterion, characterized by cohesion, c, and friction angle, ϕ, is represented there by an irregular hexagonal pyramid with the same axis, three "outer" and three "inner" edges (see Figure 1.5). The parameters q_ϕ and k_ϕ can be adjusted so that the Drucker-Prager cone will either pass through the outer or the inner edges of the Mohr-Coulomb pyramid. For the outer adjustment, we have

$$\begin{aligned} q_\phi &= \frac{6}{\sqrt{3}(3 - \sin\phi)} \sin\phi \\ k_\phi &= \frac{6}{\sqrt{3}(3 - \sin\phi)} c \cos\phi \end{aligned} \tag{1.53}$$

and for the inner adjustment, we have

$$\begin{aligned} q_\phi &= \frac{6}{\sqrt{3}(3 + \sin\phi)} \sin\phi \\ k_\phi &= \frac{6}{\sqrt{3}(3 + \sin\phi)} c \cos\phi \end{aligned} \tag{1.54}$$

In the special case $q_\phi = 0$, the Drucker-Prager criterion degenerates into the von Mises criterion, which corresponds to a cylinder in the principal stress space. The Tresca criterion is a special case of the Mohr-Coulomb criterion for which $\phi = 0$. It is represented in the principal stress space by a regular hexagonal prism. The von Mises cylinder circumscribes the prism for

$$q_\phi = 0$$
$$k_\phi = \frac{2}{\sqrt{3}} c \tag{1.55}$$

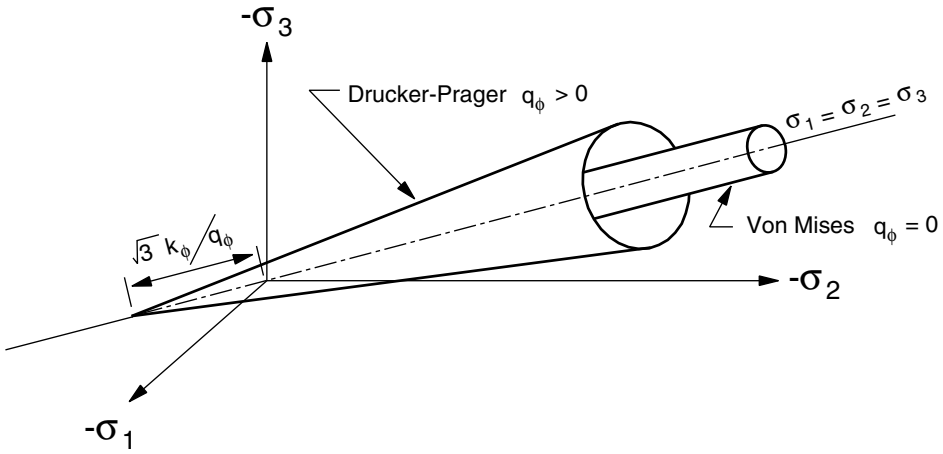

Figure 1.4 Drucker-Prager and von Mises yield surfaces in principal stress space

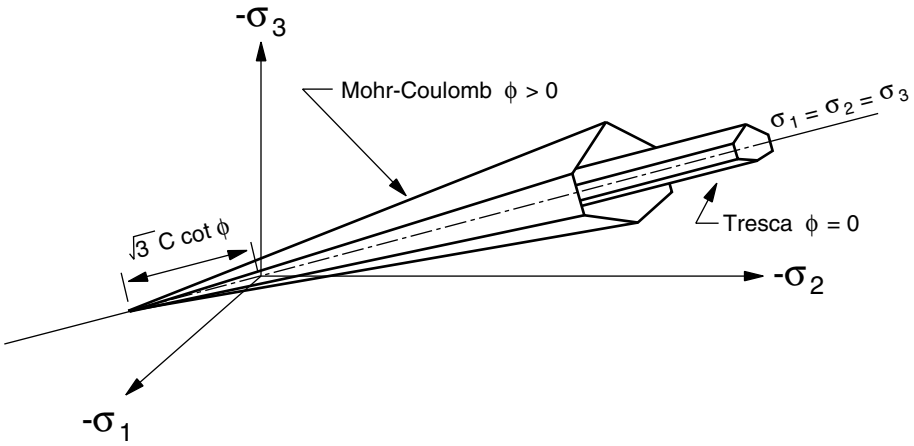

Figure 1.5 Mohr-Coulomb and Tresca yield surfaces in principal stress space

1.6.1.6 **block zone cmodel** *Command and Property Keywords*

Drucker-Prager – **block zone cmodel assign drucker-prager**

(1)	**bu**lk	elastic bulk modulus, K
(2)	**coh**esion-**dr**ucker	material parameter, k_ϕ
(3)	**dens**ity	mass density, ρ
(4)	**di**lation-**dr**ucker	material parameter, q_ψ
(5)	**fri**ction-**dr**ucker	material parameter, q_ϕ
(6)	**sh**ear	elastic shear modulus, G
(7)	**ten**sion	tension limit, σ^t

Note that the default tension limit is zero for a material with $q_\phi = 0$, and is k_ϕ / q_ϕ otherwise. The value assigned for the tension limit remains constant when tensile failure occurs.

1.6.2 Mohr-Coulomb Model

The failure envelope for this model corresponds to a Mohr-Coulomb criterion (shear yield function) with tension cutoff (tensile yield function). The shear flow rule is nonassociated, and the tensile flow rule is associated.

1.6.2.1 Incremental Elastic Law

In the implementation of this model, principal stresses σ_1, σ_2, σ_3 are used, the out-of-plane stress, σ_{zz}, being recognized as one of these. The principal stresses and principal directions are evaluated from the stress tensor components, and ordered so that (recall that compressive stresses are negative)

$$\sigma_1 \leq \sigma_2 \leq \sigma_3 \tag{1.56}$$

The corresponding principal strain increments Δe_1, Δe_2, Δe_3 are decomposed:

$$\Delta e_i = \Delta e_i^e + \Delta e_i^p \qquad i = 1, 3 \tag{1.57}$$

where the superscripts ^{e} and ^{p} refer to elastic and plastic parts, respectively, and the plastic components are nonzero only during plastic flow. The incremental expression of Hooke's law in terms of principal stress and strain has the form

$$\begin{aligned} \Delta\sigma_1 &= \alpha_1 \Delta e_1^e + \alpha_2(\Delta e_2^e + \Delta e_3^e) \\ \Delta\sigma_2 &= \alpha_1 \Delta e_2^e + \alpha_2(\Delta e_1^e + \Delta e_3^e) \\ \Delta\sigma_3 &= \alpha_1 \Delta e_3^e + \alpha_2(\Delta e_1^e + \Delta e_2^e) \end{aligned} \tag{1.58}$$

where $\alpha_1 = K + 4G/3$ and $\alpha_2 = K - 2G/3$.

1.6.2.2 Yield and Potential Functions

With the ordering convention of Eq. (1.56), the failure criterion may be represented in the plane (σ_1, σ_3) as illustrated in Figure 1.6.

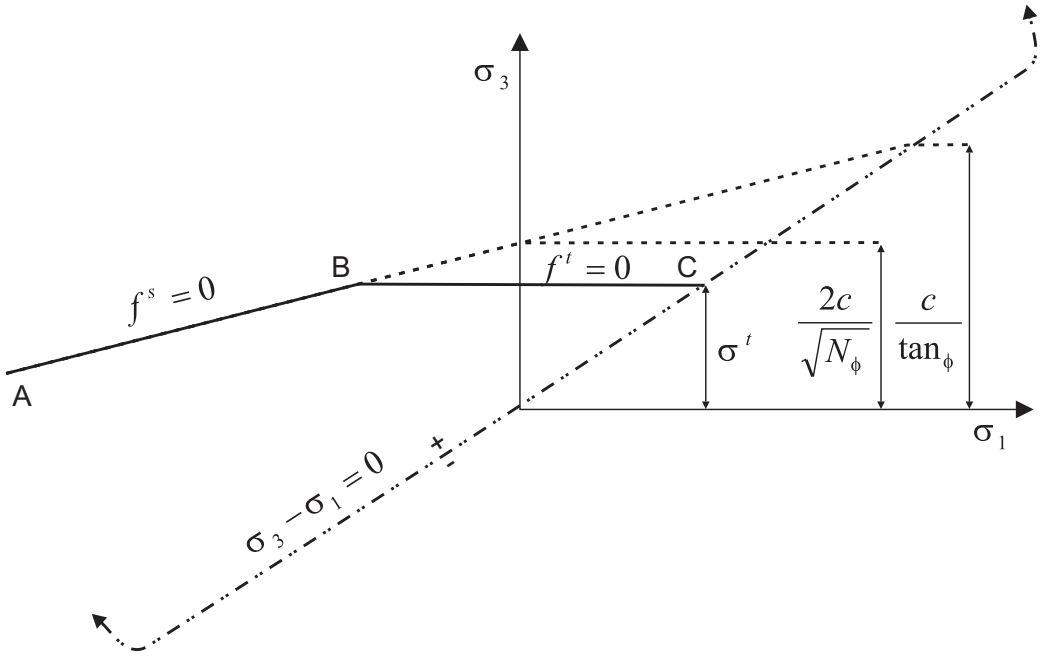

Figure 1.6 Mohr-Coulomb failure criterion

The failure envelope is defined from point A to point B by the Mohr-Coulomb yield function,

$$f^s = \sigma_1 - \sigma_3 N_\phi + 2c\sqrt{N_\phi} \tag{1.59}$$

and from B to C by a tension yield function of the form

$$f^t = \sigma^t - \sigma_3 \tag{1.60}$$

where ϕ is the friction angle, c is the cohesion, σ^t is the tensile strength and

$$N_\phi = \frac{1 + \sin\phi}{1 - \sin\phi} \tag{1.61}$$

Note that only the major and minor principal stresses are active in the shear yield formulation; the intermediate principal stress has no effect. For a material with friction, $\phi \neq 0$ and the tensile strength of the material cannot exceed the value σ^t_{max} given by

$$\sigma^t_{max} = \frac{c}{\tan \phi} \tag{1.62}$$

The shear potential function, g^s, corresponds to a nonassociated flow rule and has the form

$$g^s = \sigma_1 - \sigma_3 N_\psi \tag{1.63}$$

where ψ is the dilation angle and

$$N_\psi = \frac{1 + \sin \psi}{1 - \sin \psi} \tag{1.64}$$

The associated flow rule for tensile failure is derived from the potential function g^t, with

$$g^t = -\sigma_3 \tag{1.65}$$

The flow rules for this model are given a unique definition in the vicinity of an edge of the composite yield function in three-dimensional stress space by application of a technique (illustrated below) for the case of a shear-tension edge. A function, $h(\sigma_1, \sigma_3) = 0$, which is represented by the diagonal between the representation of $f^s = 0$ and $f^t = 0$ in the (σ_1, σ_3) plane, is defined (see Figure 1.7). This function has the form

$$h = \sigma_3 - \sigma^t + \alpha^P (\sigma_1 - \sigma^P) \tag{1.66}$$

where α^P and σ^P are constants defined as

$$\alpha^P = \sqrt{1 + N_\phi^2} + N_\phi \tag{1.67}$$

and

$$\sigma^P = \sigma^t N_\phi - 2c\sqrt{N_\phi} \tag{1.68}$$

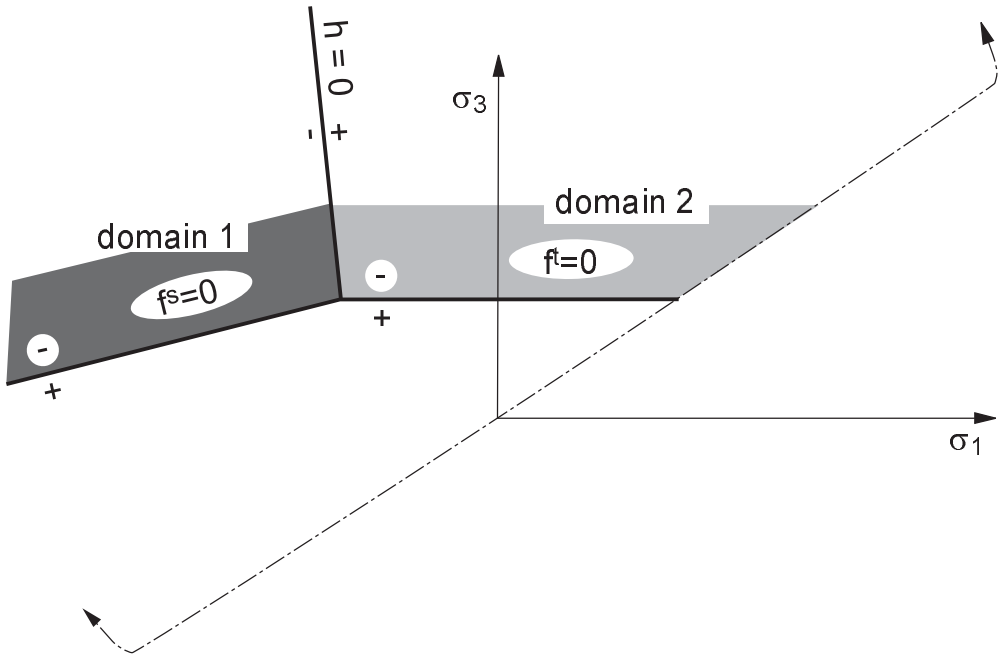

Figure 1.7 Mohr-Coulomb model: domains used in the definition of the flow rule

An elastic guess violating the failure criterion is represented by a point in the (σ_1, σ_3) plane, located either in domain 1 or 2, corresponding to negative or positive domains of $h = 0$, respectively. If in domain 1, shear failure is declared, and the stress point is brought back to the curve $f^s = 0$ using a flow rule derived using the potential function g^s. If in domain 2, tensile failure takes place, and the stress point is brought back to $f^t = 0$ using a flow rule derived using g^t.

Note that, by ordering the stresses as in Eq. (1.56), the case of a shear-shear edge is automatically handled by a variation on this technique. The technique, applicable for small-strain increments, is simple to implement: at each step, only one flow rule and corresponding stress correction is involved in the calculation of plastic flow. In particular, when a stress point follows an edge, it receives stress corrections alternating between two criteria. In this process, the two yield criteria are fulfilled to an accuracy that depends on the magnitude of the strain increment. As a validation of this approach, results obtained for the oedometric test are presented in Section 1.6.2.5.

1.6.2.3 Plastic Corrections

First consider shear failure. The flow rule has the form

$$\Delta e_i^p = \lambda^s \frac{\partial g^s}{\partial \sigma_i} \qquad i = 1, 3 \tag{1.69}$$

where λ^s is a parameter of magnitude as yet unknown. Using Eq. (1.63) for g^s, these equations become, after partial differentiation,

$$\begin{aligned} \Delta e_1^p &= \lambda^s \\ \Delta e_2^p &= 0 \\ \Delta e_3^p &= -\lambda^s N_\psi \end{aligned} \tag{1.70}$$

The elastic strain increments may be expressed from Eq. (1.57) as total increments minus plastic increments. In further using the flow rule above (Eq. (1.70)), the elastic laws in Eq. (1.58) become

$$\begin{aligned} \Delta\sigma_1 &= \alpha_1 \Delta e_1 + \alpha_2(\Delta e_2 + \Delta e_3) - \lambda^s(\alpha_1 - \alpha_2 N_\psi) \\ \Delta\sigma_2 &= \alpha_1 \Delta e_2 + \alpha_2(\Delta e_1 + \Delta e_3) - \lambda^s \alpha_2(1 - N_\psi) \\ \Delta\sigma_3 &= \alpha_1 \Delta e_3 + \alpha_2(\Delta e_1 + \Delta e_2) - \lambda^s(-\alpha_1 N_\psi + \alpha_2) \end{aligned} \tag{1.71}$$

Let the new and old stress states be referred to by the superscripts ^{N} and ^{O}, respectively. Then, by definition,

$$\sigma_i^N = \sigma_i^O + \Delta\sigma_i \qquad i = 1, 3 \tag{1.72}$$

Substituting Eq. (1.71) for $\Delta\sigma_i$, $i = 1, 3$ in these equations, we may write

$$\begin{aligned} \sigma_1^N &= \sigma_1^I - \lambda^s(\alpha_1 - \alpha_2 N_\psi) \\ \sigma_2^N &= \sigma_2^I - \lambda^s \alpha_2(1 - N_\psi) \\ \sigma_3^N &= \sigma_3^I - \lambda^s(-\alpha_1 N_\psi + \alpha_2) \end{aligned} \tag{1.73}$$

where the superscript ^{I} is used to represent the elastic guess, obtained by adding to the old stresses elastic increments computed using the total strain increments – i.e.,

$$\begin{aligned}\sigma_1^I &= \sigma_1^O + \alpha_1 \Delta e_1 + \alpha_2(\Delta e_2 + \Delta e_3)\\ \sigma_2^I &= \sigma_2^O + \alpha_1 \Delta e_2 + \alpha_2(\Delta e_1 + \Delta e_3)\\ \sigma_3^I &= \sigma_3^O + \alpha_1 \Delta e_3 + \alpha_2(\Delta e_1 + \Delta e_2)\end{aligned} \tag{1.74}$$

The parameter λ^s may now be defined by requiring that the new stress point be located on the shear yield surface. Substitution of σ_1^N and σ_3^N for σ_1 and σ_3 in $f^s = 0$ gives, after some manipulations (see Eqs. (1.59) and (1.73)),

$$\lambda^s = \frac{f^s(\sigma_1^I, \sigma_3^I)}{(\alpha_1 - \alpha_2 N_\psi) - (\alpha_2 - \alpha_1 N_\psi) N_\phi} \tag{1.75}$$

In the case of tensile failure, the flow rule has the form

$$\Delta e_i^p = \lambda^t \frac{\partial g^t}{\partial \sigma_i} \qquad i = 1, 3 \tag{1.76}$$

where the magnitude of the parameter λ^t is not yet defined. Using Eq. (1.65) for g^t, this expression gives, after partial differentiation,

$$\begin{aligned}\Delta e_1^p &= 0\\ \Delta e_2^p &= 0\\ \Delta e_3^p &= -\lambda^t\end{aligned} \tag{1.77}$$

Repeating a reasoning similar to that described above, we obtain

$$\begin{aligned}\sigma_1^N &= \sigma_1^I + \lambda^t \alpha_2\\ \sigma_2^N &= \sigma_2^I + \lambda^t \alpha_2\\ \sigma_3^N &= \sigma_3^I + \lambda^t \alpha_1\end{aligned} \tag{1.78}$$

and

$$\lambda^t = \frac{f^t(\sigma_3^I)}{\alpha_1} \tag{1.79}$$

1.6.2.4 Implementation Procedure

In the implementation of the Mohr-Coulomb model in *UDEC*, an elastic guess σ_{ij}^I is first computed, by adding to the old stress components, increments calculated by application of Hooke's law to the total strain increment for the step. Principal stresses σ_1^I, σ_2^I, σ_3^I and corresponding principal directions are calculated and ordered. If these stresses violate the composite yield criterion, a correction must be applied to the elastic guess to give the new stress state. In this situation we have that either $h(\sigma_1^I, \sigma_3^I) \leq 0$ or $h(\sigma_1^I, \sigma_3^I) > 0$ (see Eq. (1.66)). In the first case, shear failure is declared. New stresses are evaluated from Eq. (1.73) using Eq. (1.75) for λ^s. In the second case, tensile failure takes place, and new stresses are calculated from Eq. (1.78) using Eq. (1.79). The stress tensor components in the system of reference axes are then calculated from the principal values by assuming that the principal directions have not been affected by the occurrence of a plastic correction.

In *UDEC*, the default value for the tensile strength is zero. This value is set to σ_{max}^t if the value assigned to the tensile strength exceeds σ_{max}^t. If the computed value of σ_3 exceeds σ^t in a zone, the tensile strength is set to zero for that zone. This simulates instantaneous tensile softening.

The plastic strain is *not* calculated directly in this model, in order to speed the calculation. The strain-softening model can be used if plastic strains are needed and/or gradual or no tensile softening is desired.

1.6.2.5 Oedometer Test

This example concerns the determination of stresses in a Mohr-Coulomb material subjected to an oedometer test. In this experiment, two of the principal stress components are equal and, during plastic flow, the stress point evolves along an edge of the Mohr-Coulomb criterion representation in the principal stress space. The purpose is to validate the numerical technique adopted to handle such a situation. Results of a numerical experiment are presented and compared to an exact solution.

The boundary conditions for the plane-strain oedometric test are sketched in Figure 1.8. They correspond to the uniform strain rates:

$$\begin{aligned} \Delta e_x &= 0 \\ \Delta e_y &= v\Delta t/L \\ \Delta e_z &= 0 \end{aligned} \tag{1.80}$$

where x and y refer to the system of reference axes sketched in the figure, and z is out-of-plane, v is the constant y-component of the velocity applied to the sample ($v < 0$), and L is the height of the sample.

Assuming zero initial stresses, the principal directions of stresses and strains are those of the coordinate axes. For simplicity, we consider a sample of unit height $L = 1$.

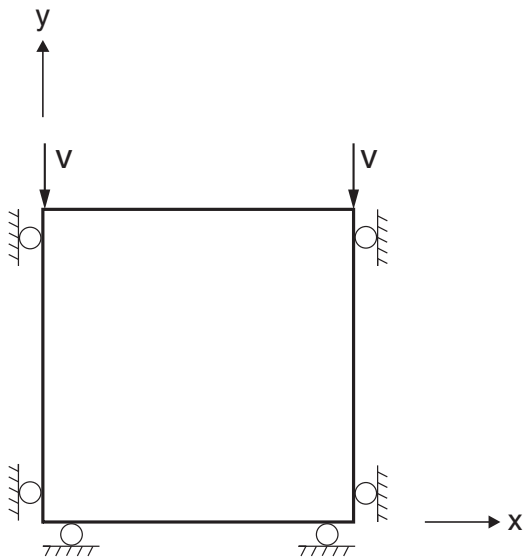

Figure 1.8 Boundary conditions for oedometer test

In the elastic range, application of Hooke's law gives, using that $e_y = vt$ at time t,

$$\begin{aligned} \sigma_x &= \alpha_2 vt \\ \sigma_y &= \alpha_1 vt \\ \sigma_z &= \sigma_x \end{aligned} \tag{1.81}$$

where $\alpha_1 = K + 4/3G$ and $\alpha_2 = K - 2/3G$.

To apply the Mohr-Coulomb failure criterion, we consider the yield functions

$$\begin{aligned} f^1 &= \sigma_y - \sigma_x N_\phi + 2c\sqrt{N_\phi} \\ f^2 &= \sigma_y - \sigma_z N_\phi + 2c\sqrt{N_\phi} \end{aligned} \tag{1.82}$$

At the onset of yield, $f^1 = f^2 = 0$ and, using Eqs. (1.81) and (1.82), we find

$$t = \frac{2c\sqrt{N_\phi}}{-v(\alpha_1 - \alpha_2 N_\phi)} \tag{1.83}$$

Hence, yielding will only take place provided $\alpha_1 - \alpha_2 N_\phi > 0$.

During plastic flow, the strain increments are composed of elastic and plastic parts, and we have

$$\begin{aligned} \Delta e_x &= \Delta e_x^e + \Delta e_x^p \\ \Delta e_y &= \Delta e_y^e + \Delta e_y^p \\ \Delta e_z &= \Delta e_z^e + \Delta e_z^p \end{aligned} \tag{1.84}$$

Using the boundary conditions Eq. (1.80), we may write

$$\begin{aligned} \Delta e_x^e &= -\Delta e_x^p \\ \Delta e_y^e &= v\Delta t - \Delta e_y^p \\ \Delta e_z^e &= -\Delta e_z^p \end{aligned} \tag{1.85}$$

The flow rule for plastic flow along the edge of the Mohr-Coulomb criterion corresponding to $\sigma_x = \sigma_z$ has the form (e.g., see Drescher 1991)

$$\begin{aligned} \Delta e_x^p &= \lambda_1 \frac{\partial g^1}{\partial \sigma_x} + \lambda_2 \frac{\partial g^2}{\partial \sigma_x} \\ \Delta e_y^p &= \lambda_1 \frac{\partial g^1}{\partial \sigma_y} + \lambda_2 \frac{\partial g^2}{\partial \sigma_y} \\ \Delta e_z^p &= \lambda_1 \frac{\partial g^1}{\partial \sigma_z} + \lambda_2 \frac{\partial g^2}{\partial \sigma_z} \end{aligned} \tag{1.86}$$

where g^1 and g^2 are the potential functions corresponding to f^1 and f^2:

$$\begin{aligned} g^1 &= \sigma_y - \sigma_x N_\psi \\ g^2 &= \sigma_y - \sigma_z N_\psi \end{aligned} \tag{1.87}$$

After partial differentiation, Eq. (1.86) becomes

$$\begin{aligned} \Delta e_x^p &= -\lambda_1 N_\psi \\ \Delta e_y^p &= \lambda_1 + \lambda_2 \\ \Delta e_z^p &= -\lambda_2 N_\psi \end{aligned} \tag{1.88}$$

In further considering that, by symmetry, $\lambda_1 = \lambda_2$, we obtain

$$\begin{aligned} \Delta e_x^p &= -\lambda_1 N_\psi \\ \Delta e_y^p &= 2\lambda_1 \\ \Delta e_z^p &= -\lambda_1 N_\psi \end{aligned} \tag{1.89}$$

The stress increments, derived from Hooke's law, are given by the relations

$$\begin{aligned} \Delta\sigma_x &= \alpha_1 \Delta e_x^e + \alpha_2 (\Delta e_y^e + \Delta e_x^e) \\ \Delta\sigma_y &= \alpha_1 \Delta e_y^e + \alpha_2 2\Delta e_x^e \\ \Delta\sigma_z &= \Delta\sigma_x \end{aligned} \tag{1.90}$$

where we have used the symmetry condition $\Delta e_x^e = \Delta e_z^e$.

Substitution of Eq. (1.85) in Eq. (1.90) yields, using Eq. (1.89),

$$\begin{aligned} \Delta\sigma_x &= \alpha_1 \lambda_1 N_\psi + \alpha_2 (v\Delta t - 2\lambda_1 + \lambda_1 N_\psi) \\ \Delta\sigma_y &= \alpha_1 (v\Delta t - 2\lambda_1) + \alpha_2 2\lambda_1 N_\psi \\ \Delta\sigma_z &= \Delta\sigma_x \end{aligned} \tag{1.91}$$

The parameter λ_1 may now be determined by expressing the condition that, during plastic flow, $\Delta f^1 = 0$. Using Eq. (1.82), this condition takes the form

$$\Delta\sigma_y - \Delta\sigma_x N_\phi = 0 \tag{1.92}$$

Substitution of Eq. (1.91) in Eq. (1.92) yields, after some manipulations, the expression

$$\lambda_1 = v\lambda\Delta t \tag{1.93}$$

where

$$\lambda = \frac{\alpha_1 - \alpha_2 N_\phi}{(\alpha_1 + \alpha_2)N_\phi N_\psi - 2\alpha_2(N_\phi + N_\psi) + 2\alpha_1} \tag{1.94}$$

The *UDEC* simulation is carried out using a single zone of unit dimensions. Several properties are used in conjunction with the Mohr-Coulomb model:

bulk modulus	200 MPa
shear modulus	200 MPa
cohesion	1 MPa
friction	10°
dilation	10° and 0°
tension	5.67 MPa

The velocity components are fixed in the x- and y-directions. A velocity of magnitude 10^{-5} m/steps is applied to the top of the model in the negative y-direction for a total of 1000 steps. The stress and displacement components in the y-direction are monitored and compared to the analytic prediction obtained from Eqs. (1.81), (1.83) and (1.91), using Eqs. (1.93) and (1.94). Two runs are carried out using the data file in Example 1.1, with values of 10° and 0° for the dilation parameter. The match is very good, as may be seen in Figures 1.9 and 1.10, where numerical and analytic solutions coincide.

Example 1.1 Oedometer test on the Mohr-Coulomb model

```
model new
;File:mohr_oed.dat
model title 'Oedometric Test - Mohr-coulomb'
;-------------------------------------------------------------------
; oedometer test
; check plastic flow along an edge of the Mohr-Coulomb criterion
;-------------------------------------------------------------------
block config
block tolerance corner-round-length 1E-2
block tolerance minimum-edge-length 2E-2
block create polygon 0 0 0 1 1 1 1 0
block zone gen quad 2.0
; fish functions to monitor results
```

```
fish define d_sigy
  c_k = bulk_mod
  c_g = shear_mod
  e1  = c_k + 4. * c_g /3.
  e2  = c_k - 2. * c_g /3.
  sf  = friction * math.degrad
  nf  = math.sin(sf)
  nf  = (1. + nf) / (1. - nf)
  sp  = dilation * math.degrad
  np  = math.sin(sp)
  np  = (1. + np) / (1. - np)
  rl  = (e1-e2*nf)/((e1+e2)*nf*np-2.*e2*(nf+np)+2.*e1)
  v_dt = -1.e-5
  vely = v_dt / block.mechanical.timestep
  dsigy = v_dt * (e1+2.*rl*(e2*np-e1))
  stepl = -2.*cohesion*math.sqrt(nf)/((e1-e2*nf)*v_dt)
end
;
fish define esigy
  whilestepping
  if global.step < stepl then
    a_sy = a_sy + e1 * v_dt
  else
    a_sy = a_sy + dsigy
  end_if
  n_sy = block.zone.stress.yy(z_pnt)
end
;
fish define z_pnt
  ib = block.head
  z_pnt = block.zone(ib)
end
@z_pnt
;
fish set @bulk_mod 200 @shear_mod 200
fish set @cohesion 1
block gridpoint apply velocity-x 0
block gridpoint apply velocity-y 0
history interval 50
block gridpoint history displacement-y 0.020967752 0.9967741
fish history @n_sy
fish history @a_sy
model save 'mohr_model.sav'
;
; Dilation 10
;
```

```
model restore 'mohr_model.sav'
model title 'Oedometric Test - Mohr-coulomb - Dilation 10'
;
fish set @friction 10 @dilation 10

block zone group 'User:Mohr - Dilation 10'
block zone cmodel assign mohr-c density 1 bulk 200 shear 200 ...
  friction 10 cohesion 1 tension 0 dilation 10 ...
  range group 'User:Mohr - Dilation 10'
block cycle 0
@d_sigy
block gridpoint apply velocity-y @vely range pos-y .9 1.1
block cycle 865
model save 'Mohr_dilation_10.sav'
;
; Dilation 0
;
model restore 'mohr_model.sav'
model title 'Oedometric Test - Mohr-coulomb - Dilation 0'
;
fish set @friction 10 @dilation 0
block zone group 'User:Mohr - Dilation 0'
block zone cmodel assign mohr-c density 1 bulk 200 shear 200 ...
  friction 10 cohesion 1 tension 0 dilation 0 ...
  range group 'User:Mohr - Dilation 0'
block cycle 0
@d_sigy
block gridpoint apply velocity-y @vely range pos-y .9 1.1
block cycle 865
model save 'Mohr_dilation_0.sav'
;
return
```

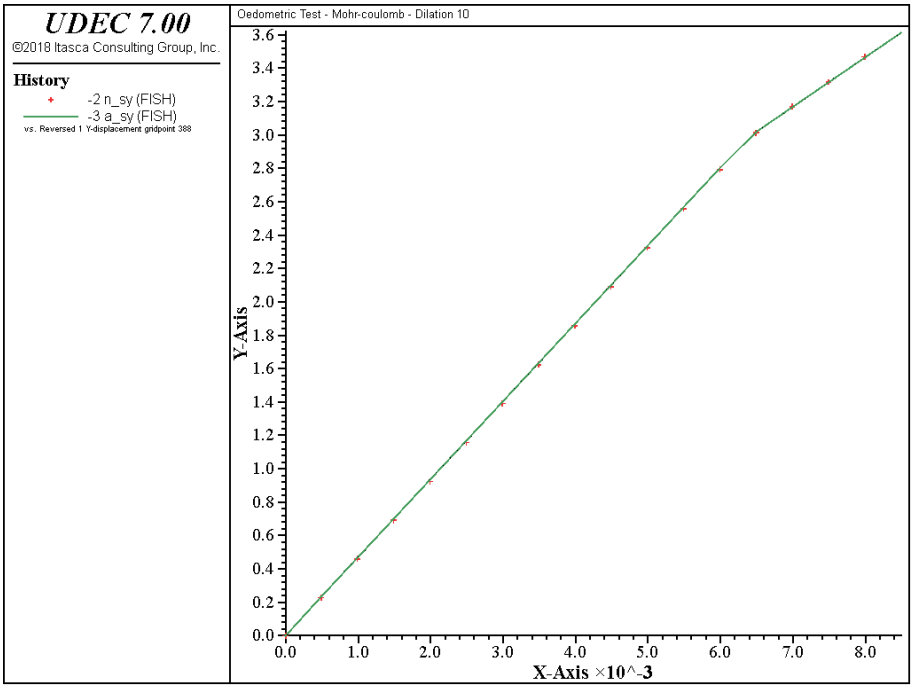

Figure 1.9 Oedometric test – comparison of numerical and analytical predictions for 10° dilation

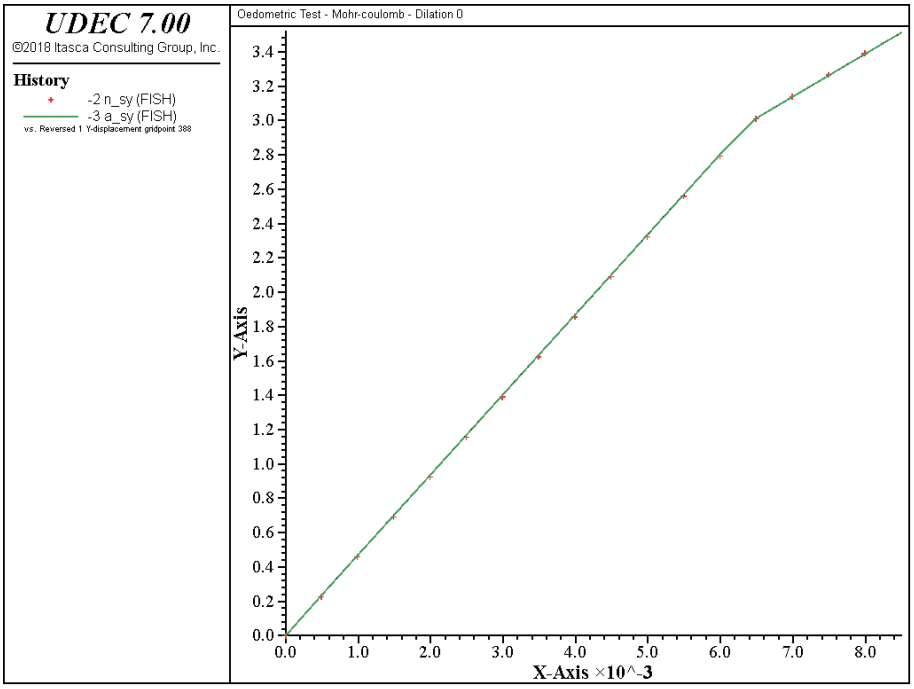

Figure 1.10 Oedometric test – comparison of numerical and analytical predictions for 0° dilation

1.6.2.6 **block zone cmodel** *Command and Property Keywords*

Mohr-Coulomb – **block zone cmodel assign mohr-coulomb**

(1)	**bu**lk	elastic bulk modulus, K
(2)	**coh**esion	cohesion, c
(3)	**dens**ity	mass density, ρ
(4)	**di**lation	dilation angle, ψ
(5)	**fl**ag-**br**ittle	tension after yield
(6)	**fri**ction	internal angle of friction, ϕ
(7)	**sh**ear	elastic shear modulus, G
(8)	**ten**sion	tension limit, σ^t

Note that the default tension limit is zero for a material with no friction, and is $c/\tan\phi$ otherwise. If tensile failure occurs in a zone, the tensile strength is set to zero for that zone.

The following property can be printed, plotted or accessed via *FISH*.

(1)	**sta**te	plastic state

1.6.3 Ubiquitous-Joint Model

In this model, which accounts for the presence of an orientation of weakness (weak plane) in a Mohr-Coulomb model, yield may occur either in the solid or along the weak plane, or both, depending on the stress state, the orientation of the weak plane, and the material properties of the solid and weak plane.

In the implementation, use is made of a technique by which general failure is first detected, and relevant plastic corrections are applied, as indicated in the Mohr-Coulomb model description. The new stresses are then analyzed for failure on the weak plane and updated accordingly. The criterion for failure on the plane is a local form of the Mohr-Coulomb yield criterion with tension cutoff. The local shear flow rule is nonassociated, and the local tension flow rule is associated. The Mohr-Coulomb model was addressed above; developments related to plastic flow on the weak plane are outlined in this section.

1.6.3.1 Weak Plane Plastic Corrections

Figure 1.11 illustrates the weak plane existing in a Mohr-Coulomb solid, and the global (xy) and local ($x'y'$) coordinate frames.

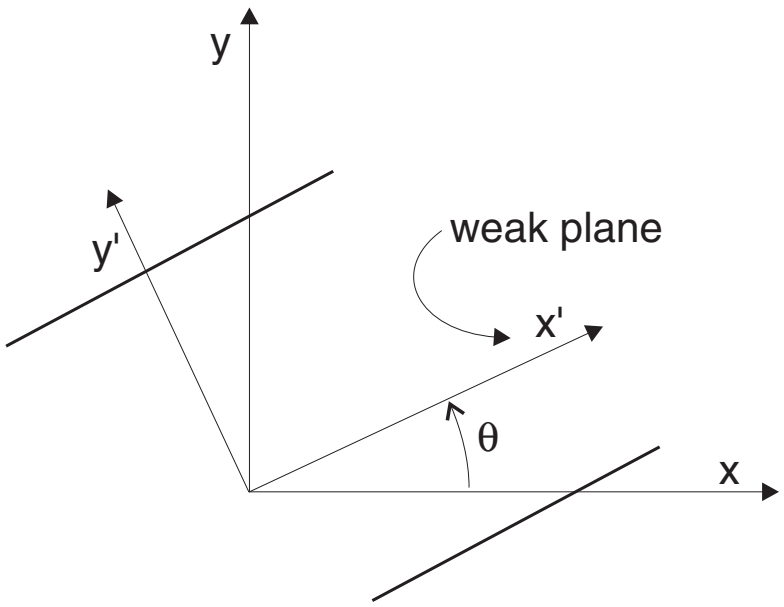

Figure 1.11 A weak plane oriented at an angle θ to the global reference frame

For simplicity, we define the global stress components by σ_{ij} (obtained after application of the plastic corrections). These global stresses are resolved into local components using the expressions

$$\begin{aligned}
\sigma'_{11} &= \sigma_{11}\ \cos^2\theta + 2\sigma_{12}\ \sin\theta\ \cos\theta + \sigma_{22}\ \sin^2\theta \\
\sigma'_{22} &= \sigma_{11}\ \sin^2\theta - 2\sigma_{12}\ \sin\theta\ \cos\theta + \sigma_{22}\ \cos^2\theta \\
\sigma'_{33} &= \sigma_{33} \\
\sigma'_{12} &= -(\sigma_{11} - \sigma_{22})\ \sin\theta\cos\theta + \sigma_{12}(\cos^2\theta - \sin^2\theta)
\end{aligned} \tag{1.95}$$

where θ is the joint angle (measured counterclockwise from the x-global axis).

By convention, let τ represent the magnitude of the tangential traction component on the weak plane, the associated strain variable is γ, and we have

$$\begin{aligned}
\tau &= |\sigma'_{12}| \\
\gamma &= |e'_{12}|
\end{aligned} \tag{1.96}$$

With this notation, the local expression of the incremental elastic laws have the form

$$\begin{aligned}
\Delta\sigma'_{11} &= \alpha_1 \Delta e'^{e}_{11} + \alpha_2(\Delta e'^{e}_{22} + \Delta e'^{e}_{33}) \\
\Delta\sigma'_{22} &= \alpha_1 \Delta e'^{e}_{22} + \alpha_2(\Delta e'^{e}_{11} + \Delta e'^{e}_{33}) \\
\Delta\sigma'_{33} &= \alpha_1 \Delta e'^{e}_{33} + \alpha_2(\Delta e'^{e}_{11} + \Delta e'^{e}_{22}) \\
\Delta\tau &= 2G\Delta\gamma^e
\end{aligned} \tag{1.97}$$

where $\alpha_1 = K + 4G/3$, $\alpha_2 = K - 2G/3$, and the superscript ^{e} stands for "elastic part."

The weak-plane failure criterion may be represented in the (σ'_{22}, τ) plane, as illustrated in Figure 1.12.

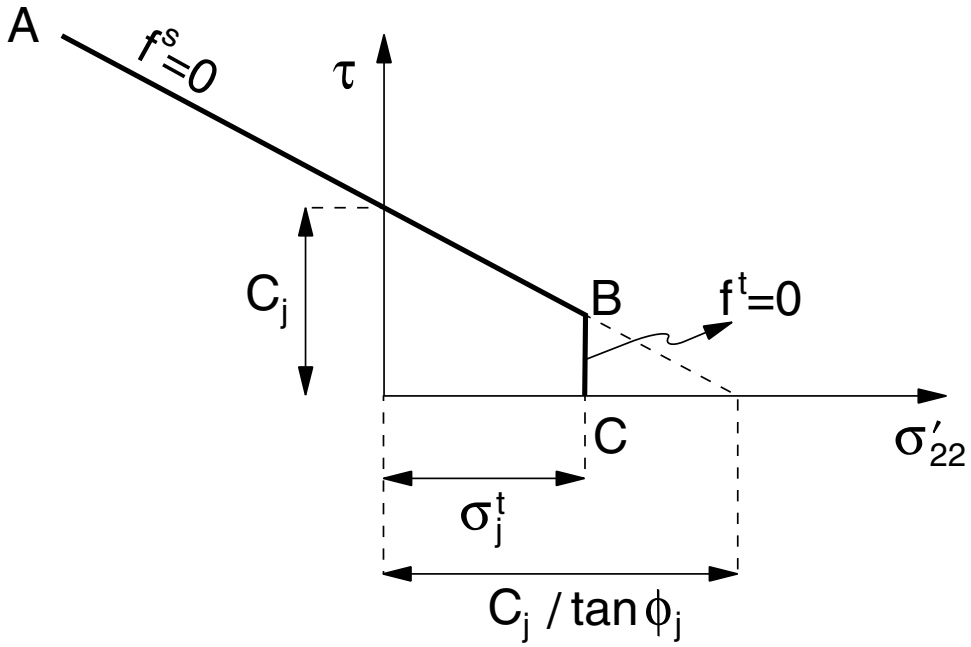

Figure 1.12 Weak-plane failure criterion

The local failure envelope is defined from point A to B by a Mohr-Coulomb failure criterion defined as $f^s = 0$, with

$$f^s = -\tau - \sigma'_{22} \tan \phi_j + c_j \tag{1.98}$$

and from B to C by a tension failure criterion of the form $f^t = 0$, with

$$f^t = \sigma_j^t - \sigma'_{22} \tag{1.99}$$

where ϕ_j, c_j and σ_j^t are the friction, cohesion and tensile strength of the weak plane, respectively. Note that, for a weak plane with a nonzero friction angle, the maximum value of the tensile strength is given by

$$\sigma_{j,max}^t = \frac{c_j}{\tan \phi_j} \tag{1.100}$$

The shear and tensile potential functions g^s and g^t correspond to a nonassociated flow rule with dilatancy, ψ_j, and an associated flow rule, respectively. They have the form

$$g^s = -\tau - \sigma'_{22} \tan \psi_j \tag{1.101}$$

and

$$g^t = -\sigma'_{22} \tag{1.102}$$

The flow rule is given a unique definition in the vicinity of the failure criterion edge by application of a technique already described in the context of the Mohr-Coulomb model. Here, a function, $h(\sigma'_{22}, \tau) = 0$, which may be represented by the diagonal between the representation of $f^s = 0$ and $f^t = 0$ in the (σ'_{22}, τ) plane, is used (see Figure 1.13). This function has the form

$$h = \tau - \tau_j^P - \alpha_j^P (\sigma'_{22} - \sigma_j^t) \tag{1.103}$$

where τ_j^P and α_j^P are constants defined as

$$\begin{aligned} \tau_j^P &= c_j - \tan \phi_j \sigma_j^t \\ \alpha_j^P &= \sqrt{1 + \tan \phi_j^2} - \tan \phi_j \end{aligned} \tag{1.104}$$

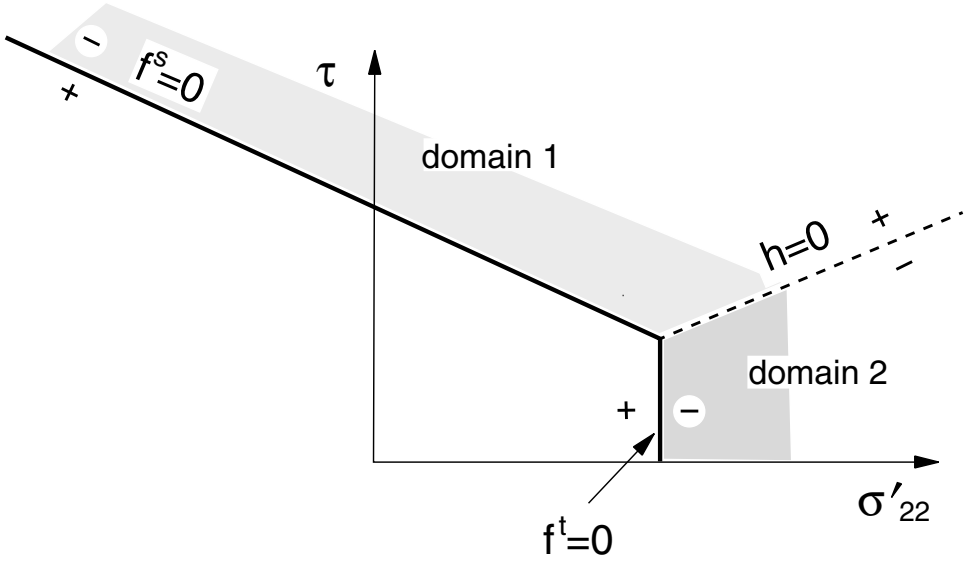

Figure 1.13 Ubiquitous-joint model: domains used in the definition of the weak-plane flow rule

A stress state violating the local failure criterion is represented by a point in the (σ'_{22}, τ) plane, located either in domain 1 or 2, corresponding to positive or negative domain of $h = 0$, respectively. If in domain 1, shear failure is declared on the plane, and the stress point is brought back to the curve $f^s = 0$ using a flow rule derived using the potential function g^s. If in domain 2, local tensile failure takes place, and the stress point is brought back to $f^t = 0$ using a flow rule derived using g^t.

First consider shear failure on the plane; the flow rule has the form

$$\begin{aligned} \Delta e'^{p}_{11} &= \lambda^s \frac{\partial g^s}{\partial \sigma'_{11}} \\ \Delta e'^{p}_{22} &= \lambda^s \frac{\partial g^s}{\partial \sigma'_{22}} \\ \Delta e'^{p}_{33} &= \lambda^s \frac{\partial g^s}{\partial \sigma'_{33}} \\ \Delta \gamma^p &= \lambda^s \frac{\partial g^s}{\partial \tau} \end{aligned} \tag{1.105}$$

where the superscript ^{p} refers to plastic parts associated with failure on the weak plane, and the magnitude of λ^s is as yet unknown. Using Eq. (1.101) for g^s, these equations become, after partial differentiation,

$$\begin{aligned} \Delta e'^{p}_{11} &= 0 \\ \Delta e'^{p}_{22} &= -\lambda^s \tan \psi_j \\ \Delta e'^{p}_{33} &= 0 \\ \Delta \gamma^p &= -\lambda^s \end{aligned} \tag{1.106}$$

The elastic strain increments in the elastic relations Eq. (1.97) are expressed as differences between total and plastic strain increments for the step. Assuming that the plastic contributions of general and local failure are additive, we follow a reasoning similar to that used in the derivation of the stress corrections for the Mohr-Coulomb criterion, in which we interpret the elastic guesses there as the stresses here, obtained after application of the plastic corrections relating to general failure. (This technique is approximate only when failure occurs both in the matrix and on the weak plane.) Using this approach, it may be shown that the new stress state may be expressed as

$$\begin{aligned} \sigma'^{N}_{11} &= \sigma'_{11} + \alpha_2 \tan \psi_j \lambda^s \\ \sigma'^{N}_{22} &= \sigma'_{22} + \alpha_1 \tan \psi_j \lambda^s \\ \sigma'^{N}_{33} &= \sigma'_{33} + \alpha_2 \tan \psi_j \lambda^s \\ \tau^N &= \tau + 2G\lambda^s \end{aligned} \tag{1.107}$$

where G is the shear modulus, and λ^s is given by

$$\lambda^s = \frac{f^s(\sigma'_{22}, \tau)}{2G + \alpha_1 \tan\phi_j \tan\psi_j} \tag{1.108}$$

The new shear stress on the weak plane may be derived from τ^N and τ, using the relation

$$\sigma'^N_{12} = \sigma'_{12}\frac{\tau^N}{\tau} \tag{1.109}$$

The local stress corrections have the form

$$\begin{aligned}
\Delta\sigma'_{11} &= \alpha_2 \tan\psi_j \lambda^s \\
\Delta\sigma'_{22} &= \alpha_1 \tan\psi_j \lambda^s \\
\Delta\sigma'_{33} &= \alpha_2 \tan\psi_j \lambda^s \\
\Delta\sigma'_{12} &= \sigma'_{12}\frac{\tau^N - \tau}{\tau}
\end{aligned} \tag{1.110}$$

where λ^s is given by Eq. (1.108).

Finally, the global stress corrections for shear failure on the plane, obtained by resolution of the local stress corrections into the global axes, may be expressed as

$$\begin{aligned}
\Delta\sigma_{11} &= -2\Delta\sigma'_{12}\,(\cos\theta\ \ \sin\theta) + \Delta\sigma'_{11}\cos^2\theta + \Delta\sigma'_{22}\sin^2\theta \\
\Delta\sigma_{22} &= 2\Delta\sigma'_{12}\,(\cos\theta\ \ \sin\theta) + \Delta\sigma'_{11}\sin^2\theta + \Delta\sigma'_{22}\cos^2\theta \\
\Delta\sigma_{33} &= \Delta\sigma'_{33} \\
\Delta\sigma_{12} &= \Delta\sigma'_{12}\,(\cos^2\theta\ \ -\sin^2\theta) + (\Delta\sigma'_{11} - \Delta\sigma'_{22})\sin\theta\cos\theta
\end{aligned} \tag{1.111}$$

These corrections are added to the stress components σ_{ij}, which include the stress corrections for general failure, if any, to provide the new stress state for the step.

We now consider tensile failure on the plane. In this case, the flow rule has the form

$$\begin{aligned} \Delta e'^{p}_{11} &= \lambda^t \frac{\partial g^t}{\partial \sigma'_{11}} \\ \Delta e'^{p}_{22} &= \lambda^t \frac{\partial g^t}{\partial \sigma'_{22}} \\ \Delta e'^{p}_{33} &= \lambda^t \frac{\partial g^t}{\partial \sigma'_{33}} \\ \Delta \gamma^p &= \lambda^t \frac{\partial g^t}{\partial \tau} \end{aligned} \tag{1.112}$$

where λ^t is a parameter of magnitude as yet unknown. Using Eq. (1.102) for g^t, these equations become, after partial differentiation,

$$\begin{aligned} \Delta e'^{p}_{11} &= 0 \\ \Delta e'^{p}_{22} &= -\lambda^t \\ \Delta e'^{p}_{33} &= 0 \\ \Delta \gamma^p &= 0 \end{aligned} \tag{1.113}$$

Using the same reasoning as described above, we obtain

$$\begin{aligned} \sigma'^{N}_{11} &= \sigma'_{11} + \lambda^t \alpha_2 \\ \sigma'^{N}_{22} &= \sigma'_{22} + \lambda^t \alpha_1 \\ \sigma'^{N}_{33} &= \sigma'_{33} + \lambda^t \alpha_2 \\ \tau^N &= \tau \end{aligned} \tag{1.114}$$

and

$$\lambda^t = \frac{f^t(\sigma'_{22})}{\alpha_1} \tag{1.115}$$

The local stress corrections for tensile failure on the weak plane may be expressed, after substitution of Eq. (1.115) for λ^t in Eq. (1.114), as

$$\begin{aligned} \Delta\sigma'_{11} &= (\sigma^t - \sigma'_{22})\frac{\alpha_2}{\alpha_1} \\ \Delta\sigma'_{22} &= (\sigma^t - \sigma'_{22}) \\ \Delta\sigma'_{33} &= (\sigma^t - \sigma'_{22})\frac{\alpha_2}{\alpha_1} \end{aligned} \tag{1.116}$$

where use has been made of Eq. (1.99) for f^t.

After resolution into global axes, the stress corrections become

$$\begin{aligned} \Delta\sigma_{11} &= (\sigma^t - \sigma'_{22})\left(\frac{\alpha_2}{\alpha_1}\cos^2\theta + \sin^2\theta\right) \\ \Delta\sigma_{22} &= (\sigma^t - \sigma'_{22})\left(\frac{\alpha_2}{\alpha_1}\sin^2\theta + \cos^2\theta\right) \\ \Delta\sigma_{33} &= (\sigma^t - \sigma'_{22})\frac{\alpha_2}{\alpha_1} \\ \Delta\sigma_{12} &= -(\sigma^t - \sigma'_{22})(1 - \frac{\alpha_2}{\alpha_1})\sin\theta\cos\theta \end{aligned} \tag{1.117}$$

In large-strain mode, the orientation θ of the weak plane is adjusted to account for rigid body rotations, and rotations due to deformations. The correction $\Delta\theta$, evaluated as average over all triangles in a zone, has the form

$$\Delta\theta = e'_{12} + \omega \tag{1.118}$$

where

$$\begin{aligned} e'_{12} &= -(e_{11} - e_{22})\sin\theta\cos\theta + e_{12}(\cos^2\theta - \sin^2\theta) \\ \omega &= \frac{1}{2}(\dot{u}_{1,2} - \dot{u}_{2,1}) \end{aligned} \tag{1.119}$$

and $\Delta\theta$ is expressed in radians.

1.6.3.2 Implementation Procedure

In the implementation of the ubiquitous-joint model, stresses corresponding to the elastic guess for the step are first analyzed for general failure, and relevant plastic corrections are made, as described in the Mohr-Coulomb model. The resulting stress components (labeled σ_{ij} in this section) are then examined for failure on the weak plane.

The corresponding local stress components σ'_{22} and τ are calculated using Eqs. (1.95) and (1.96). If these stresses violate the weak-plane composite yield criterion (see Eqs. (1.98) and (1.99)), corrections must be applied to the components σ_{ij} to give the new stress state for the step. In this situation we have that either $h(\sigma'_{22}, \tau) > 0$ or $h(\sigma'_{22}, \tau) \leq 0$ (see Eqs. (1.103) and (1.104)). In the first case, shear failure takes place on the weak plane. New stresses are evaluated by adding the corrections Eq. (1.111) to σ_{ij}. In the second case, weak-plane tensile failure is declared, and new stresses are calculated using the corrections Eq. (1.117).

In large-strain mode, the orientation of the weak plane is adjusted to account for body rotations (see Eqs. (1.118) and (1.119)).

The default value for the weak-plane tensile strength is zero if $\phi_j = 0$, and $\sigma^t_{j,max}$ otherwise (see Eq. (1.100)). This last value is also retained in the code if the value assigned for the weak-plane tensile strength exceeds $\sigma^t_{j,max}$. If the computed value of σ'_{22} exceeds $\sigma^t_{j,max}$ in a zone, then the tensile strength is set to zero for that zone. This simulates instantaneous softening.

1.6.3.3 **block zone cmodel** *Command and Property Keywords*

Ubiquitous-Joint – **block zone cmodel assign ubiquitous-joint**

(1)	**bu**lk	elastic bulk modulus, K
(2)	**coh**esion	cohesion of matrix, c
(3)	**dens**ity	mass density, ρ
(4)	**di**lation	dilation angle of matrix, ψ
(5)	**fri**ction	internal angle of friction of matrix, ϕ
(6)	**ja**ngle	joint angle taken counterclockwise from the x-axis, θ
(7)	**jo**int-**co**hesion	joint cohesion, c_j
(8)	**jo**int-**di**lation	joint dilation angle, ψ_j
(9)	**jo**int-**fri**ction	joint friction angle, ϕ_j
(10)	**jo**int-**ten**sion	joint tension limit, σ_j^t
(11)	**sh**ear	elastic shear modulus, G
(12)	**ten**sion	tension limit of matrix, σ^t

Note that the default tension limit of the matrix, σ^t, is the same as that for the Mohr-Coulomb model. The default joint tension limit, σ_j^t, is zero if $\phi_j = 0$, and is $c_j / tan\phi_j$ otherwise. If tension failure occurs on the joint, then the joint tensile strength is set to zero.

The following property can be printed, plotted or accessed via *FISH*.

(1)	**sta**te	plastic state

1.6.4 Strain-Hardening/Softening Model

This model is based on the *UDEC* Mohr-Coulomb model with nonassociated shear and associated tension flow rules, as described earlier. The difference, however, lies in the possibility that the cohesion, friction, dilation and tensile strength may harden or soften after the onset of plastic yield. In the Mohr-Coulomb model, those properties are assumed to remain constant. Here, the user can define the cohesion, friction and dilation as piecewise-linear functions of a hardening parameter measuring the plastic shear strain. A piecewise-linear softening law for the tensile strength can also be prescribed in terms of another hardening parameter measuring the plastic tensile strain. The code measures the total plastic shear and tensile strains by incrementing the hardening parameters at each timestep, and causes the model properties to conform to the user-defined functions.

The yield and potential functions, plastic flow rules and stress corrections are identical to those of the Mohr-Coulomb model, as discussed in Section 1.6.2.

1.6.4.1 Hardening/Softening Parameters

Plastic shear strain is measured by the shear hardening parameter e^{ps}, whose incremental form is defined as (see Equation 6.4 in Vermeer and deBorst 1984)

$$\Delta e^{ps} = \left\{ \frac{1}{2}\left(\Delta e_1^{ps} - \Delta e_m^{ps}\right)^2 + \frac{1}{2}\left(\Delta e_m^{ps}\right)^2 + \frac{1}{2}\left(\Delta e_3^{ps} - \Delta e_m^{ps}\right)^2 \right\}^{\frac{1}{2}} \tag{1.120}$$

where

$$\Delta e_m^{ps} = \frac{1}{3}\left(\Delta e_1^{ps} + \Delta e_3^{ps}\right)$$

and Δe_j^{ps}, $j = 1, 3$ are the principal plastic shear strain increments.

The tensile hardening parameter e^{pt} measures the accumulated tensile plastic strain; its increment is defined as

$$\Delta e^{pt} = \Delta e_3^{pt} \tag{1.121}$$

where Δe_3^{pt} is the increment of tensile plastic strain in the direction of the major principal stress (recall that tensile stresses are positive).

The notation used above (and in similar expressions to be presented later) needs some clarification. The term Δe_i^{ps} is identical to Δe_i^{p} (defined previously in Eq. (1.70)), where $i = 1, 2, 3$. The added superscript ^{s} denotes that the plastic strain is related to the *shear* yield surface (rather than the tensile yield surface). Note that Δe_i^{ps} are plastic principal strain increments, not shear strain increments.

Similarly, Δe_3^{pt} is identical to Δe_3^{p}, defined in Eq. (1.77); here, the superscript ^{t} denotes that the plastic strain is related to the tensile yield surface.

The following example demonstrates the relation between the incremental hardening parameter and the axial strain increment for an unconfined compression test of an axisymmetric sample of frictionless material. The results show that the average value for the plastic strain increment is equal to the axial strain increment.

Example 1.2 Relation between incremental hardening parameter and axial strain increment for an axial compression test

```
model new
;file: ss_1.dat
block config axisymmetry
block  smallstrain
block tolerance corner-round-length 0.01
block tolerance minimum-edge-length 0.02
block create polygon 0 0 0 10 5 10 5 0
block zone gen edge 1.0
block zone group 'mat1'
block zone cmodel assign strain-softening density 1 bulk 1E8 shear 1E8 ...
  friction 0 cohesion 1E5 tension 1E20 range group 'mat1'
block gridpoint apply velocity-y 0 range pos-x -0.1 5.1 pos-y -0.1 0.1
block gridpoint apply velocity-y 1.728 range pos-x -0.1 5.1 pos-y 9.9 10.1
block zone history stress-yy 0.0 0.0
fish define results
  sum = 0.0
  count = 0
  iab = block.head
  loop while iab # 0
    iaz= block.zone(iab)
    loop while iaz # 0
       sum = sum + block.zone.prop(iaz,'strain-shear-plastic')
       count = count + 1
       iaz = block.zone.next(iaz)
    endloop
    iab=block.next(iab)
  endloop
  av_ep    = sum / count
  igp = block.gp.near(0, 10)
  ax_e_inc = block.gp.disp.y(igp)/block.gp.pos.y(igp)
  ii = io.out(' Average plastic strain increment = '+ ...
    string(av_ep,10,' ',4,'E'))
  ii = io.out(' Axial strain increment           = '+ ...
    string(ax_e_inc,10,' ',4,'E'))
end
```

```
block cycle 1500
block zone property strain-shear-plastic 0
block gridpoint initialize displacement-x 0.0
block gridpoint initialize displacement-y 0.0
block cycle 40
@results
```

1.6.4.2 User-Defined Functions for Cohesion, Friction, Dilation and Tensile Strength

Consider a one-dimensional stress-strain curve $\sigma - e$, which softens upon yield and attains some residual strength:

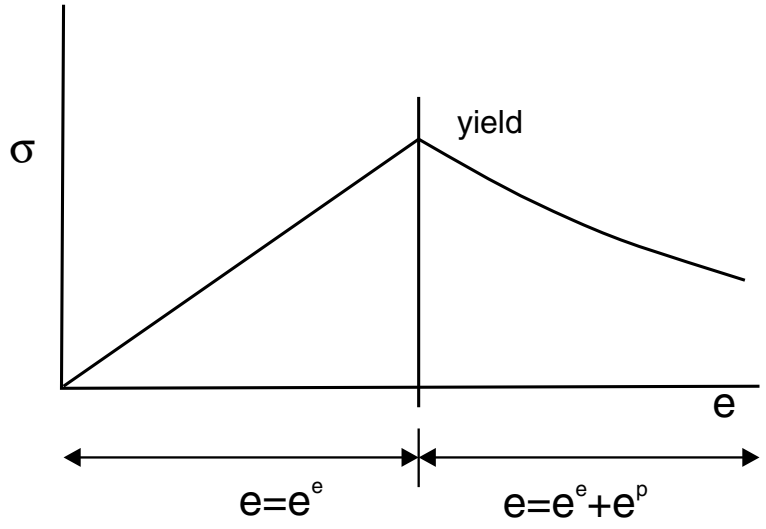

Figure 1.14 Example stress-strain curve

The curve is linear to the point of yield; in that range, the strain is elastic only (i.e., $e = e^e$). After yield, the total strain is composed of elastic and plastic parts (i.e., $e = e^e + e^p$). In the softening/hardening model, the user defines the cohesion, friction, dilation and tensile strength variance as functions of the plastic portion, e^p, of the total strain. Examples of these functions are sketched in Figure 1.15, and may be approximated in *UDEC* as sets of linear segments (see Figure 1.16).

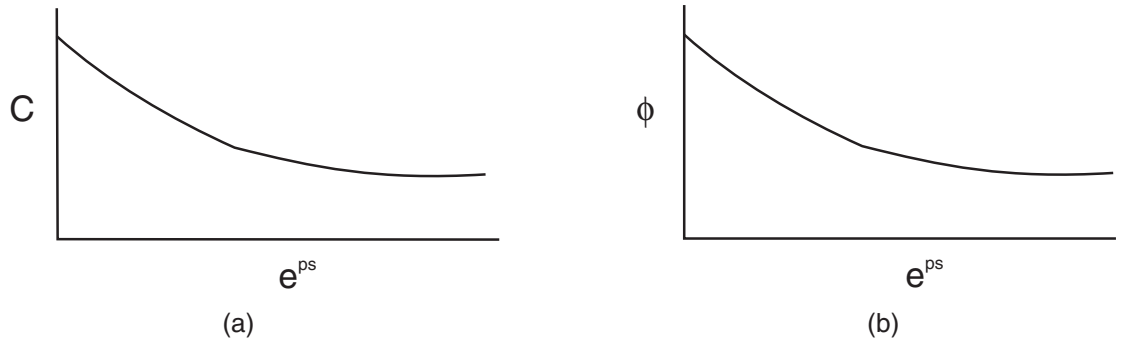

Figure 1.15 Variation of cohesion (a) and friction angle (b) with plastic strain

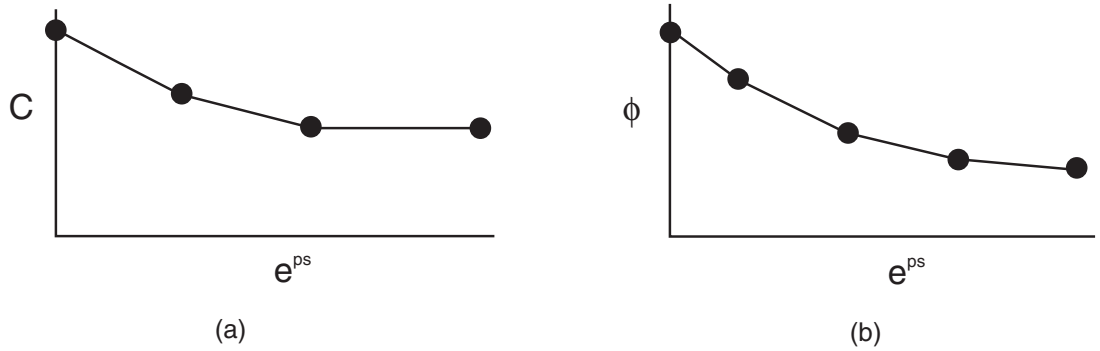

Figure 1.16 Approximation by linear segments

Hardening and softening behaviors for the cohesion, friction and dilation in terms of the shear parameter e^{ps} (see Eq. (1.120)) are provided by the user in the form of tables. Each table contains pairs of values: one for the parameter, and one for the corresponding property value. It is assumed that the property varies linearly between two consecutive parameter entries in the table. Softening of the tensile strength is described in a similar manner using the parameter e^{pt} (see Eq. (1.121)).

For example, the input in Example 1.3 illustrates a piecewise-linear definition of softening properties.

Example 1.3 Piecewise linear definition of softening properties

```
;file: ss_2.dat
block zone cmodel assign strain-softening density 2E3 bulk 8.62E9 ...
  shear 1.15E10 friction 40 cohesion 2E7 tension 1.5E7 dilation 10 ...
  table-friction 1 table-coh 2 table-tension 4 table-dilation 3 ...
  range group 'mat1'
table 1 add 0,40   .01,30
table 2 add 0,20e6 .01,10e6
table 3 add 0,10   .01,5
table 4 add 0,15e6 .01,0.0
```

Here, the friction function is defined in table 1, the cohesion in table 2, the dilation in table 3 and the tensile strength in table 4. Note that the initial friction, cohesion, dilation and tensile strength must be defined (here, as 40°, 20 MPa, 10° and 15 MPa, respectively). The functions each consist of two linear segments, as shown in Figure 1.17. The values remain constant for plastic strains greater than the last table value.

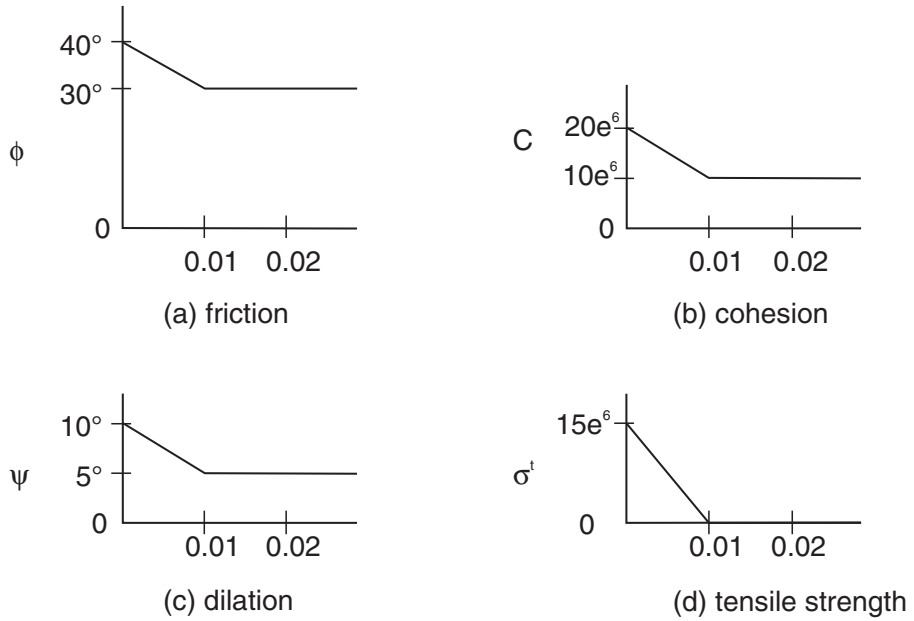

Figure 1.17 Friction (a), cohesion (b), dilation (c) and tensile strength (d) defined by two linear segments

Hardening behavior for the cohesion, friction and dilation can be produced by an increase in these properties with increasing plastic strain measure.

1.6.4.3 Implementation Procedure

In the implementation of this model, new stresses for the step are computed, as described in the *UDEC* Mohr-Coulomb model description, using the current values of the model properties. Plastic shear and tensile strain increments are evaluated from Eqs. (1.70) and (1.77) using Eq. (1.75) of λ^s and Eq. (1.79) of λ^t. Hardening increments are calculated as the surface average of values obtained from Eqs. (1.120) and (1.121) for all triangles involved in the zone. The hardening parameters are updated, and new model properties are evaluated by linear interpolation in the tables. These properties are stored for use in the next step. The hardening or softening lags one timestep behind the corresponding plastic deformation. In an explicit code, this error is small because the steps are small.

For a material with friction, the maximum value of the tensile strength is evaluated from Eq. (1.62) using the new cohesion and friction angle. This value is retained by the code if it is smaller than the tensile strength updated from the table.

1.6.4.4 **block zone cmodel** *Command and Property Keywords*

Strain-Hardening/Softening – **block zone cmodel assign strain-softening**

(1)	**bu**lk	elastic bulk modulus, K
(2)	**coh**esion	cohesion, c
(3)	**dens**ity	mass density, ρ
(4)	**di**lation	dilation angle, ψ
(5)	**fri**ction	angle of internal friction, ϕ
(6)	**sh**ear	elastic shear modulus, G
(7)	**ta**ble-**co**hesion	number of table relating cohesion to plastic shear strain
(8)	**ta**ble-**dil**ation	number of table relating dilation angle to plastic shear strain
(9)	**ta**ble-**fri**ction	number of table relating friction angle to plastic shear strain
(10)	**ta**ble-**ten**sion	number of table relating tension limit to plastic tensile strain
(11)	**ten**sion	tension limit, σ^t

The strain-hardening/softening behavior is controlled by the variation in friction, cohesion and dilation as a function of plastic shear strain, and tension limit as a function of plastic tensile strain, given by a specified table of values. Note that if table numbers are given as 0 (default), the properties will take the values given (i.e., with **cohesion**, **dilation**, **friction** or **tension** keyword).

The following properties can be printed, plotted or accessed via *FISH*.

(1)	**sta**te	plastic state
(2)	**stra**in-**sh**ear-**pl**astic	accumulated plastic shear strain
(3)	**stra**in-**ten**sion-**pl**astic	accumulated plastic tensile strain

1.6.5 Bilinear Strain-Hardening/Softening Ubiquitous-Joint Model

The bilinear strain-hardening/softening ubiquitous-joint model is a generalization of the ubiquitous-joint model described in Section 1.6.4. In the bilinear model, the failure envelopes for the matrix and joint are the composite of two Mohr-Coulomb criteria with a tension cutoff that can harden or soften according to specified laws. A nonassociated flow rule is used for shear-plastic flow, and an associated flow rule for tensile-plastic flow.

The softening behaviors for the matrix and the joint are specified in tables in terms of four independent hardening parameters (two for the matrix and two for the joint), which measure the amount of plastic shear and tensile strain, respectively. In this numerical model, general failure is first detected for the step, and relevant plastic corrections are applied. The new stresses are then analyzed for failure on the weak plane and updated accordingly. The hardening parameters are incremented if plastic flow has taken place, and the parameters of cohesion, friction, dilation and tensile strength are adjusted for the matrix and the joint using the tables.

1.6.5.1 Failure Criterion and Flow Rule for the Matrix

The criterion for failure in the matrix used in this model is sketched in the principal stress plane (σ_1, σ_3) in Figure 1.18. (Recall that compressive stresses are negative and, by convention, $\sigma_1 \leq \sigma_2 \leq \sigma_3$.)

The failure envelope is defined by two Mohr-Coulomb failure criteria ($f_2^s = 0$ and $f_1^s = 0$ for segments $A - B$ and $B - C$) and a tension failure criterion ($f^t = 0$ for segment $C - D$).

The shear failure criterion has the general form $f^s = 0$. Failure is characterized by a cohesion, c, and a friction angle, ϕ. For segment $A - B$, cohesion and friction angle are defined by c_2, and ϕ_2, respectively. For segment $B - C$, cohesion and friction angle are defined by c_1 and ϕ_1, respectively. The tensile failure criterion is specified by means of the tensile strength, σ^t (positive value); thus we have

$$f^s = \sigma_1 - \sigma_3 \, N_\phi + 2c\sqrt{N_\phi} \tag{1.122}$$

$$f^t = \sigma_3 - \sigma^t \tag{1.123}$$

where

$$N_\phi = \frac{1 + \sin\phi}{1 - \sin\phi} \tag{1.124}$$

The value of σ_3 corresponding to the intersection of $f_2^s = 0$ and $f_1^s = 0$ is given by

$$\sigma_3^I = \frac{2c_2\sqrt{N_{\phi_2}} - 2c_1\sqrt{N_{\phi_1}}}{N_{\phi_2} - N_{\phi_1}} \tag{1.125}$$

Note that the tensile cap acts on segment $B - C$ of the shear envelope, and for a material with nonzero friction angle ϕ_1, the maximum value of the tensile strength is given by

$$\sigma^t{}_{max} = \frac{c_1}{\tan \phi_1} \tag{1.126}$$

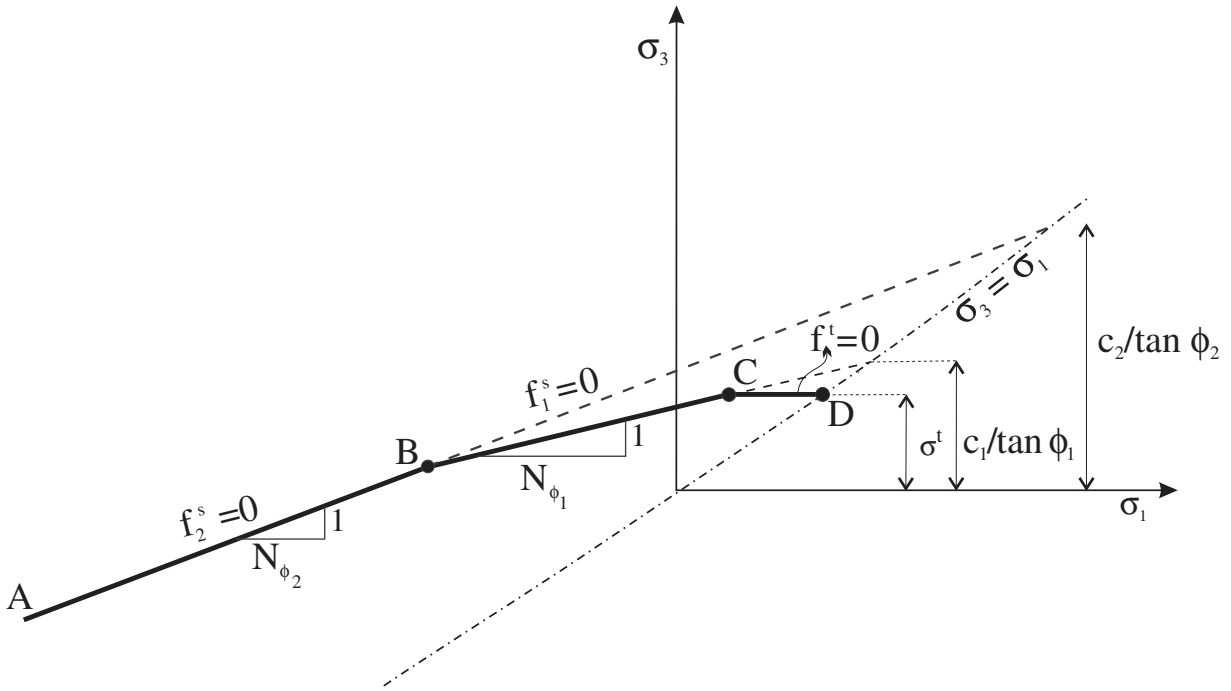

Figure 1.18 UDEC bilinear matrix failure criterion

In the model formulation, elastic guesses for the stresses are first evaluated for the step using total strain increments. Plastic yielding is detected if the corresponding stress point (σ_1^I, σ_3^I) lies outside the failure surface representation in Figure 1.18. In this case, a stress correction must be applied to the elastic guess. It is determined by allowing plastic flow to occur in order to restore the condition $f_2^s = 0$, $f_1^s = 0$ or $f^t = 0$, depending on the position of the stress point above $A - B$, $B - C$ or $C - D$. (Bisectors are used at B and C to delimit the domain of failure attached to a particular segment of the yield surface.)

The usual assumption is made: that total strain increments can be decomposed into elastic and plastic parts. The flow rule for plastic yielding has the form

$$\Delta e_i^p = \lambda \frac{\partial g}{\partial \sigma_i} \tag{1.127}$$

where $i = 1, 3$. The potential function g for shear yielding is g^s. This function corresponds to the nonassociated law,

$$g^s = \sigma_1 - \sigma_3 N_\psi \tag{1.128}$$

where ψ, the dilation angle, is equal to ψ_2 for failure along $A - B$, ψ_1 along $B - C$, and

$$N_\psi = \frac{1 + \sin \psi}{1 - \sin \psi} \tag{1.129}$$

The potential function for tensile yielding is g^t. It corresponds to the associated flow rule,

$$g^t = \sigma_3 \tag{1.130}$$

It may be shown that the plastic strain increments for shear failure have the form

$$\begin{aligned} \Delta e_1^{p_s} &= \lambda^s \\ \Delta e_2^{p_s} &= 0 \\ \Delta e_3^{p_s} &= -\lambda^s N_\psi \end{aligned} \tag{1.131}$$

The stress corrections for shear failure are

$$\begin{aligned} \Delta \sigma_1 &= -\lambda^s (\alpha_1 - \alpha_2 N_\psi) \\ \Delta \sigma_2 &= -\lambda^s \alpha_2 (1 - N_\psi) \\ \Delta \sigma_3 &= -\lambda^s (-\alpha_1 N_\psi + \alpha_2) \end{aligned} \tag{1.132}$$

where

$$\lambda^s = \frac{\sigma_1^I - \sigma_3^I \, N_\phi + 2c\sqrt{N_\phi}}{(\alpha_1 - \alpha_2 \, N_\psi) - (-\alpha_1 \, N_\psi + \alpha_2) \, N_\phi} \tag{1.133}$$

and, by definition,

$$\begin{aligned} \alpha_1 &= K + \frac{4}{3} \, G \\ \alpha_2 &= K - \frac{2}{3} \, G \end{aligned} \tag{1.134}$$

In turn, the plastic strain increments for tensile failure have the form

$$\begin{aligned} \Delta e_1^{p_t} &= 0 \\ \Delta e_2^{p_t} &= 0 \\ \Delta e_3^{p_t} &= \lambda^t \end{aligned} \tag{1.135}$$

The stress corrections for tensile failure are

$$\begin{aligned} \Delta\sigma_1 &= -\lambda^t \alpha_2 \\ \Delta\sigma_2 &= -\lambda^t \alpha_2 \\ \Delta\sigma_3 &= -\lambda^t \alpha_1 \end{aligned} \tag{1.136}$$

where

$$\lambda^t = \frac{\sigma_3^I - \sigma^t}{\alpha_1} \tag{1.137}$$

1.6.5.2 Failure Criterion and Flow Rule for the Weak Plane

The stresses, corrected for plastic flow in the matrix, are resolved into components parallel and perpendicular to the weak plane, and tested for ubiquitous-joint failure. The failure criterion is expressed in terms of the magnitude of the tangential traction component, $\tau = |\sigma'_{12}|$, and the normal traction component, σ'_{22}, on the weak plane.

The failure criterion is represented in Figure 1.19 and corresponds to two Mohr-Coulomb failure criteria ($f_2^s = 0$ for segment $A - B$; $f_1^s = 0$ for segment $B - C$) and a tension failure criterion ($f^t = 0$, for segment $C - D$). Each shear criterion has the general form $f^s = 0$, and is characterized by a cohesion and a friction angle c_j, ϕ_j, equal to c_{j_2}, ϕ_{j_2} along segment $A - B$ and c_{j_1}, ϕ_{j_1} along $B - C$. The tensile criterion is specified by means of the tensile strength, σ_j^t (positive value). Thus we have

$$f^s = \tau + \sigma'_{22} \tan\phi_j - c_j \tag{1.138}$$

$$f^t = \sigma'_{22} - \sigma_j^t \tag{1.139}$$

Note that for a weak plane with nonzero friction angle ϕ_{j_1}, the maximum value of the tensile strength is given by

$$\sigma_{j\,max}^t = \frac{c_{j_1}}{\tan\phi_{j_1}} \tag{1.140}$$

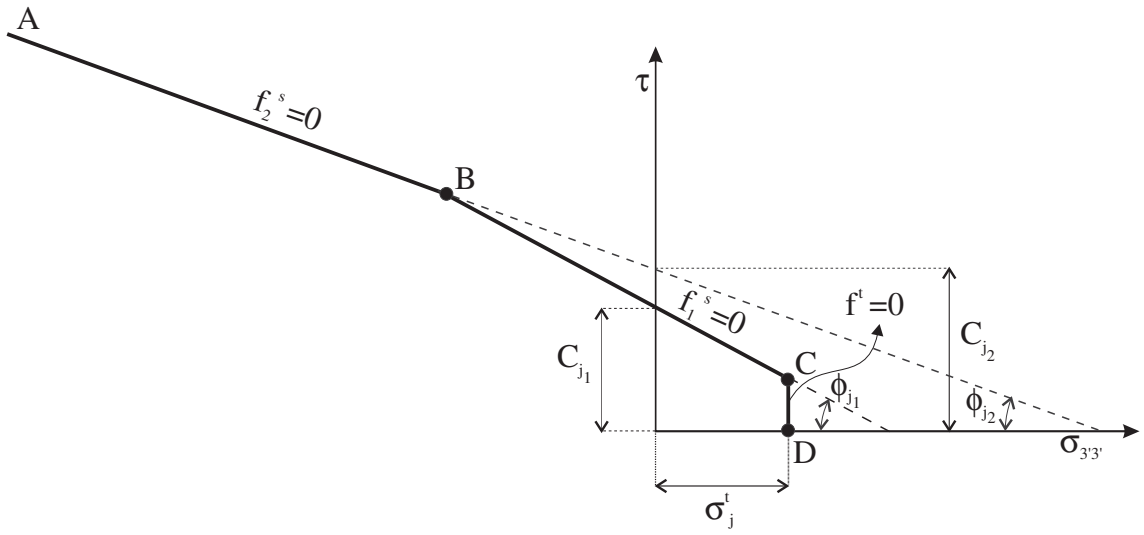

Figure 1.19 UDEC bilinear joint failure criterion

Yield is detected, and stress corrections applied, using a technique similar to the one described in the matrix context.

Here, the flow rule for plastic yielding has the form

$$\Delta e'^{p_s}_{22} = \lambda \frac{\partial g}{\partial \sigma'_{22}}$$

$$\Delta \gamma^{p_s} = \lambda \frac{\partial g}{\partial \tau} \tag{1.141}$$

where γ is the strain variable associated to τ, and we have

$$\Delta \gamma^{p_s} = |\Delta e'^{p_s}_{12}| \tag{1.142}$$

The potential function, g, for shear yielding on the weak plane is g^s. It corresponds to the nonassociated law,

$$g^s = \tau + \sigma'_{22} \tan \psi_j \tag{1.143}$$

where ψ_j, the dilation angle, is equal to ψ_{j_2} for failure along $A - B$, and ψ_{j_1} along $B - C$.

The potential function, g, for tensile yielding on the weak plane is g^t. It corresponds to the associated flow rule,

$$g^t = \sigma'_{22} \tag{1.144}$$

It may be shown that the local plastic strain increments for shear failure are such that

$$\Delta e'^{p_s}_{22} = \lambda^s \tan \psi_j$$

$$\Delta \gamma^{p_s} = \lambda^s \tag{1.145}$$

The stress corrections for shear failure are

$$\Delta\sigma'_{11} = -\lambda^s \alpha_2 \tan\psi_j$$

$$\Delta\sigma'_{22} = -\lambda^s \alpha_1 \tan\psi_j$$

$$\Delta\sigma'_{33} = -\lambda^s \alpha_2 \tan\psi_j$$

$$\Delta\tau = -\lambda^s 2G \tag{1.146}$$

where

$$\lambda^s = \frac{\tau^O + \sigma'^O_{22} \tan\phi_j - c_j}{2G + \alpha_1 \tan\psi_j \tan\phi_j} \tag{1.147}$$

and the superscript ^{O} indicates values obtained just before detection of failure on the weak plane.

The plastic corrections for the local shear stress components on the weak plane are derived by scaling

$$\Delta\sigma'_{12} = \Delta\tau \frac{\sigma'^O_{12}}{\tau^O} \tag{1.148}$$

In turn, local plastic strain increments for tensile failure have the form

$$\Delta e'^{p_t}_{22} = \lambda^t$$

$$\Delta\gamma^{p_t} = 0 \tag{1.149}$$

The stress corrections for tensile failure are

$$\Delta\sigma'_{11} = -\lambda^t \alpha_2$$

$$\Delta\sigma'_{22} = -\lambda^t \alpha_1 \tag{1.150}$$

$$\Delta\sigma'_{33} = -\lambda^t \alpha_2$$

where

$$\lambda^t = \frac{\sigma'^{O}_{22} - \sigma^t_j}{\alpha_1} \tag{1.151}$$

1.6.5.3 Large-Strain Update of Orientation

In large-strain, the orientation of the weak plane is adjusted, per zone, to account for rigid-body rotations, and rotations due to deformations. The corrections are identical to those described in Section 1.6.3.1.

1.6.5.4 Hardening Parameters

In the bilinear strain-hardening/softening ubiquitous-joint model, some or all of the zone yielding parameters (cohesion, friction, dilation and tensile strength) for the matrix and joint are modified automatically after the onset of plasticity, according to piecewise linear laws specified on input, in terms of a range of values for the hardening parameters. (See Section 1.6.4.2.) One table number must be specified in the **block zone cmodel property** command for each softening parameter. (If no table property number is specified, the parameter is taken as constant.) The corresponding table data contain pairs of values for the parameter and the property between which a linear variation is assumed. The last property value is used for values of the hardening parameter beyond the last one specified in the table.

Four independent hardening parameters are used in this model:

(1) κ^s measures the matrix plastic shear strain, and is used to update the matrix cohesion, friction and dilation;

(2) κ^t measures the matrix plastic volumetric tensile strain, and is used to update the matrix tensile strength;

(3) κ^s_j estimates the joint plastic shear strain, and controls the joint cohesion, friction and dilation update; and

(4) κ^t_j evaluates the joint plastic volumetric tensile strain, and controls the joint tensile strength update.

The parameters are defined as the sum of incremental measures of plastic strain for the zone. The zone-hardening increments are calculated as the average of hardening increments over all triangles involved in the zone.

The shear-hardening increment for a triangle is the square root of the second invariant of the incremental plastic shear-strain deviator tensor for the step. For the matrix, it is given as

$$\Delta\kappa^s = \frac{1}{\sqrt{2}}\sqrt{(\Delta e_1^{p_s} - \Delta e_m^{p_s})^2 + (\Delta e_m^{p_s})^2 + (\Delta e_3^{p_s} - \Delta e_m^{p_s})^2} \tag{1.152}$$

where $\Delta e_m^{p_s}$ is the volumetric plastic shear strain increment,

$$\Delta e_m^{p_s} = \frac{1}{3}(\Delta e_1^{p_s} + \Delta e_3^{p_s}) \tag{1.153}$$

and the plastic strain increments are given by Eq. (1.131), using Eq. (1.133) for λ^s.

For the joint, the formula is

$$\Delta \kappa_j^s = \sqrt{\frac{1}{3}(\Delta e'^{p_s}_{22})^2 + (\Delta e'^{p_s}_{12})^2} \tag{1.154}$$

where the plastic strain increments are given by Eq. (1.145) (see Eq. (1.142)), using Eq. (1.147) for λ^s.

The tetrahedron tensile-hardening increment is the plastic volumetric tensile-strain increment.

For the matrix, we have

$$\Delta \kappa^t = \Delta \epsilon_3^{p_t} \tag{1.155}$$

where the plastic strain increment is given by Eq. (1.135), using Eq. (1.137) for λ^t.

For the joint, the expression is

$$\Delta \kappa_j^t = \Delta e'^{p_t}_{22} \tag{1.156}$$

where the plastic strain increment is given by Eq. (1.149), using Eq. (1.151) for λ^t.

1.6.5.5 Implementation Procedure

The implementation of the bilinear model proceeds as indicated above. An elastic guess, σ_{ij}^{I}, is first computed using stress increments for the step evaluated by application of Hooke's law to the total strain increments, Δe_{ij}. Principal stresses are calculated, ordered such that $\sigma_1^I \leq \sigma_2^I \leq \sigma_3^I$, and tested for failure in the matrix using the yield criteria Eqs. (1.122) and (1.123). In principle, matrix failure is declared if the representation of the stress point (σ_1^I, σ_3^I) falls outside the yield surface in Figure 1.18. In this case, stress corrections are applied to the principal values of the elastic guess, which depend on the position of the stress point above $A-B$, $B-C$ or $C-D$. (Bisectors are used at B and C to delimit the domain of failure attached to a particular segment of the yield surface.)

The stress corrections for shear failure in the matrix are given by Eqs. (1.132) and (1.133), where the parameters of cohesion, c, friction, ϕ, and dilation, ψ, have values c_2, ϕ_2, ψ_2 for failure along $A-B$, and c_1, ϕ_1, ψ_1 for failure along $B-C$.

The stress corrections for tensile failure in the matrix are given by Eqs. (1.136) and (1.137).

The stress tensor components in the system of reference axes, σ_{ij}^{O}, are then calculated from the corrected principal values by assuming that the principal directions have not changed during plastic flow.

Local traction components on the weak plane are defined as σ'_{22} and τ, with σ'_{22} being the normal component, and $\tau = |\sigma'_{12}|$ being the magnitude of the tangential traction component. These stresses are resolved from σ_{ij}^{O}, and examined for ubiquitous-joint failure using the yield criteria Eqs. (1.138) and (1.139). In principle, ubiquitous-joint failure is declared if the representation of the stress point $(\sigma'^{O}_{22}, \tau^{O})$ falls outside the yield surface in Figure 1.19. In this case, local stress corrections, which depend on the position of the stress point in the vicinity of $A-B$, $B-C$ or $C-D$, are applied. (Bisectors are used at B and C to delimit the domain of failure attached to a particular segment of the yield surface.)

The stress corrections for shear joint failure are given by Eqs. (1.146) to (1.148), where the parameters of cohesion, c_j, friction, ϕ_j, and dilation, ψ_j, have values c_{j_2}, ϕ_{j_2}, ψ_{j_2} for failure along $A-B$, and c_{j_1}, ϕ_{j_1}, ψ_{j_1} for failure along $B-C$.

The stress corrections for tensile joint failure are given by Eqs. (1.150) and (1.151).

Finally, the local stress components are resolved back into global axes.

In large-strain mode, the unit normal to the weak plane is adjusted per zone to account for body rotations.

After determination of the new stresses for the step, the hardening parameters are incremented using Eqs. (1.152), (1.154), (1.155) and (1.156). These parameters are then used to determine new values of cohesion, friction, dilation and tensile strength for the matrix and the joint from the available input tables.

It is assumed that the tensile strength of the material can never increase. Also, for material with friction, the value will not exceed the maximum value σ^t_{max} or $\sigma^t_{j\ max}$ (see Eqs. (1.126) and (1.140)).

Note that, by default, the yield model is linear in both the matrix and the joint, in which case only section 1 (where $f^s_1 = 0$) and section 3 (where $f^t = 0$) of the yield curve are recognized (even if properties are assigned for section 2, where $f^s_2 = 0$). To activate the bilinear laws, the property **flag-bilinear** and/or **flag-bilinear-joint** must be set to 1.

Also, if the friction angles for sections 1 and 2 become equal, the model will be considered as linear and section 2 will be ignored (for the matrix and/or the joint, as appropriate). Section 2 will also be ignored if the intersection of section 1 and 2 corresponds to a stress point which violates the tensile criterion.

1.6.5.6 **block zone cmodel** *Command and Property Keywords*

Strain-Softening/Hardening Ubiquitous-Joint – **block zone cmodel assign softening-ubiquitous**

(1) **bu**lk — elastic bulk modulus, K

(2) **coh**esion — matrix cohesion, c_1

(3) **coh**esion**-2** — matrix cohesion, c_2

(4) **dens**ity — mass density, ρ

(5) **di**lation**-2** — matrix dilation angle, ψ_2

(6) **di**lation — matrix dilation angle, ψ_1

(7) **fl**ag**-bi**linear — = 0 for matrix linear model (default);
= 1 for matrix bilinear model

(8) **fl**ag**-bi**linear**-jo**int — = 0 for joint linear model (default);
= 1 for joint bilinear model

(9) **fri**ction — matrix friction angle, ϕ_1

(10) **fri**ction**-2** — matrix friction angle, ϕ_2

(11) **ja**ngle — angle of ubiquitous plane measured counterclockwise from x-axis (2D models)

(12) **jo**int**-co**hesion**-2** — joint cohesion, c_{j2}

(13) **jo**int**-co**hesion — joint cohesion, c_{j1}

(14) **jo**int**-di**lation**-2** — joint dilation angle, ψ_{j2}

(15) **jo**int**-di**lation — joint dilation angle, ψ_{j1}

(16) **jo**int**-fri**ction**-2** — joint friction angle, ϕ_{j2}

(17) **jo**int**-fri**ction — joint friction angle, ϕ_{j1}

(18) **jo**int**-ten**sion — joint tension limit, σ_j^t

(19) **sh**ear — elastic shear modulus, G

(20) **ta**ble**-co**hesion — number of table relating matrix cohesion c_1 to matrix plastic shear strain

(21) **ta**ble**-co**hesion**-2** — number of table relating matrix cohesion c_2 to matrix plastic shear strain

(22) **ta**ble**-di**lation — number of table relating matrix dilation angle ψ_1 to matrix plastic shear strain

(23) **ta**ble**-di**lation**-2** — number of table relating matrix dilation ψ_2 to matrix plastic shear strain

(24) **ta**ble**-fri**ction — number of table relating matrix friction ϕ_1 angle to matrix plastic shear strain

(25) **ta**ble**-fri**ction**-2** — number of table relating matrix friction angle ϕ_2 to matrix plastic shear strain

(26) **ta**ble-**jo**int-**co**hesion number of table relating joint cohesion c_{j1} to joint plastic shear strain

(27) **ta**ble-**jo**int-**co**hesion-**2** number of table relating joint cohesion c_{j2} to joint plastic shear strain

(28) **ta**ble-**jo**int-**di**lation number of table relating joint dilation ψ_{j1} to joint plastic shear strain

(29) **ta**ble-**jo**int-**di**lation-**2** number of table relating joint dilation ψ_{j2} to joint plastic shear strain

(30) **ta**ble-**jo**int-**fri**ction number of table relating joint friction angle ϕ_{j1} to joint plastic shear strain

(31) **ta**ble-**jo**int-**fri**ction-**2** number of table relating joint friction angle ϕ_{j2} to joint plastic shear strain

(32) **ta**ble-**jo**int-**ten**sion number of table relating joint tension limit σ_j^t to joint plastic tensile strain

(33) **ta**ble-**ten**sion number of table relating matrix tension limit σ^t to matrix plastic tensile strain

(34) **ten**sion matrix tension limit, σ^t

Table 1.1 lists the properties by matrix and joint failure segments.

Note that the default tension limits for the matrix and weakness planes are the same as those in the ubiquitous-joint model.

The following properties can be printed, plotted or accessed via *FISH*.

(1) **sta**te plastic state

(2) **stra**in-**she**ar-**pl**astic accumulated matrix plastic shear strain

(3) **stra**in-**she**ar-**pl**astic-**jo**int accumulated joint plastic shear strain

(4) **stra**in-**ten**sile-**pl**astic accumulated matrix plastic tensile strain

(5) **stra**in-**ten**sile-**pl**astic-**jo**int accumulated joint plastic tensile strain

Table 1.1 Property groups by failure segment for the bilinear, strain-hardening/softening ubiquitous-joint model

Properties			Description
general			
	bulk		bulk modulus
	density		mass density
	flag-**bi**linear-**jo**int		1 for bilinear joint law 0 for linear joint law (default)
	flag-**b**ilinear		1 for bilinear matrix law 0 for linear matrix law (default)
	jangle		angle of weakness plane measured counterclockwise from x-axis (2D models)
	tension-**jo**int	<**ta**ble-**jo**int-**ten**sion>	tension limit of joint segments 1 and 2
	shear		shear modulus
	tension	<**ta**ble-**ten**sion>	tension limit of matrix segments 1 and 2
matrix	segment 1		
	cohesion	<**ta**ble-**co**hesion>	cohesion
	dilation	<**ta**ble-**di**lation>	dilation (degree)
	friction	<**table-friction**>	friction (degree)
matrix	segment 2		
	cohesion-**2**	<**ta**ble-**co**hesion-**2**>	cohesion
	dilation-**2**	<**ta**ble-**di**lation-**2**>	dilation (degree)
	friction-**2**	<**ta**ble-**fri**ction-**2**>	friction (degree)
joint	segment 1		
	cohesion	<**ta**ble-**coh**esion>	cohesion
	joint-**di**lation	<**ta**ble-**jo**int-**di**lation>	dilation (degree)
	joint-**fri**ction	<**ta**ble-**jo**int-**fri**ction>	friction (degree)
joint	segment 2		
	joint-**co**hesion-**2**	<**ta**ble-**jo**int-**co**hesion>	cohesion
	joint-**di**lation-**2**	<**ta**ble-**jo**int-**di**lation-**2**>	dilation (degree)
	joint-**fri**ction-**2**	<**ta**ble-**jo**int-**fri**ction-**2**>	friction (degree)

1.6.6 Double-Yield Model

Permanent volume changes caused by the application of isotropic pressure are taken into account in this model by including, in addition to the shear and tensile failure envelopes in the strain-softening/hardening model, a volumetric yield surface (or "cap"). For simplicity, the cap surface, defined by the "cap pressure" $p_c > 0$, is independent of shear stress; it consists of a vertical line on a plot of shear stress versus mean stress. The hardening behavior of the cap pressure is activated by volumetric plastic strain, and follows a piecewise-linear law prescribed in a user-supplied table (like that described in Section 1.6.4.2). The tangential bulk and shear moduli evolve as plastic volumetric strain takes place according to a special law defined in terms of a factor, R, assumed to be constant, and defined as the ratio of elastic bulk modulus to plastic bulk modulus.

Only two material parameters and a table are required in addition to those associated with the strain-softening model:

(1) the initial value of p_c, which corresponds to the maximum mean pressure that the material has experienced in the past;

(2) the value of R, greater than unity, which controls the slope of the stress-strain curve on volumetric unloading (the "swelling" line, in soil mechanics terms); and

(3) the table representation of the "hardening curve," which relates cap pressure, p_c, to plastic volume strain, e^{pv}.

Hence, any laboratory-determined hardening behavior may be modeled within the constraints imposed by a two-parameter model.

1.6.6.1 Incremental Elastic Law

In the *UDEC* implementation of this model, principal stresses σ_1, σ_2, σ_3 are used, the out-of-plane stress, σ_{zz}, being recognized as one of these. The principal stresses and principal directions are evaluated from the stress tensor components, and ordered so that (recall that compressive stresses are negative)

$$\sigma_1 \leq \sigma_2 \leq \sigma_3 \tag{1.157}$$

The corresponding principal strain increments Δe_1, Δe_2, Δe_3 are decomposed:

$$\Delta e_i = \Delta e_i^e + \Delta e_i^p \qquad i = 1, 3 \tag{1.158}$$

where the superscripts ^{e} and ^{p} refer to elastic and plastic parts, respectively, and the plastic components are nonzero only during plastic flow. (Note that extensional strains are positive.) It is assumed that the plastic contributions of shear, tensile and volumetric yielding are additive, so we may write

$$\Delta e_i^p = \Delta e_i^{ps} + \Delta e_i^{pt} + \Delta e_i^{pv} \tag{1.159}$$

where the superscripts ^{ps}, ^{pt} and ^{pv} stand for plastic shear, plastic tensile and plastic volumetric strain. By convention in this section, the symbol Δe is used to refer to the *minus* volumetric strain increment ($\Delta e_1 + \Delta e_2 + \Delta e_3$) with plastic part Δe^p and elastic part Δe^e. The symbol Δe^{pv} refers to *minus* the value of the plastic volumetric strain ($\Delta e_1^{pv} + \Delta e_2^{pv} + \Delta e_3^{pv}$).

The incremental expression of Hooke's law in terms of principal stress and strain has the form

$$\begin{aligned} \Delta\sigma_1 &= \alpha_1 \Delta e_1^e + \alpha_2(\Delta e_2^e + \Delta e_3^e) \\ \Delta\sigma_2 &= \alpha_1 \Delta e_2^e + \alpha_2(\Delta e_1^e + \Delta e_3^e) \\ \Delta\sigma_3 &= \alpha_1 \Delta e_3^e + \alpha_2(\Delta e_1^e + \Delta e_2^e) \end{aligned} \tag{1.160}$$

where $\alpha_1 = K_c + 4G_c/3$, $\alpha_2 = K_c - 2G_c/3$, and K_c and G_c are the current tangential bulk and shear moduli, defined according to the following considerations.

Consider an isotropic compression test with increasing pressure, p_c. As the material becomes more compact, its plastic stiffness (dp_c/de^{pv}) usually increases; it seems reasonable that the elastic stiffness will also increase, since the grains are being forced closer together. A simple rule is adopted in this model, whereby under general loading conditions the incremental elastic stiffness, K_c, is a constant factor, R, multiplied by the current incremental plastic stiffness. The values of bulk and shear modulus, K and G, supplied by the user, are taken as upper limits to K_c and G_c, and it is assumed that the ratio K_c/G_c remains constant and equal to K/G. Using incremental notation, this law is defined by the relations

$$K_c = R\,\frac{\Delta p_c}{\Delta e^{pv}} \qquad K_c := \min(K_c, K)$$

$$G_c = G\,\frac{K_c}{K} \tag{1.161}$$

where the factor R is given, and $\Delta p_c/\Delta e^{pv}$ is the current slope of the table of p_c values.

The type of behavior exhibited by the double-yield model is illustrated in Figure 1.20, which shows a nonlinear volumetric loading curve with several unloading excursions; these excursions are elastic, with slope related by R to the plastic stiffness at the point of unloading.

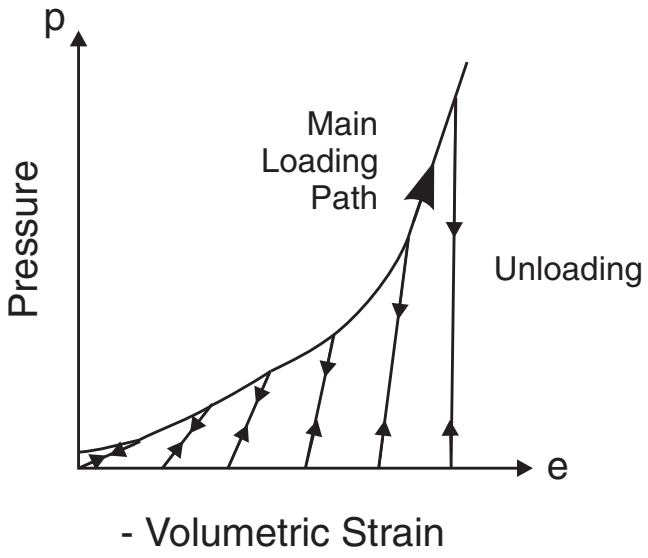

Figure 1.20 Elastic volumetric loading/unloading paths

1.6.6.2 Yield and Potential Functions

The shear and tensile yield functions, referred to as f^s and f^t, have the form

$$f^s = \sigma_1 - \sigma_3 N_\phi + 2c\sqrt{N_\phi} \tag{1.162}$$

$$f^t = \sigma^t - \sigma_3 \tag{1.163}$$

where

$$N_\phi = (1 + \sin\phi)/(1 - \sin\phi)$$

and ϕ is the friction angle, c is the cohesion and σ^t is the tensile strength.

The volumetric yield function, f^v, is defined as

$$f^v = \frac{1}{3}\left(\sigma_1 + \sigma_2 + \sigma_3\right) + p_c \tag{1.164}$$

where p_c is the cap pressure.

The shear potential function, g^s, corresponds to a nonassociated flow rule, and the tensile and volumetric potential functions, g^t and g^v, correspond to associated laws. They have the form

$$\begin{aligned} g^s &= \sigma_1 - \sigma_3 N_\psi \\ g^t &= -\sigma_3 \\ g^v &= \frac{1}{3}(\sigma_1 + \sigma_2 + \sigma_3) \end{aligned} \tag{1.165}$$

where

$$N_\psi = (1 + \sin\psi)/(1 - \sin\psi)$$

and ψ is the dilation angle.

1.6.6.3 Hardening/Softening Parameters

The shear and volume yield surfaces can harden (or soften), and the tensile yield surface can soften, according to hardening rules that are specified by look-up tables (see Section 1.6.4.2). Entry to the tables is by hardening parameters that record some measure of accumulated plastic strain. In shear and tension, the hardening parameter incremental forms are

$$\begin{aligned} \Delta e^{ps} &= \left\{ \frac{1}{2}\left(\Delta e_1^{ps} - \Delta e_m^{ps}\right)^2 + \frac{1}{2}\left(\Delta e_m^{ps}\right)^2 + \frac{1}{2}\left(\Delta e_3^{ps} - \Delta e_m^{ps}\right)^2 \right\}^{\frac{1}{2}} \\ \Delta e^{pt} &= e_3^{pt} \end{aligned} \tag{1.166}$$

where

$$\Delta e_m^{ps} = 1/3\left(\Delta e_1^{ps} + \Delta e_3^{ps}\right)$$

Δe_j^{ps}, $j = 1, 3$ and Δe_3^{pt} are plastic shear and tensile strain increments in the principal directions.

In the volumetric direction, the hardening parameter increment is

$$\Delta e^{pv} = |\Delta e_1^{pv} + \Delta e_2^{pv} + \Delta e_3^{pv}| \tag{1.167}$$

where Δe_j^{pv}, $j = 1, 3$ are plastic volumetric strain increments in the principal directions.

These hardening parameters are used in the tables to determine new values of friction, cohesion, dilation, tensile strength and cap pressure. The current bulk and shear moduli are also calculated from the table values as defined by Eq. (1.161).

1.6.6.4 Plastic Corrections

Let the superscript ^{I} be used to represent the elastic guess, obtained by adding to the old stresses, σ_{ij}^O, elastic increments computed using the total strain increments. In principal axes we then have

$$\begin{aligned}
\sigma_1^I &= \sigma_1^O + \alpha_1 \Delta e_1 + \alpha_2 (\Delta e_2 + \Delta e_3) \\
\sigma_2^I &= \sigma_2^O + \alpha_1 \Delta e_2 + \alpha_2 (\Delta e_1 + \Delta e_3) \\
\sigma_3^I &= \sigma_3^O + \alpha_1 \Delta e_3 + \alpha_2 (\Delta e_1 + \Delta e_2)
\end{aligned} \tag{1.168}$$

In the *UDEC* implementation, shear yield is detected if $f^s(\sigma_1^I, \sigma_3^I) < 0$, volumetric yield if $f_v(\sigma_1^I, \sigma_2^I, \sigma_3^I) < 0$, and tensile yield if $f^t(\sigma_3^I) < 0$. Corresponding plastic corrections are evaluated using the following techniques.

We first consider the case where tensile failure is *not* detected for the step, but both shear and volumetric yield conditions are exceeded. Using Eqs. (1.158) and (1.159), the principal strain increments may be expressed as

$$\Delta e_i = \Delta e_i^e + \Delta e_i^{ps} + \Delta e_i^{pv} \qquad i = 1, 3 \tag{1.169}$$

The flow rules for shear and volumetric yielding are

$$\begin{aligned}
\Delta e_i^{ps} &= \lambda^s \frac{\partial g^s}{\partial \sigma_i} \\
\Delta e_i^{pv} &= \lambda^v \frac{\partial g^v}{\partial \sigma_i}
\end{aligned} \tag{1.170}$$

where $i = 1, 3$. Using Eq. (1.165), these expressions become, after differentiation,

$$\begin{aligned}
\Delta e_1^{ps} &= \lambda^s \\
\Delta e_2^{ps} &= 0 \\
\Delta e_3^{ps} &= -\lambda^s N_\psi
\end{aligned} \tag{1.171}$$

and

$$\begin{aligned}\Delta e_1^{pv} &= \frac{1}{3}\lambda^v \\ \Delta e_2^{pv} &= \frac{1}{3}\lambda^v \\ \Delta e_3^{pv} &= \frac{1}{3}\lambda^v\end{aligned} \tag{1.172}$$

Substituting in Eq. (1.169), we obtain

$$\begin{aligned}\Delta e_1^e &= \Delta e_1 - \lambda^s - \lambda^v/3 \\ \Delta e_2^e &= \Delta e_2 - \lambda^v/3 \\ \Delta e_3^e &= \Delta e_3 + \lambda^s N_\psi - \lambda^v/3\end{aligned} \tag{1.173}$$

With these expressions for the elastic strain increments, Hooke's incremental equations yield (see Eq. (1.160))

$$\begin{aligned}\sigma_1^N &= \sigma_1^I - \lambda^s(\alpha_1 - \alpha_2 N_\psi) - \lambda^v K \\ \sigma_2^N &= \sigma_2^I - \alpha_2\lambda^s(1 - N_\psi) - \lambda^v K \\ \sigma_3^N &= \sigma_3^I - \lambda^s(\alpha_2 - \alpha_1 N_\psi) - \lambda^v K\end{aligned} \tag{1.174}$$

where σ_i^I, $i = 1, 3$ are the initial trial stresses in Eq. (1.168), and $\sigma_i^N = \sigma_i^O + \Delta\sigma_i$, $i = 1, 3$ are the new principal stresses for the step.

To determine the multipliers λ^s and λ^v, we require that if shear and volumetric yielding occur, the new stresses lie on both yield surfaces, and we must have $f^s(\sigma_1^N, \sigma_3^N) = 0$, and $f^\sigma(\sigma_1^N, \sigma_2^N, \sigma_3^N) = 0$. Substituting Eq. (1.174) for σ_i, $i = 1, 3$ in Eqs. (1.162) and (1.164), and solving for λ^s, we obtain

$$\lambda^s = \frac{f^{sI} - f^{vI}(1 - N_\phi)}{\alpha_1 - \alpha_2 N_\psi - \alpha_2 N_\phi + \alpha_1 N_\phi N_\psi - K(1 - N_\phi)(1 - N_\psi)} \tag{1.175}$$

Hence,

$$\lambda^v = \frac{f^{vI}}{K} - \lambda^s(1 - N_\psi) \tag{1.176}$$

In these equations, the notation f^I stands for the function f evaluated for the initial trial stresses.

Eqs. (1.175) and (1.176) can now be used to evaluate the new stresses from Eq. (1.174). These stresses simultaneously satisfy both yield conditions and both flow rules.

If the element is only yielding in shear, then

$$\begin{aligned} \lambda^v &= 0 \\ \lambda^s &= \frac{f^{sI}}{\alpha_1 - \alpha_2 N_\psi - \alpha_2 N_\phi + \alpha_1 N_\phi N_\psi} \end{aligned} \tag{1.177}$$

If the element is only yielding in volume, then

$$\begin{aligned} \lambda^s &= 0 \\ \lambda^v &= \frac{f^{vI}}{K} \end{aligned} \tag{1.178}$$

Eq. (1.177) or Eq. (1.178) may be used in Eq. (1.174), as appropriate, to compute new stresses.

We now consider the case where tensile failure is detected by the condition $f^t(\sigma_3^I) < 0$. If volumetric failure is *not* detected, we use the same technique and stress corrections as described in the Mohr-Coulomb model. If volumetric failure is detected in addition to tensile failure, then either $f^s(\sigma_1^I, \sigma_3^I) \leq 0$ or $f^s(\sigma_1^I, \sigma_3^I) > 0$. We begin by assuming that all three yield conditions are exceeded. We assume that the plastic contributions of shear, volumetric and tensile yielding are additive – i.e.,

$$\Delta e_i = \Delta e_i^e + \Delta e_i^{ps} + \Delta e_i^{pv} + \Delta e_i^{pt} \qquad i = 1, 3 \tag{1.179}$$

The flow rule for tensile yielding has the form

$$\Delta e_i^{pt} = \lambda^t \frac{\partial g^t}{\partial \sigma_i} \qquad i = 1, 3 \tag{1.180}$$

Using Eq. (1.165), these expressions become, after partial differentiation,

$$\begin{aligned} \Delta e_1^{pt} &= 0 \\ \Delta e_2^{pt} &= 0 \\ \Delta e_3^{pt} &= -\lambda^t \end{aligned} \tag{1.181}$$

Using the same reasoning as above, and Eqs. (1.171) and (1.172) for the shear and volumetric flow rule, we obtain

$$\begin{aligned}
\sigma_1^N &= \sigma_1^I - \lambda^s(\alpha_1 - \alpha_2 N_\psi) - \lambda^v K + \lambda^t \alpha_2 \\
\sigma_2^N &= \sigma_2^I - \alpha_2 \lambda^s (1 - N_\psi) - \lambda^v K + \lambda^t \alpha_2 \\
\sigma_3^N &= \sigma_3^I - \lambda^s(\alpha_2 - \alpha_1 N_\psi) - \lambda^v K + \lambda^t \alpha_1
\end{aligned} \tag{1.182}$$

The multipliers λ^s, λ^v and λ^t are determined by solving the system of three equations: $f^s(\sigma_1^N, \sigma_3^N) = 0$, $f^v(\sigma_1^N, \sigma_2^N, \sigma_3^N) = 0$ and $f^t(\sigma_3^N) = 0$. This gives

$$\begin{aligned}
\lambda^s &= \frac{f^{tI}(1 + 2N_\phi) + 3f^{vI} - 2f^{sI}}{\alpha_2 - \alpha_1} \\
\lambda^v &= \frac{f^{vI}}{K} + \frac{-3(1 + N_\phi) f^{tI} - 6f^{vI} + 3f^{sI}}{\alpha_2 - \alpha_1} \\
\lambda^t &= \frac{-f^{tI}[N_\psi(1 + 2N_\phi) + 2 + N_\phi] - 3(1 + N_\psi) f^{vI} + (1 + 2N_\psi) f^{sI}}{\alpha_2 - \alpha_1}
\end{aligned} \tag{1.183}$$

Substitution of those expressions in Eq. (1.182) yields

$$\begin{aligned}
\sigma_1^N &= \sigma^t N_\phi - 2c\sqrt{N_\phi} \\
\sigma_2^N &= -3p_c - \sigma^t(1 + N_\phi) + 2c\sqrt{N_\phi} \\
\sigma_3^N &= \sigma_t
\end{aligned} \tag{1.184}$$

If only tensile and volumetric yield are detected, then $\lambda^s = 0$ in Eq. (1.182). The constants λ^v and λ^t are determined by requiring that both conditions, $f^v(\sigma_1^N, \sigma_2^N, \sigma_3^N) = 0$ and $f^t(\sigma_3^N) = 0$, be fulfilled. After some manipulation, we obtain

$$\begin{aligned}
\lambda^v &= \frac{\alpha_1 f^{vI} + K f^{tI}}{K(\alpha_1 - K)} \\
\lambda^t &= \frac{f^{vI} + f^{tI}}{\alpha_1 - K}
\end{aligned} \tag{1.185}$$

Substitution of those expressions in Eq. (1.182) gives

$$\begin{aligned}\sigma_1^N &= \sigma_1^I - \frac{3f^{vI} + f^{tI}}{2} \\ \sigma_2^N &= \sigma_2^I - \frac{3f^{vI} + f^{tI}}{2} \\ \sigma_3^N &= \sigma_t\end{aligned} \tag{1.186}$$

1.6.6.5 Implementation Procedure

Hardening and softening behaviors for the cohesion, friction and dilation in terms of the shear parameter e^{ps} (see Eq. (1.166)) are provided by the user in the form of tables. Softening of the tensile strength is described in a similar manner, using the parameter e^{pt} (see Eq. (1.166)). In turn, the variation of cap pressure is specified in a table in terms of the parameter e^{pv} (see Eq. (1.167)). Each table contains pairs of values: one for the parameter and one for the corresponding property value. It is assumed that the property varies linearly between two consecutive parameter entries in the table.

In the implementation of the double-yield model in *UDEC*, new stresses for the step are computed using the current values of the model properties. In this process, an elastic guess σ_{ij}^I is first computed by, adding to the old stress components, increments calculated by application of Hooke's law to the total strain increment for the step. Principal stresses $\sigma_1^I, \sigma_2^I, \sigma_3^I$ and corresponding principal directions are calculated and ordered. If these stresses violate the composite yield criterion, corrections are applied to the elastic guess as described in Section 1.6.6.4 to give the new stress state. The stress tensor components in the system of reference axes are then calculated from the principal values by assuming that the principal directions have not been affected by the occurrence of a plastic correction.

Plastic strain increments are evaluated from Eqs. (1.171), (1.172) and (1.181), using relevant expressions of λ^s, λ^t and λ^v for the mode of failure taking place. Zone hardening increments are then calculated as the surface average of values obtained from Eqs. (1.166) and (1.167) for all triangles involved in the zone. The hardening parameters are updated, and new zone properties for cohesion, friction, dilation, tensile strength and cap pressure are evaluated by linear interpolation in the tables. New elastic constants are derived from the cap pressure table using Eq. (1.161). All of these properties are stored for use in the next step. The hardening or softening lags one timestep behind the corresponding plastic deformation. In an explicit code, this error is small because the steps are small.

For a material with friction, the maximum value of the tensile strength is evaluated from Eq. (1.62), using the new cohesion and friction angle. This value is retained by the code if it is smaller than the tensile strength updated from the table.

1.6.6.6 Choice of Volumetric Properties

The "hardening curve" and ratio, R, of elastic bulk modulus to plastic bulk modulus are volumetric properties that may be derived from the results of a triaxial test in which axial stress and confining pressure, p, are kept equal. This test, for which $de^p = de^{pv}$, is recommended because it is best to determine the parameters related to a particular mode of failure from a test which *only* involves that failure mode.

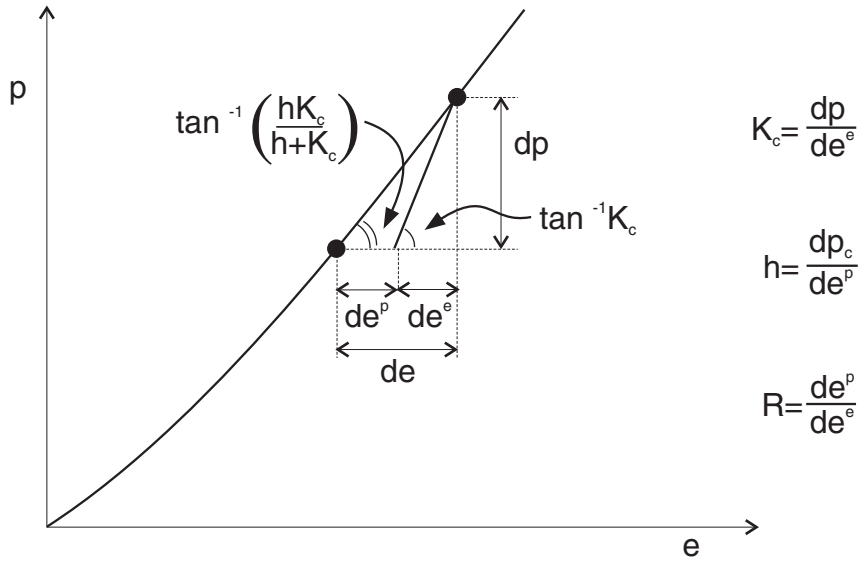

Figure 1.21 Isotropic consolidation test

Consider the experimental graph of minus mean stress (pressure) versus minus volumetric strain for an increasing stress level, with a small unloading excursion, obtained from such a test and presented in Figure 1.21. The volumetric strain increment, de, at a point of the main loading path (assuming that we are above any initial pre-consolidation stress level) is composed of an elastic part, de^e, and a plastic part, de^p. (Recall that in this section, de, de^e and de^p refer to *minus* the value of the volumetric strain.) The observed tangent modulus may be expressed as

$$\frac{dp}{de} = \frac{hK_c}{h + K_c} \tag{1.187}$$

where h is the plastic modulus, K_c is the elastic modulus and, by definition,

$$h = \frac{dp_c}{de^p}$$
$$K_c = \frac{dp}{de^e} \tag{1.188}$$

With the preceding notation convention, the volumetric property R may be defined as

$$R = K_c / h \tag{1.189}$$

and Eq. (1.187) becomes

$$\frac{dp}{de} = \frac{K_c}{1 + R} \tag{1.190}$$

Expressing R from this relation, we obtain

$$R = \frac{K_c}{dp/de} - 1 \tag{1.191}$$

Values for dp/de and K_c can be estimated from main loading and unloading increments on the graph. Hence, R can be calculated from Eq. (1.191). Note that, in the context of this model, the ratio R is assumed to be constant. Using that $K_c = Rh$ and $h = dp_c/de^p$ in Eq. (1.187), we may write, after some manipulation,

$$\frac{dp_c}{de^p} = h = \left(\frac{1 + R}{R}\right) \frac{dp}{de} \tag{1.192}$$

From this, it follows that values of p_c for a particular e^p can be obtained, to the first approximation, by multiplying the value p on the graph corresponding to $e = e^p$ by the ratio $(1 + R)/R$. For example, if $R = 5$, then the graph curve must be scaled by a factor of 1.2 to convert it to table values, assuming no overconsolidation.

To be sure that input parameters are reasonable, a single-element test should be done with *UDEC*, exercising the double-yield model over stress paths similar to those of the physical tests, and plotting similar graphs.

As an illustration, the data file in Example 1.4 exercises the double-yield model for a material that exhibits a response eleven times stiffer upon unloading than loading.

Example 1.4 Exercising the double-yield model

```
model new
;file: dy.dat
model title 'Double-Yield'
block config axisymmetry
block tolerance corner-round-length 0.01
block create polygon 0 0 0 1 1 1 1 0
block zone gen edge 1
block zone group 'mat1'
block zone cmodel assign double-yield density 1E3 bulk-maximum 1.11E9 ...
  shear 5.077E8 cohesion 1E10 tension 1E10 table-pr-cap 1 multiplier 10 ...
  range group 'mat1'
table 1 add 0 0 1 1.1e7
block gridpoint apply velocity-x 0 range pos-x -0.1 0.1 pos-y 0 1
block gridpoint apply velocity-y 0 range pos-x 0 1 pos-y -0.1 0.1
block gridpoint apply velocity-y -5.35e-3 range pos-x 0 1 pos-y 0.9 1.1
block gridpoint apply velocity-x -5.35e-3 range pos-x 0.9 1.1 pos-y 0 1
fish define _syy
  count = 0
  _tsyy = 0
  ib = block.head
  iz = block.zone(ib)
  loop while iz # 0
     _tsyy = _tsyy + block.zone.stress.yy(iz)
     iz = block.zone.next(iz)
     count = count + 1
   endloop
   _syy = -_tsyy / count
   _ydis = -block.gp.disp.y(block.gp.near(0,1))
end
fish history @_syy
fish history @_ydis
block cycle 1000
block gridpoint apply velocity-y 5.35e-4 range pos-x 0 1 pos-y 0.9 1.01
block gridpoint apply velocity-x 5.35e-4 range pos-x 0.9 1.1 pos-y 0 1
block cycle 900
hist name 1 label 'Average vertical stress'
hist name 2 label 'Vertical displacement'

return
```

The loading tangent modulus, dp/de, observed in the physical test was constant and equal to 10 MPa. The slope of unloading increments corresponded to a value $K_c = 110$ MPa. To define the volumetric properties of the numerical model, we substitute those values in Eq. (1.191) and find that $R = 10$. As can be seen from Eq. (1.192), the hardening curve has a constant slope

corresponding to $dp_c/de^p = h = 11$ MPa. The hardening table is derived from this result, assuming no overconsolidation.

Note that the input value for bulk modulus, K, must be higher than K_c (see Eq. (1.161)). The input shear modulus controls the ratio of G/K. In this example,

$$G_c = G\frac{K_c}{K} = 50.77 \text{ MPa}$$

and the Poisson's ratio is

$$v = \frac{3K_c - 2G_c}{2(3K_c + G_c)} = 0.3$$

Results of the numerical test are presented in the plot of minus vertical stress versus minus vertical strain in Figure 1.22. The loading slope is 10 MPa, and the unloading slope is eleven times stiffer, as expected.

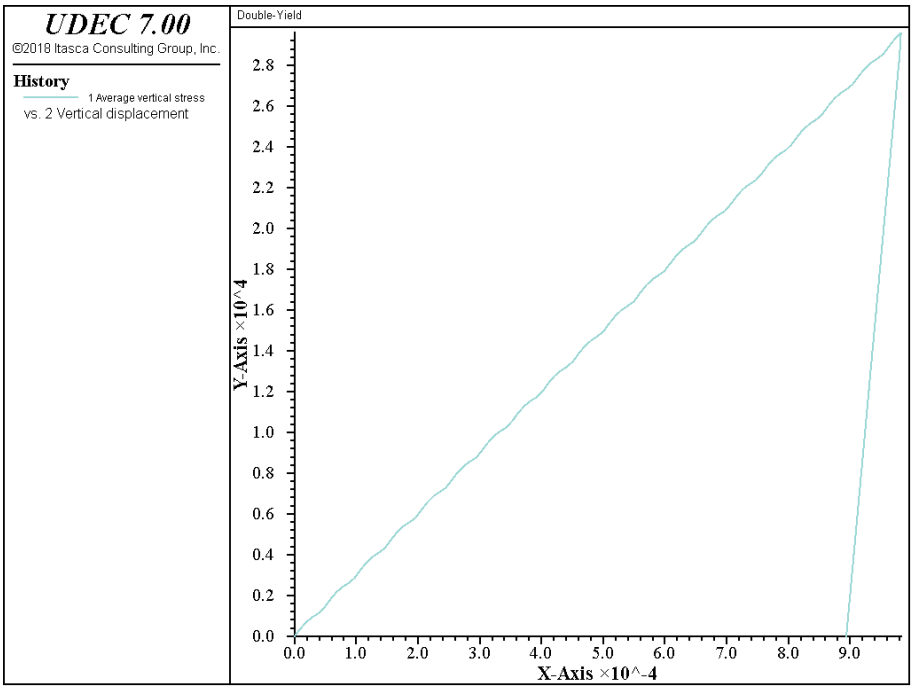

Figure 1.22 Single-element test in which unloading is eleven times stiffer than loading

The maximum elastic moduli, **bulk-maximum** and **shear-maximum**, should be estimated for the maximum pressure likely to be produced in the model. They should not be set larger than this

because mass scaling (for a stable timestep) is calculated on the basis of the moduli. Setting them too high will give rise to a sluggish response (e.g., the model may be slow to converge to a steady-state solution). The elastic moduli also act as a limit on plastic moduli.

If a material to be modeled has experienced some initial compaction (i.e., it is overconsolidated), then p_c may be set to this "pre-consolidation" pressure. In this case, e^p must also be set, in order to be consistent with p_c and the given table (use **block zone cmodel property model strain-volumetric-plastic** to set e^p).

1.6.6.7 **block zone cmodel** *Command and Property Keywords*

Double-Yield – **block zone cmodel assign double-yield**

(1)	**bu**lk	maximum elastic bulk modulus, K
(2)	**coh**esion	cohesion, c
(3)	**dens**ity	mass density, ρ
(4)	**di**lation	dilation angle, ψ
(5)	**fri**ction	angle of internal friction, ϕ
(6)	**mu**ltiplier	multiplier on current plastic cap modulus to give elastic bulk and shear moduli, R
(7)	**pr**essure-**ca**p	current intersection of volumetric yield surface (cap) with pressure (mean stress) axis, p_c
(8)	**sh**ear	maximum elastic shear modulus, G
(9)	**ta**ble-**co**hesion	number of table relating cohesion to plastic shear strain
(10)	**ta**ble-**di**lation	number of table relating dilation angle to plastic shear strain
(11)	**ta**ble-**fri**ction	number of table relating friction angle to plastic shear strain
(11)	**ta**ble-**pr**essure-**ca**p	number of table relating cap pressure to plastic volumetric strain
(12)	**ta**ble-**ten**sion	number of table relating tensile limit to plastic tensile strain
(13)	**ten**sion	tension limit, σ^t

The strain-hardening/softening behavior is controlled by the variation in friction, cohesion and dilation as a function of plastic shear strain, and tension limit as a function of plastic tensile strain, given by a specified table of values. The variation in cap pressure is a function of plastic volumetric strain. Note that if table numbers are given as 0 (default), the properties will take the values given (i.e., with **cohesion**, **dilation**, **friction**, **tension** or **pressure-cap** keyword).

The following properties can be printed, plotted or accessed via *FISH*.

(1)	**sta**te	plastic state*
(2)	**stra**in-**sh**ear-**pl**astic	accumulated plastic shear strain
(3)	**stra**in-**ten**sion-**pl**astic	accumulated plastic tensile strain
(4)	**stra**in-**vo**lumetric-**pl**astic	accumulated plastic volumetric strain

---

* plastic state codes for double-yield model: (1) currently at yield in shear; (2) currently at yield in tension; (4) shear yield in past; (8) tension yield in past; (256) current volumetric yield; (512) volumetric yield in past.

1.6.7 Modified Cam-Clay Model

The modified Cam-clay model is an incremental hardening/softening elastoplastic model. Its features include a particular form of nonlinear elasticity, and a hardening/softening behavior governed by volumetric plastic strain ("density" driven). The failure envelopes are similar in shape, and correspond to ellipsoids of rotation about the mean stress axis in the principal stress space. The shear flow rule is associated; no resistance to tensile mean stress is offered in this model. See Roscoe and Burland (1968) and Wood (1990) for detailed discussions on the modified Cam-clay model. (For convenience, we drop the qualifier "modified" in the following discussion. Recall that all models are expressed in terms of effective stresses. In particular, all pressures referred to in this section are effective pressures.)

1.6.7.1 Incremental Elastic Law

The Cam-clay model is expressed in terms of three variables: the mean effective pressure, p; the deviatoric stress, q; and the specific volume, v. In the *UDEC* implementation of this model, principal stresses $\sigma_1, \sigma_2, \sigma_3$ are used, the out-of-plane stress, σ_{zz}, being recognized as one of these. (By convention, traction and dilation are positive.)

The generalized stress components p and q may be expressed in terms of principal stresses:

$$\begin{aligned} p &= -\frac{1}{3}(\sigma_1 + \sigma_2 + \sigma_3) \\ q &= \frac{1}{\sqrt{2}}\sqrt{(\sigma_1 - \sigma_2)^2 + (\sigma_2 - \sigma_3)^2 + (\sigma_1 - \sigma_3)^2} \end{aligned} \tag{1.193}$$

(Note that $q = \sqrt{3J_2}$, where J_2 is the second invariant of the effective stress deviator tensor.)

The incremental strain variables associated with $-p$ and q are the volumetric strain increment, Δe, and distortional strain increment, Δe_q, and we have

$$\begin{aligned} \Delta e &= \Delta e_1 + \Delta e_2 + \Delta e_3 \\ \Delta e_q &= \frac{\sqrt{2}}{3}\sqrt{(\Delta e_1 - \Delta e_2)^2 + (\Delta e_2 - \Delta e_3)^2 + (\Delta e_1 - \Delta e_3)^2} \end{aligned} \tag{1.194}$$

where Δe_j, $j = 1, 3$ are principal strain increments. The principal strain increments may be decomposed into elastic and plastic parts so that

$$\Delta e_i = \Delta e_i^e + \Delta e_i^p \qquad i = 1, 3 \tag{1.195}$$

The specific volume v is defined as

$$v = \frac{V}{V_s} \tag{1.196}$$

where V_s is the volume of solid particles (assumed incompressible) contained in a volume, V, of soil. The incremental relation between volumetric strain, e, and specific volume has the form

$$\Delta e = \frac{\Delta v}{v} \tag{1.197}$$

Starting with an initial specific volume, v_0, we may thus write, for small volumetric strain increments,

$$v = v_0(1 + e) \tag{1.198}$$

where e is the current accumulated volumetric strain.

The incremental expression of Hooke's law in principal axes may be expressed in the form

$$\begin{aligned} \Delta\sigma_1 &= \alpha_1 \Delta e_1^e + \alpha_2(\Delta e_2^e + \Delta e_3^e) \\ \Delta\sigma_2 &= \alpha_1 \Delta e_2^e + \alpha_2(\Delta e_1^e + \Delta e_3^e) \\ \Delta\sigma_3 &= \alpha_1 \Delta e_3^e + \alpha_2(\Delta e_1^e + \Delta e_2^e) \end{aligned} \tag{1.199}$$

where $\alpha_1 = K + 4G/3$; and

$\alpha_2 = K - 2G/3$.

Alternatively, using deviatoric parts of incremental stress and strain tensors, we may write

$$\begin{aligned} \Delta s_i &= 2G\Delta\epsilon_i^e \qquad i = 1, 3 \\ -\Delta p &= K\Delta e^e \end{aligned} \tag{1.200}$$

where $\Delta s_i = \Delta\sigma_i + \Delta p$;

$\Delta\epsilon_i^e = \Delta e_i^e - \Delta e^e/3$; and

$\Delta e^e = \Delta e_1^e + \Delta e_2^e + \Delta e_3^e$.

In the Cam-clay model, the tangential bulk modulus, K, in the volumetric relation Eq. (1.200) is updated to reflect a nonlinear law derived experimentally from isotropic compression tests. The results of a typical isotropic compression test are presented in the semi-logarithmic plot of Figure 1.23.

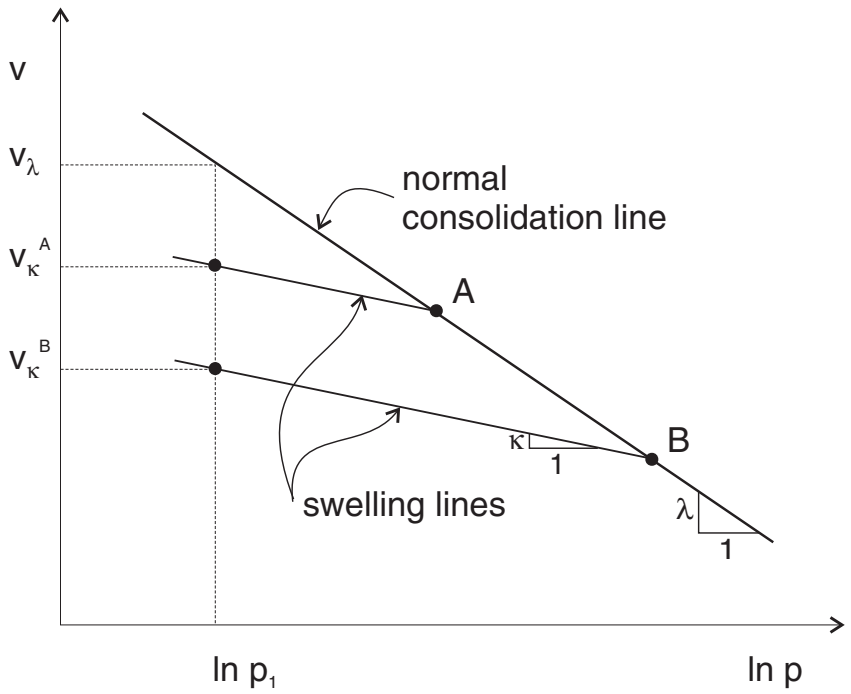

Figure 1.23 Normal consolidation line and unloading-reloading (swelling) line for an isotropic compression test

As the normal consolidation pressure, p, increases, the specific volume, v, of the material decreases. The point representing the state of the material moves along the *normal consolidation line* defined by the equation

$$v = v_\lambda - \lambda \ln \frac{p}{p_1} \tag{1.201}$$

where λ* and v_λ are two material parameters, and p_1 is a reference pressure. (Note that v_λ is the value of the specific volume at the reference pressure.)

---

* λ is used by Wood (1990) to define the slope of the normal consolidation line. It should not be confused with the plastic (volumetric) multiplier, λ^s, used in the plasticity flow rule given in Section 1.6.7.3.

An unloading-reloading excursion, from point A or B on the figure, will move the point along an *elastic swelling line* of slope κ, back to the normal consolidation line where the path will resume. The equation of the swelling lines has the form

$$v = v_\kappa - \kappa \ln \frac{p}{p_1} \tag{1.202}$$

where κ is a material constant, and the value of v_κ for a particular line depends on the location of the point on the normal consolidation line from which unloading was performed.

The recoverable change in specific volume Δv^e may be expressed in incremental form after differentiation of Eq. (1.202):

$$\Delta v^e = -\kappa \frac{\Delta p}{p} \tag{1.203}$$

After division of both members by v, and comparing with Eq. (1.197), we may write

$$-\Delta p = \frac{vp}{\kappa} \Delta e^e \tag{1.204}$$

In the Cam-clay model it is assumed that any change in mean pressure is accompanied by elastic change in volume according to the above expression. Comparison with Eq. (1.200) hence suggests the following expression for the tangent bulk modulus of the Cam-clay material:

$$K = \frac{vp}{\kappa} \tag{1.205}$$

Under more general loading conditions, the state of a particular point in the medium might be represented by a point, such as A, located below the normal consolidation line in the $(v, \ln p)$ plane (see Figure 1.24). By virtue of the law adopted in Eq. (1.203), an elastic path from that point proceeds along the swelling line through A.

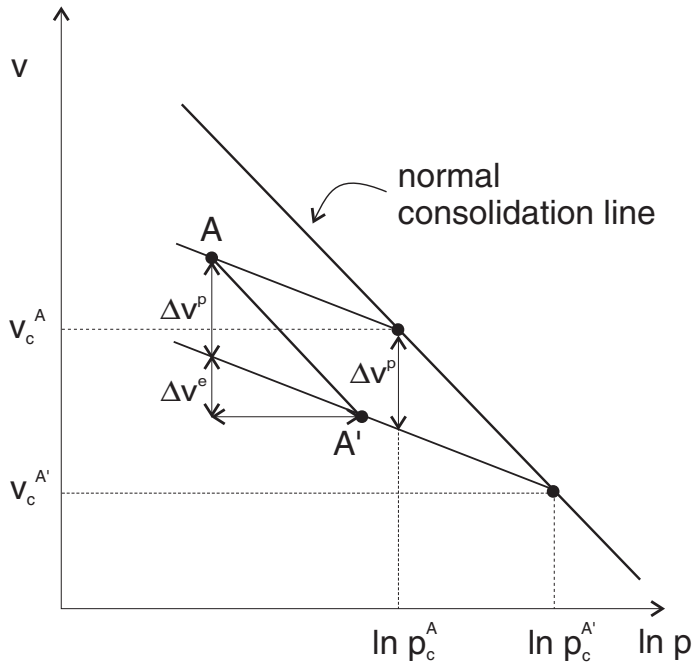

Figure 1.24 Plastic volume change corresponding to an incremental consolidation pressure change

The specific volume and mean pressure at the intersection of swelling line and normal consolidation line are referred to as *(normal) consolidation (specific) volume* and *(normal) consolidation pressure*: v_c^A and p_c^A, in the case of point A. Consider an incremental change in stress bringing the point from state A to state A'. At A' there is a corresponding consolidation volume, $v_c^{A'}$, and consolidation pressure, $p_c^{A'}$. The increment of plastic volume change, Δv^p, is measured on the figure by the vertical distance between swelling lines (associated with points A and A'), and we may write, using incremental notation,

$$\Delta v^p = -(\lambda - \kappa)\frac{\Delta p_c}{p_c} \tag{1.206}$$

After division of the left and right member by v, we obtain, comparing with Eq. (1.197),

$$\Delta e^p = -\frac{\lambda - \kappa}{v}\frac{\Delta p_c}{p_c} \tag{1.207}$$

Hence, whereas elastic changes in volume occur whenever the mean pressure changes, plastic changes of volume occur only when the consolidation pressure changes.

1.6.7.2 Yield and Potential Functions

The yield function corresponding to a particular value p_c of the consolidation pressure has the form

$$f = q^2 + M^2 p(p - p_c) \tag{1.208}$$

where M is a material constant. The yield condition $f = 0$ is represented by an ellipse with horizontal axis, p_c, and vertical axis, Mp_c, in the (q, p) plane (see Figure 1.25). Note that the ellipse passes through the origin. Hence, the material in this model is not able to support an all-around tensile stress.

The failure criterion is represented in the principal stress space by an ellipsoid of rotation about the mean stress axis (any section through the yield surface at constant mean effective stress, p, is a circle).

The potential function g corresponds to an associated flow rule and we have

$$g = q^2 + M^2 p(p - p_c) \tag{1.209}$$

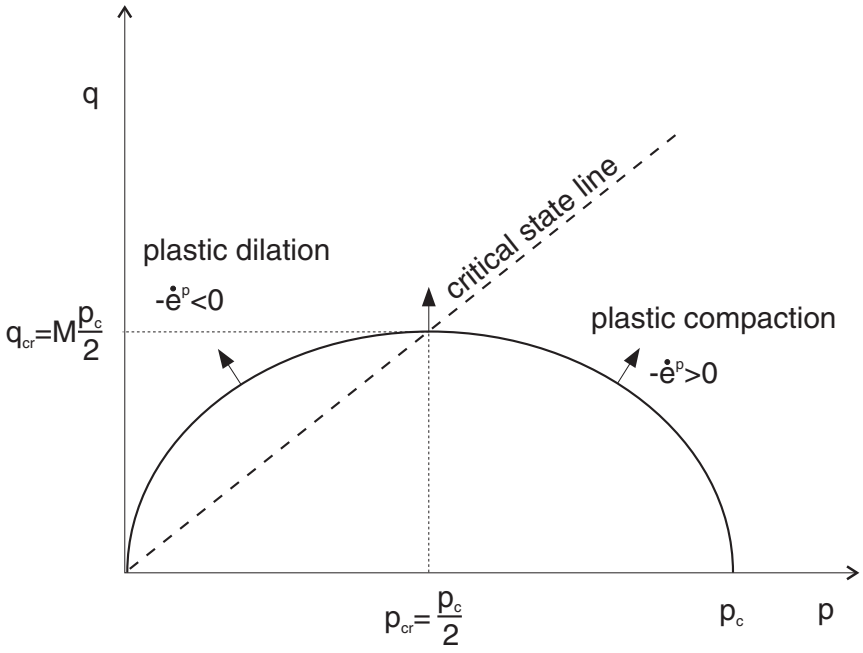

Figure 1.25 Cam-clay failure criterion in UDEC

1.6.7.3 Plastic Corrections

The flow rule used to describe plastic flow has the form

$$\Delta e_i^p = \lambda^s \frac{\partial g}{\partial \sigma_i} \qquad i = 1, 3 \tag{1.210}$$

where λ^s is a parameter whose magnitude remains to be defined.

Using Eq. (1.209) for g, these expressions give, after partial differentiation,

$$\begin{aligned} \Delta e_1^p &= \lambda^s c_a \\ \Delta e_2^p &= \lambda^s c_b \\ \Delta e_3^p &= \lambda^s c_c \end{aligned} \tag{1.211}$$

where

$$\begin{aligned} c_a &= \frac{M^2}{3}(2p - p_c) + (\sigma_1 - \sigma_2) + (\sigma_1 - \sigma_3) \\ c_b &= \frac{M^2}{3}(2p - p_c) + (\sigma_2 - \sigma_1) + (\sigma_2 - \sigma_3) \\ c_c &= \frac{M^2}{3}(2p - p_c) + (\sigma_3 - \sigma_1) + (\sigma_3 - \sigma_2) \end{aligned} \tag{1.212}$$

The elastic strain increments may be expressed from Eq. (1.195) as total increments minus plastic increments. In further using Eq. (1.211), the elastic laws in Eq. (1.199) become

$$\begin{aligned} \Delta\sigma_1 &= \alpha_1 \Delta e_1 + \alpha_2(\Delta e_2 + \Delta e_3) \\ &\quad - \lambda^s \left[\alpha_1 c_a + \alpha_2(c_b + c_c)\right] \\ \Delta\sigma_2 &= \alpha_1 \Delta e_2 + \alpha_2(\Delta e_1 + \Delta e_3) \\ &\quad - \lambda^s \left[\alpha_1 c_b + \alpha_2(c_a + c_c)\right] \\ \Delta\sigma_3 &= \alpha_1 \Delta e_3 + \alpha_2(\Delta e_1 + \Delta e_2) \\ &\quad - \lambda^s \left[\alpha_1 c_c + \alpha_2(c_a + c_b)\right] \end{aligned} \tag{1.213}$$

Let the new and old stress states be referred to by the superscripts ^{N} and ^{O}, respectively. Then, by definition,

$$\sigma_i^N = \sigma_i^O + \Delta\sigma_i \qquad i = 1, 3 \tag{1.214}$$

Substitution of Eq. (1.213) gives

$$\begin{aligned}
\sigma_1^N &= \sigma_1^I - \lambda^s \left[\alpha_1 c_a + \alpha_2 (c_b + c_c)\right] \\
\sigma_2^N &= \sigma_2^I - \lambda^s \left[\alpha_1 c_b + \alpha_2 (c_a + c_c)\right] \\
\sigma_3^N &= \sigma_3^I - \lambda^s \left[\alpha_1 c_c + \alpha_2 (c_a + c_b)\right]
\end{aligned} \tag{1.215}$$

where the superscript ^{I} is used to represent the elastic guess, obtained by adding to the old stresses, elastic increments computed using the total strain increments – i.e.,

$$\begin{aligned}
\sigma_1^I &= \sigma_1^O + \alpha_1 \Delta e_1^e + \alpha_2 (\Delta e_2^e + \Delta e_3^e) \\
\sigma_2^I &= \sigma_2^O + \alpha_1 \Delta e_2^e + \alpha_2 (\Delta e_1^e + \Delta e_3^e) \\
\sigma_3^I &= \sigma_3^O + \alpha_1 \Delta e_3^e + \alpha_2 (\Delta e_1^e + \Delta e_2^e)
\end{aligned} \tag{1.216}$$

The parameter λ^s may now be defined by requiring that the new stress point be located on the yield surface. Substitution of σ_i^N, as given by Eq. (1.215) for σ_i, $i = 1, 3$ in $f = 0$ give, after some manipulations (see Eq. (1.208)),

$$a\lambda^{s\,2} + b\lambda^s + c = 0 \tag{1.217}$$

where

$$\begin{aligned}
a =& 2G^2 \left[(c_a - c_b)^2 + (c_b - c_c)^2 + (c_c - c_a)^2\right] + M^2 K^2 (c_a + c_b + c_c)^2 \\
b =& -2G \left[(\sigma_1^I - \sigma_2^I)(c_a - c_b) + (\sigma_2^I - \sigma_3^I)(c_b - c_c) + (\sigma_3^I - \sigma_1^I)(c_c - c_a)\right] \\
& - M^2 K (c_a + c_b + c_c)(2p^I - p_c) \\
c =& f(q^I, p^I)
\end{aligned} \tag{1.218}$$

Of the two roots of this equation, the one with the smallest modulus must be retained.

Note that at the *critical* point corresponding to $p_{cr} = p_c/2, q_{cr} = Mp_c/2$ in Figure 1.25, the normal to the yield curve, $f = 0$, is parallel to the q-axis. Since the flow rule is associated, the plastic volumetric strain rate component vanishes there. As a result of the hardening rule Eq. (1.207), the consolidation pressure, p_c, will not change. The corresponding material point has reached the *critical state*, in which unlimited shear strains occur with no accompanying change in specific volume or stress level.

1.6.7.4 Hardening/Softening Rule

The size of the yield curve is dependent on the value of the consolidation pressure, p_c (see Eq. (1.208)). This pressure is a function of the plastic volume change, and varies with the specific volume, as indicated in Eq. (1.207).

The consolidation pressure, p_c, corresponding to new values for v and p may easily be found by intersection of the consolidation line with the swelling line through $(v, \ln p)$. This gives, using Eqs. (1.201) and (1.202),

$$p_c = p_1 e^{(v_\lambda - v_\kappa)/(\lambda - \kappa)} \tag{1.219}$$

where

$$v_\kappa = v + \kappa \ln \frac{p}{p_1} \tag{1.220}$$

1.6.7.5 Initial Stress State

The Cam-clay model in *UDEC* is only applicable to material in which the stress state corresponds to a compressive mean effective stress. This model is not designed to predict the behavior of material in which this condition is not met. In particular, the initial state of the material (just before application of the Cam-clay model) must be consistent with this requirement. The initial state may be specified using the **pressure-initial** command, or may be the result of a run in which another constitutive model has been used. In any case, the initial effective pressure, defined as p_0, must be positive throughout the medium.

1.6.7.6 Overconsolidation Ratio

The overconsolidation ratio, R, is defined as the ratio of initial pre-consolidation pressure to initial pressure – i.e.,

$$R = \frac{p_{c0}}{p_0} \tag{1.221}$$

This ratio is useful in characterizing the behavior of Cam-clay material.

1.6.7.7 Implementation Procedure

In the implementation of the Cam-clay model in *UDEC*, an elastic guess, σ_{ij}^{I}, is first computed by adding to the old stress components, increments calculated by application of Hooke's law to the total strain increment for the step. The principal stresses σ_i^I, $i = 1, 3$ and corresponding principal directions are then evaluated.

Elastic guesses for the mean pressure, p^I, and deviator stress, q^I, are calculated using Eq. (1.193). If these stresses violate the yield criterion and $f(q^I, p^I) < 0$ (see Eq. (1.208)), plastic deformation takes place and the consolidation pressure changes. In this situation, a correction must be applied to the elastic guess to give the new stress state: new principal stresses are derived from Eqs. (1.212) and (1.215). These equations use a value for λ^s corresponding to the root of Eqs. (1.217) and (1.218), and using the smallest modulus. Note that, in this version of the code, Eq. (1.212) is evaluated using the elastic guess. However, the error associated with this technique is small, provided the steps are small. New stress tensor components in the system of reference axes are then evaluated, assuming the principal directions have not been affected by the occurrence of plastic flow.

Volumetric strain increment, Δe, and mean pressure, p, for the zone are computed as average over all involved triangles (see Eqs. (1.193) and (1.194)). The zone volumetric strain, e, is incremented, and the zone specific volume, v, updated, using Eq. (1.198). In turn, the new zone consolidation pressure is calculated from Eq. (1.219), and the tangential bulk modulus is updated using Eq. (1.205). If a nonzero value for the Poisson's ratio property is imposed, a new shear modulus is calculated from the expression $G = 1.5(1 - 2\nu)K/(1 + \nu)$. Otherwise, G is left unchanged as long as the condition $0 \leq \nu \leq 0.5$ is satisfied. If it is not, G is assigned a value corresponding to $\nu = 0$ or $\nu = 0.5$, as appropriate. The new values for the consolidation pressure, and shear and bulk moduli, are then stored for use in the next timestep. The material properties thus lag one timestep behind the corresponding calculation. In an explicit code, this error is small because the steps are small.

1.6.7.8 Determination of the Input Parameters

Frictional constant M – M is the ratio of q/p_{cr} at the critical state line. Therefore, a series of triaxial tests (drained or undrained with pore pressure measurement) can be used to obtain this constant. These tests should be carried out to large strains to ensure that the final values of p_{cr} and q are close to the critical state line. The slope of a best-fitting line of q vs p_{cr} will be the parameter M.

M is related to the effective stress friction angle, ϕ', of the Mohr-Coulomb yield function. However, since the Cam-clay critical state line is dependent on the intermediate stress, σ_2, while Mohr-Coulomb is not, the relation between M and ϕ' will be different for different values of σ_2 at yield. (This condition is similar to the relation between Mohr-Coulomb and Drucker-Prager yield functions – see Section 1.6.1.5.) For triaxial compression tests,

$$M = \frac{6 \sin \phi'}{3 - \sin \phi'} \tag{1.222}$$

while for triaxial extension tests,

$$M = \frac{6 \sin \phi'}{3 + \sin \phi'} \tag{1.223}$$

The slopes of the normal consolidation and swelling lines (λ and κ) – Ideally, these two parameters should be obtained from an isotropically loaded triaxial test ($q = 0$) with several unloading excursions. The slope of the normal compression line in a v versus ln p plot will be the parameter λ. The slope of an unloading excursion in the same plot will be the parameter κ.

These two parameters can also be derived from an oedometer test, making certain assumptions. Let σ_v and σ_H be the vertical and horizontal stresses in an oedometer test. In most oedometer apparatus, it is not possible to measure the horizontal stresses, σ_H, so the mean stress, $p = (\sigma_v + 2\sigma_H)/3$, is not known. However, experimental data show that the ratio of horizontal to vertical effective stresses, K_0, is constant during normal compression. Since $p = \sigma_v(1 + 2K_0)/3$ along the normal compression line, the slope of v vs ln p will be equal to the slope of e versus ln σ_v, where e is the void ratio = $v - 1$.

The compression index, C_c, is calculated as the slope of e vs $\log_{10}(\sigma_v)$. So the parameter λ will be

$$\lambda = C_c / \ln(10) \tag{1.224}$$

Experimental data show that along a swelling line in an oedometer test, K_0 is *not* constant, so an estimate of κ based on the swelling coefficient, C_s, will only be an approximation:

$$\kappa \approx C_s / \ln(10) \tag{1.225}$$

In practice, κ is usually chosen in the range of one-fifth to one-third of λ.

Location of the normal consolidation line in the v versus ln p plot – In order to determine the location of the normal consolidation line in the v versus ln p plot, a point (v_λ, ln p_1) on this line must be specified. The obvious way to determine this point is to perform an isotropic triaxial test. There is an alternative way to determine this point based on the undrained shear strength (for details, see Britto and Gunn 1987).

The equation of the normal consolidation line is (see Eq. (1.201))

$$v = v_\lambda - \lambda \ln \frac{p}{p_1} \tag{1.226}$$

The specific volume Γ at the critical state line for $p = p_1$ is given by

$$\Gamma = v_\lambda - (\lambda - \kappa) \times \ln(2) \tag{1.227}$$

In a soil, the undrained shear strength, c_u, is uniquely related to the specific volume, v_{cr}, by the equation

$$c_u = \frac{Mp_1}{2} \exp\left(\frac{\Gamma - v_{cr}}{\lambda}\right) \tag{1.228}$$

Thus, the value of Γ for a given p_1, and therefore v_λ, can be calculated if the undrained shear strength for a particular specific volume, v_{cr}, along with the parameters M, λ and κ, is known.

Pre-consolidation pressure, p_{c0} – The pre-consolidation pressure determines the initial size of the yield surface in the equation

$$q^2 = M^2[p(p_{c0} - p)] \tag{1.229}$$

If a sample has been submitted to an isotropic loading path, p_{c0} will be the maximum past mean effective stress. If the sample has followed other non-isotropic paths, p_{c0} has to be calculated from the maximum previous p and q, using Eq. (1.229).

The maximum vertical effective stress can be calculated from an oedometer test using Casagrande's method (for details, see Britto and Gunn 1987). Some hypothesis has to be made about the maximum horizontal effective stress. A common hypothesis is Jaky's relation (e.g., see Britto and Gunn 1987),

$$K_{nc} = \frac{\sigma_{h\,\max}}{\sigma_{v\,\max}} \simeq 1 - \sin\phi' \tag{1.230}$$

where K_{nc} is the coefficient of horizontal $\sigma_{h\,\max}$ to vertical $\sigma_{v\,\max}$ stress at rest for normally consolidated soil. For example, if a soil with an effective friction angle of 20° has experienced a maximum vertical effective stress, $\sigma_{v\,\max} = 1$ MPa. Then, using Jaky's relation,

$$K_{nc} = 1 - \sin 20^\circ = 0.658 \tag{1.231}$$

and the maximum horizontal stress is

$$\sigma_{h\,\max} = 0.658 \text{ MPa} \tag{1.232}$$

The maximum values of p and q are

$$p_{\max} = \frac{\sigma_{v\,\max} + 2\sigma_{h\,\max}}{3} = 0.772 \text{ MPa}$$
$$q_{\max} = \sigma_{v\,\max} - \sigma_{h\,\max} = 0.342 \text{ MPa} \tag{1.233}$$

Substituting these two values in the yield function Eq. (1.229), we obtain the pre-consolidation pressure

$$p_{c0} = p_{\max} + \frac{q_{\max}^2}{M^2\, p_{\max}} = 1.026 \text{ MPa} \tag{1.234}$$

Initial values for specific volume v_0 ***and current bulk modulus*** K – Given an initial effective pressure, p_0, the initial specific volume, v_0, must be consistent with the choice of parameters κ, λ, p_1 and p_{c0}. The initial value, v_0, is calculated by the code to correspond to the value of the specific volume corresponding to p_0 on the swelling line, through the point on the normal consolidation line at which $p = p_{c0}$. From Figure 1.26, it follows that

$$v_0 = v_\lambda - \lambda \ln\left(\frac{p_{c0}}{p_1}\right) + \kappa \ln\left(\frac{p_{c0}}{p_0}\right) \tag{1.235}$$

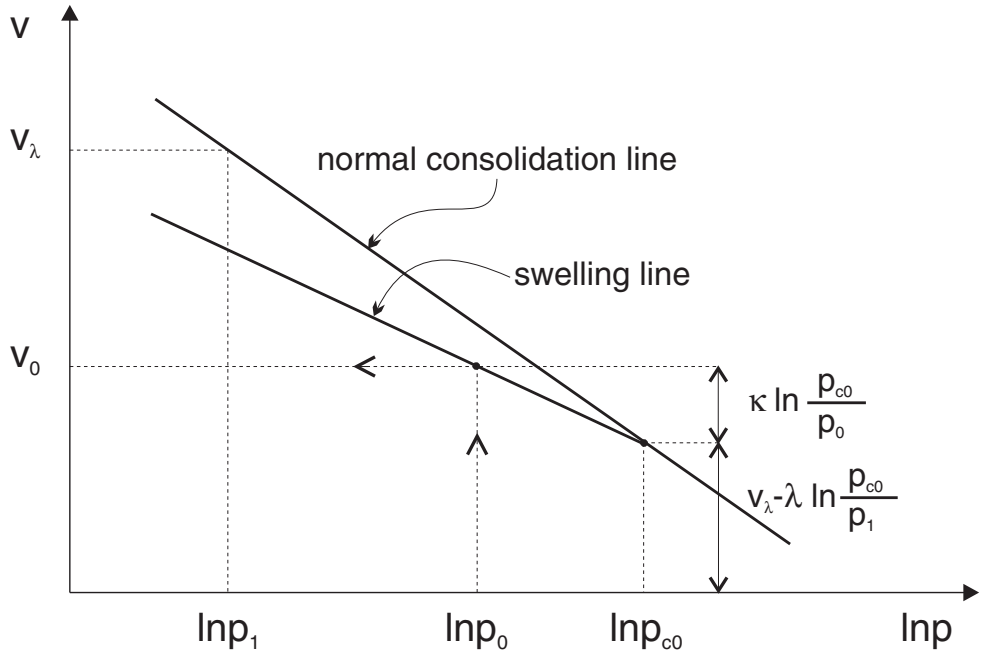

Figure 1.26 Determination of initial specific volume

The initial value of the current bulk modulus (**bulk**) may in turn be evaluated using Eq. (1.205), which gives

$$K = \frac{v_0 p_0}{\kappa} \tag{1.236}$$

In *UDEC*, the default values for v_0 and K are evaluated using Eqs. (1.235) and (1.236) when the first step command is issued.

Maximum value of the elastic parameters K ***and*** G – In the Cam-clay model, the value of the current bulk modulus (**bulk**) changes as a function of the specific volume and the mean stress:

$$K = \frac{vp}{\kappa} \tag{1.237}$$

The input values of K_{max} (**bulk**) and G (**shear**) are used in the mass scaling calculation performed in *UDEC*, to ensure numerical stability (see Section 1.2.9 in **Theory and Background**). This calculation is done once every time a **block cycle step** command is issued. These input values should be chosen so as to give an upper bound to the sum $(K + 4/3G)$, as evaluated by the model between two consecutive **block cycle step** commands. However, values should not be set too high, or the model may be slow to converge. They should be selected based on the stress level in the problem.

G ***or*** ν – The modified Cam-clay model in *UDEC* allows the user to specify either a constant shear modulus or a constant Poisson's ratio.

If no Poisson's ratio is specified, a constant shear modulus equal to the input value is assumed. Then the Poisson's ratio will vary as a function of the specific volume and the mean stress:

$$\nu = \frac{3\left(\frac{vp}{\kappa}\right) - 2G}{6\left(\frac{vp}{\kappa}\right) + 2G} \tag{1.238}$$

If a nonzero Poisson's ratio is specified, the shear modulus will vary at the same rate as the bulk modulus in order to maintain a constant Poisson's ratio:

$$G = \frac{3\left(\frac{vp}{\kappa}\right)(1 - 2\nu)}{2\,(1 - 2\nu)} \tag{1.239}$$

1.6.7.9 Oedometer Test

The numerical simulation of an oedometer test on a Cam-clay sample is presented in this example. It may be shown that, in the framework of the modified Cam-clay model, the stress path for one-dimensional normal compression corresponds to a straight line in the p-q-plane (see Wood 1990). The slope of this line, η, may be derived from the expression

$$\frac{\eta(1+\nu)(1-\Lambda)}{3(1-2\nu)} + \frac{3\eta\Lambda}{M^2-\eta^2} = 1 \tag{1.240}$$

where ν is the constant Poisson's ratio for the test $\Lambda = (\lambda - \kappa)/\lambda$, and M, λ and κ are Cam-clay model properties.

The boundary conditions for the oedometer test are represented in Figure 1.27. In this test, the ratio, K_0, of horizontal to vertical stresses is related to η by the formula

$$K_0 = \frac{3-\eta}{3+2\eta} \tag{1.241}$$

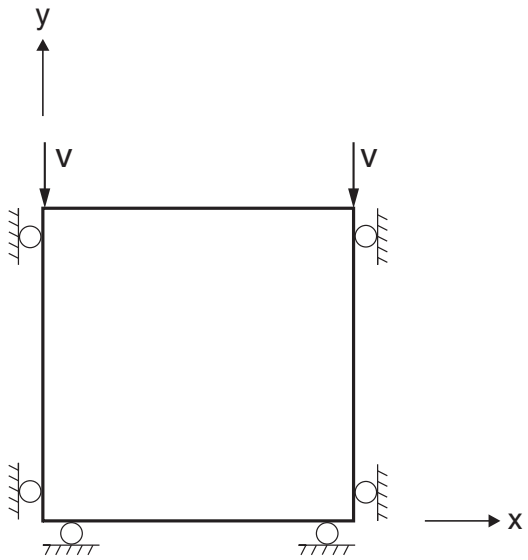

Figure 1.27 Boundary conditions for oedometer test

In soils that have a history of one-dimensional deformation, this ratio is called the "coefficient of earth pressure at rest." The coefficient K_0 is evaluated numerically using the data file in Example 1.5, and compared to the analytic value derived from the above expression.

The simulation is carried out using a single zone of unit dimensions. Several properties are used in conjunction with the Cam-clay model:

bulk modulus(maximum value), K	50000 Pa
Poisson's ratio, ν	0.3
frictional constant, M	1.02
slope of normal consolidation line, λ	0.2
slope of elastic swelling line, κ	0.05
reference pressure, p_1	1 Pa
specific volume, v_λ	3.32

The analytical value of K_0 is evaluated using the *FISH* function **c_konc**. A nonzero initial stress state is specified with values $\sigma_{yy} = -5$ Pa and $\sigma_{xx} = \sigma_{zz} = K_0\sigma_{yy}$. The initial value of p_c corresponds to a normally consolidated state, and is calculated using Eq. (1.234). The velocity components are fixed in the x- and y-directions. A velocity of magnitude 10^{-5} m/steps is applied to the top of the model in the negative y-direction for a total of 1000 steps. The ratio of horizontal to vertical stress is monitored and compared to the analytic prediction for K_0. The match is very good where numerical and analytic solutions coincide, as may be seen in Figure 1.28. The stress paths in the $(\sigma_{yy}, \sigma_{xx})$ and (p, q) planes are represented in Figures 1.29 and 1.30; they correspond to straight line trajectories, as expected.

Example 1.5 Oedometer test on a Cam-clay material

```
model new
;file: cam_clay.dat
model title 'Cam-Clay'
;-------------------------------------------------------------
; Oedometric test on cam-clay sample (drained)
; 'coefficient of earth pressure' konc: comparison between
; numerical and analytical predictions
; Wood, Soil behaviour and critical soil mechanics, p314-319
;-------------------------------------------------------------
block config axisymmetry
block tolerance corner-round-length 0.001
block tolerance minimum-edge-length 0.002
block create polygon 0 0 0 1 1 1 1 0
block zone gen edge 2
; --- model properties ---
block zone group 'mat1'
block zone cmodel assign modified-cam-clay density 1 bulk-maximum 5E4 ...
  shear 250 poisson 0.3 kappa 0.05 lambda 0.2 ratio-critical-state 1.02 ...
  pressure-reference 1 specific-volume-reference 3.32 ...
  range group 'mat1'
;
```

```
; --- boundary conditions ---
block gridpoint apply velocity-x 0
block gridpoint apply velocity-y 0 range pos-x -0.01 1.01 pos-y -0.01 0.01
block gridpoint apply velocity-y -3.167e-3 ...
   range pos-x -0.01 1.01 pos-y 0.99 1.01
;
; --- fish functions ---
; ... analytical value for konc ...
fish define c_konc
  bi = block.head
  zi = block.zone(bi)
  c_l = 1. - block.zone.prop(zi,'kappa')/block.zone.prop(zi,'lambda')
  c_b = 3.*c_l
  c_a = (1.+block.zone.prop(zi,'poisson'))*(1.-c_l)/(3.*...
     (1.-2.*block.zone.prop(zi,'poisson')))
  m2  = block.zone.prop(zi,'ratio-critical-state')* ...
    block.zone.prop(zi,'ratio-critical-state')
  a1  = -1./c_a
  a2  = -(c_a*m2+c_b)/c_a
  a3  = m2/c_a
  bq  = (a1*a1-3.*a2)/9.
  br  = (a1*(2.*a1*a1-9.*a2)+27.*a3)/54.
  aux = br*br-bq*bq*bq
  eta = 0.0
  if aux > 0.0 then
   aux = (math.sqrt(aux)+math.abs(br))^(1./3.)
   eta = -math.sgn(br)*(aux+bq/aux)-a1/3.
   konc = (3.-eta)/(3.+2.*eta)
  else
   aux = math.sqrt(-aux)/math.abs(br)
   teta= math.atan(aux)+math.pi
   aux1 = 2.*math.sqrt(bq)
   aux2 = a1/3.
   eta1 = -aux1*math.cos((teta)/3.)-aux2
   eta2 = -aux1*math.cos((teta+2.*math.pi)/3.)-aux2
   eta3 = -aux1*math.cos((teta+4.*math.pi)/3.)-aux2
   konc1 = (3.-eta1)/(3.+2.*eta1)
   konc2 = (3.-eta2)/(3.+2.*eta2)
   konc3 = (3.-eta3)/(3.+2.*eta3)
   konc = math.max(konc1,konc2)
   konc = math.max(konc,konc3)
 end_if
; ... Jaky,s approximate expression for konc = 1 - sin(phi) ...
 kjaky = 1.-3.*block.zone.prop(zi,'ratio-critical-state')/...
   (6.+block.zone.prop(zi,'ratio-critical-state'))
end
```

```
; ... initial, normally consolidated state ...
fish define i_state
  isyy = -5.0
  p_i = -isyy * (1.0 + 2.0 * konc) / 3.
  q_i = -isyy * (1.0 - konc)
  val = q_i / (block.zone.prop(zi,'ratio-critical-state')*p_i)
  bi = block.head
  zi = block.zone(bi)
  loop while zi # 0
    block.zone.stress.xx(zi) = isyy * konc
    block.zone.stress.yy(zi) = isyy
    block.zone.stress.zz(zi) = isyy * konc
    block.zone.prop(zi, 'pressure-preconsolidation') = ...
      p_i * (1.0 + val * val)
    zi = block.zone.next(zi)
  endloop
end
;
fish define camclay_ini_p
  bi = block.head
  zi = block.zone(bi)
  loop while zi # 0
    mean_p = -(block.zone.stress.xx(zi) + block.zone.stress.yy(zi)  + ...
      block.zone.stress.zz(zi) )/3. - block.zone.pp(zi)
    block.zone.prop(zi, 'pressure-effective') = mean_p
    zi = block.zone.next(zi)
  endloop
end
; ... numerical values for p, q, v ...
fish define path
  zi = block.zone(block.head)
  zoneNum = 0
  s1 = 0.0
  s2 = 0.0
  s3 = 0.0
  sp = 0.0
  sq = 0.0
  loop while zi # 0
    s1   = s1 + block.zone.stress.yy(zi)
    s2   = s2 + block.zone.stress.zz(zi)
    s3   = s3 + block.zone.stress.xx(zi)
    sp = sp + block.zone.prop(zi,'pressure-effective')
    sq = sq + block.zone.prop(zi,'stress-deviatoric')
    zoneNum = zoneNum +1
    zi = block.zone.next(zi)
  endloop
```

```
  zi = block.zone(block.head)
  s1 = -s1/zoneNum
  s2 = -s2/zoneNum
  s3 = -s3/zoneNum
  k0   = 0.0
  if s1 # 0 then
    k0 = s3 / s1
  end_if
  sp     = sp/zoneNum
  sq     = sq/zoneNum
  dif    = sq / sp - 3.*(1.-k0)/(1.+2.*k0)
  sqcr   = sp*block.zone.prop(zi,'ratio-critical-state')
  lnp    = math.ln(sp)
  logsy  = math.log(s1)
  c_sv   = block.zone.prop(zi,'specific-volume')
  void_ratio=c_sv-1.
  mk     = block.zone.prop(zi,'bulk')
  mg     = block.zone.prop(zi,'shear')
  s1konc = s1 * konc
end
;
; ... loading-unloading excursions ...
fish define trip
  loop i (1,3)
    command
      block gridpoint apply velocity-y -5E-5 ...
        range pos-x -0.01 10.01 pos-y 9.99 10.01
      block cycle 2000
      block gridpoint apply velocity-y 5E-6 ...
        range pos-x -0.01 10.01 pos-y 9.99 10.01
      block cycle 1500
      block gridpoint apply velocity-y -5E-6 ...
        range pos-x -0.01 10.01 pos-y 9.99 10.01
      block cycle 2500
    end_command
  end_loop
end
;
; --- histories ---
his interval 20
block mechanical history unbalanced-maximum
fish history @path
fish history @sp
fish history @lnp
fish history @logsy
fish history @sq
```

```
fish history @sqcr
fish history @c_sv
fish history @mk
fish history @mg
block gridpoint history displacement-y 0 1
fish history @k0
fish history @konc
fish history @s1
fish history @s3
fish history @s1konc
fish history @dif
fish history @void_ratio
; --- test ---
@c_konc
@i_state
@camclay_ini_p
@trip
block cycle 1000
;plot hold hist 12 cross 13   vs -11 ywin 0 1
;plot hold hist 15 cross 16 vs 14
;plot hold hist 6 vs 3 ywin 1.44 1.58
return
```

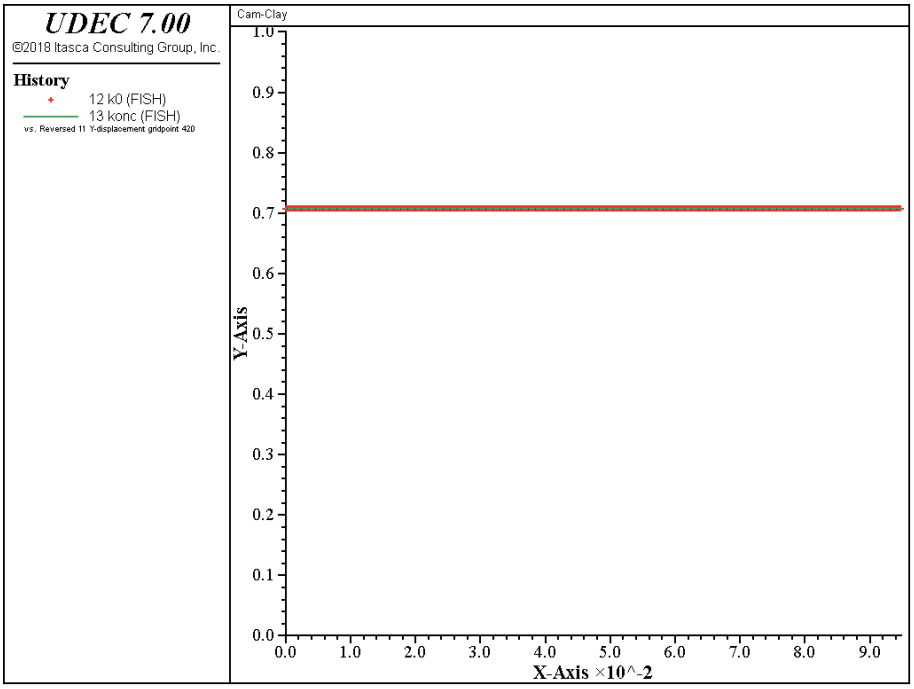

Figure 1.28 Oedometric test – comparison of numerical and analytical values for K_0

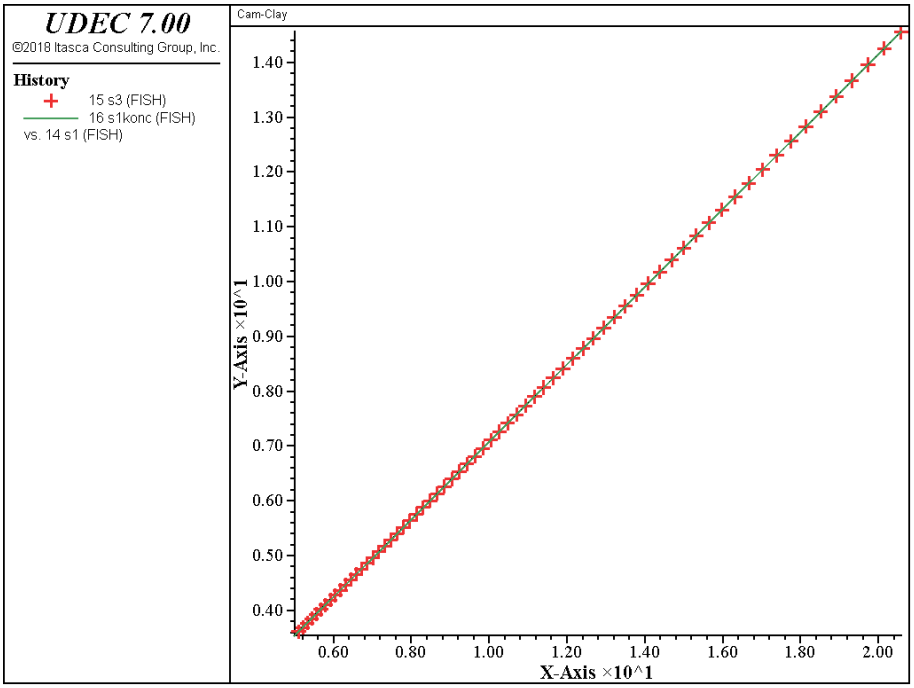

Figure 1.29 Oedometric test – history of vertical versus horizontal stresses

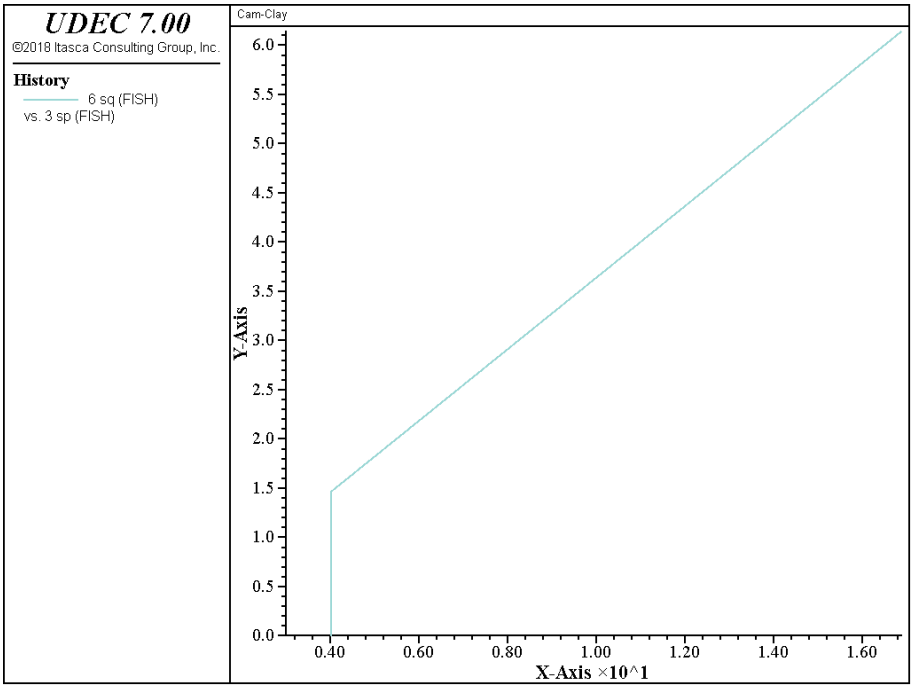

Figure 1.30 Oedometric test – history of stresses q versus p

1.6.7.10 **block zone cmodel** *Command and Property Keywords*

Modified Cam-Clay – **block zone cmodel assign cam-clay**

(1)	**bu**lk-**max**imum	maximum elastic bulk modulus, K_{max}
(2)	**dens**ity	mass density, ρ
(3)	**ka**ppa	slope of elastic swelling line, κ
(4)	**la**mbda	slope of normal consolidation line, λ
(5)	**po**isson	Poisson's ratio, ν
(6)	**pr**essure-**re**ference	reference pressure, p_1
(7)	**pr**essure-**pre**consolidation	pre-consolidation pressure, p_c
(8)	**ra**tio-**cr**itical-**sta**te	frictional constant, M
(9)	**sh**ear	elastic shear modulus, G
(10)	**sp**ecific-**vo**lume	initial specific volume, v_0 (by default, calculated internally)
(11)	**sp**ecifi-**vo**lume-**re**ference	specific volume at reference pressure, p_1, on normal consolidation line, v_λ

If Poisson's ratio, **poisson**, is not given, and a nonzero shear modulus, **shear_mod**, is specified, then the shear modulus remains constant; Poisson's ratio will change as bulk modulus changes. If a nonzero **poisson** is given, then the shear modulus will change as the bulk modulus changes; Poisson's ratio remains constant.

The following properties can be printed, plotted or accessed via *FISH*.

(1)	**bu**lk	current elastic bulk modulus, K
(2)	**pr**essure-**ef**fective	current mean effective stress, p
(3)		accumulated plastic volumetric strain
(4)	**stre**ss-**de**viatoric	current mean deviatoric stress, q

1.6.8 Hoek-Brown-PAC Model

The Hoek-Brown failure criterion is an empirical relation that characterizes the stress conditions that lead to failure in intact rock and rock masses. It has been used very successfully in design approaches that use limit equilibrium solutions, but there has been little direct use in numerical solution schemes. Numerical solution methods require full constitutive models, which relate stress to strain in a general way; in addition to a failure (or yield) criterion, a "flow rule" is also necessary, in order to provide a relation between the components of strain rate at failure. There have been several attempts to develop a full constitutive model from the Hoek-Brown criterion (e.g., Pan and Hudson 1988, Carter et al. 1993 and Shah 1992). These formulations assume that the flow rule has some fixed relation to the failure criterion, and that the flow rule is isotropic, whereas the Hoek-Brown criterion is not. In the formulation described here, there is no fixed form for the flow rule; it is assumed to depend on the stress level, and possibly some measure of damage.*

In what follows, the failure criterion is taken as a yield surface, using the terminology of plasticity theory. Usually, a failure criterion is assumed to be a fixed, limiting stress condition that corresponds to ultimate failure of the material. However, numerical simulations of elastoplastic problems allow continuing the solution after "failure" has taken place, and the failure condition itself may change as the simulation progresses (by either hardening or softening). In this event, it is more reasonable to speak of "yielding" than failure. There is no implied restriction on the type of behavior that is modeled: both ductile and brittle behavior may be represented, depending on the softening relation used.

1.6.8.1 The General Formulation

The "generalized" Hoek-Brown criterion (Hoek and Brown 1980 and 1998), adopting the convention of positive compressive stress, is

$$\sigma_1 = \sigma_3 + \sigma_{ci}\left\{m_b \frac{\sigma_3}{\sigma_{ci}} + s\right\}^a \tag{1.242}$$

where σ_1 and σ_3 are the major and minor effective principal stresses, and σ_{ci}, m_b, s and a are material constants that can be related to the Geological Strength Index and rock damage (Hoek et al. 2002). For interest, the unconfined compressive strength is given by $\sigma_c = \sigma_{ci}\ s^a$, and the tensile strength by $\sigma_t = -\ s\ \sigma_{ci}\ /\ m_b$. Note that the criterion (Eq. (1.242)) does not depend on the intermediate principal stress, σ_2. Thus, the failure envelope is not isotropic.

Assume that the current principal stresses are (σ_1,σ_2, σ_3), and that initial trial stresses (σ_1^t,σ_2^t, σ_3^t) are calculated by using incremental elasticity:

---

* *UDEC* simulations using the Hoek-Brown-PAC model have shown that the model with a stress-dependent flow rule works well at high confining stress states, but can produce excessive dilation at low confinement conditions. An alternative formulation, the *modified Hoek-Brown* model, which allows the user to input a dilation angle and specify a stress-independent flow rule, is available (see Section 1.6.9).

$$\begin{aligned}\sigma_1^t &= \sigma_1 + E_1\Delta e_1 + E_2(\Delta e_2 + \Delta e_3)\\ \sigma_2^t &= \sigma_2 + E_1\Delta e_2 + E_2(\Delta e_1 + \Delta e_3)\\ \sigma_3^t &= \sigma_3 + E_1\Delta e_3 + E_2(\Delta e_1 + \Delta e_2)\end{aligned} \tag{1.243}$$

where $E_1 = K + 4G/3$ and $E_2 = K - 2G/3$, and $(\Delta e_1, \Delta e_2, \Delta e_3)$ is the set of principal strain increments. If the yield criterion (Eq. (1.242)) is violated by this set of stresses, then the strain increments (prescribed as independent inputs to the model) are assumed to be composed of elastic and plastic parts:

$$\begin{aligned}\Delta e_1 &= \Delta e_1^e + \Delta e_1^p\\ \Delta e_2 &= \Delta e_2^e\\ \Delta e_3 &= \Delta e_3^e + \Delta e_3^p\end{aligned} \tag{1.244}$$

Note that plastic flow does not occur in the intermediate principal stress direction. The final stresses (σ_1^f,σ_2^f, σ_3^f) output from the model are related to the elastic components of the strain increments. Hence,

$$\begin{aligned}\sigma_1^f - \sigma_1 &= E_1(\Delta e_1 - \Delta e_1^p) + E_2(\Delta e_2 + \Delta e_3 - \Delta e_3^p)\\ \sigma_2^f - \sigma_2 &= E_1\Delta e_2 + E_2(\Delta e_1 - \Delta e_1^p + \Delta e_3 - \Delta e_3^p)\\ \sigma_3^f - \sigma_3 &= E_1(\Delta e_3 - \Delta e_3^p) + E_2(\Delta e_1 - \Delta e_1^p + \Delta e_2)\end{aligned} \tag{1.245}$$

Eliminating the current stresses, using Eq. (1.243) and Eq. (1.245),

$$\begin{aligned}\sigma_1^f &= \sigma_1^t - E_1\Delta e_1^p - E_2\Delta e_3^p\\ \sigma_2^f &= \sigma_2^t - E_2(\Delta e_1^p + \Delta e_3^p)\\ \sigma_3^f &= \sigma_3^t - E_1\Delta e_3^p - E_2\Delta e_1^p\end{aligned} \tag{1.246}$$

We assume the flow rule

$$\Delta e_1^p = \gamma\Delta e_3^p \tag{1.247}$$

where the factor γ depends on stress, and is recomputed at each timestep. Eliminating Δe_1^p from Eq. (1.246):

$$\begin{aligned}\sigma_1^f &= \sigma_1^t - \Delta e_3^p(\gamma E_1 + E_2)\\ \sigma_2^f &= \sigma_2^t - \Delta e_3^p E_2(1+\gamma)\\ \sigma_3^f &= \sigma_3^t - \Delta e_3^p(\gamma E_2 + E_1)\end{aligned} \tag{1.248}$$

At yield, Eq. (1.242) is satisfied by the final stresses. That is,

$$F = \sigma_1^f - \sigma_3^f - \sigma_{ci}\left\{m_b\frac{\sigma_3^f}{\sigma_{ci}} + s\right\}^a = 0 \tag{1.249}$$

By substituting values of σ_1^f and σ_3^f from Eq. (1.248), Eq. (1.249) can be solved iteratively (using Newton's method or a bisection method) for Δe_3^p, which is then substituted in Eq. (1.248) to give the final stresses. The method of solution is described later, but first the evaluation of γ is discussed.

1.6.8.2 Flow Rules

We need to consider an appropriate flow rule, which describes the volumetric behavior of the material during yield. In general, the flow parameter γ will depend on stress, and possibly history. It is not meaningful to speak of a "dilation angle" for a material when its confining stress is low or tensile, because the mode of failure is typically by axial splitting, not shearing. Although the volumetric strain depends in a complicated way on stress level, we consider certain specific cases for which behavior is well-known, and determine the behavior for intermediate conditions by interpolation. Four cases are considered below.

Associated Flow Rule

It is known that many rocks under unconfined compression exhibit large rates of volumetric expansion at yield, associated with axial splitting and wedging effects. The associated flow rule provides the largest volumetric strain rate that may be justified theoretically. This flow rule is expected to apply in the vicinity of the uniaxial stress condition ($\sigma_3 \approx 0$). An associated flow rule is one in which the vector of plastic strain rate is normal to the yield surface (when both are plotted on similar axes). Thus,

$$\Delta e_i^p = -\gamma\frac{\partial F}{\partial \sigma_i} \tag{1.250}$$

where the subscripts denote the components in the principal stress directions, and F is defined by Eq. (1.249). Differentiating this expression, and using Eq. (1.247),

$$\gamma_{\text{af}} = -\frac{1}{1 + a\sigma_{ci}(m_b\sigma_3/\sigma_{ci} + s)^{a-1}(m_b/\sigma_{ci})} \tag{1.251}$$

Radial Flow Rule

Under the condition of uniaxial tension, we might expect that the material would yield in the direction of the tensile traction. If the tension is isotropically applied, we imagine (since the test is almost impossible to perform) that the material would deform isotropically. Both of these conditions are fulfilled by the radial flow rule, which is assumed to apply when all principal stresses are tensile. For a flow-rate vector to be coaxial with the principal stress vector, we obtain

$$\gamma_{\text{rf}} = \frac{\sigma_1}{\sigma_3} \tag{1.252}$$

Constant-Volume Flow Rule

As the confining stress is increased, a point at which the material no longer dilates during yield is reached. A constant-volume flow rule is therefore appropriate when the confining stress is above some user-prescribed level, $\sigma_3 = \sigma_3^{\text{cv}}$. This flow rule is given by

$$\gamma_{\text{cv}} = -1 \tag{1.253}$$

Composite Flow Rule

We propose to assign the flow rule (and, thus, a value for γ) according to the stress condition. In the fully tensile region, the radial flow rule (γ_{rf}) will be used. For compressive σ_1 and tensile or zero σ_3, the associated flow rule (γ_{af}) is applied. For the interval $0 < \sigma_3 < \sigma_3^{\text{cv}}$, the value of γ is linearly interpolated between the associated and constant-volume limits:

$$\gamma = \frac{1}{\frac{1}{\gamma_{\text{af}}} + (\frac{1}{\gamma_{\text{cv}}} - \frac{1}{\gamma_{\text{af}}})\frac{\sigma_3}{\sigma_3^{\text{cv}}}} \tag{1.254}$$

Finally, when $\sigma_3 > \sigma_3^{\text{cv}}$, the constant-volume value, $\gamma = \gamma_{\text{cv}}$, is used.

Note that if σ_3^{cv} is set equal to zero, then the model condition approaches a nonassociated flow rule with a zero dilation angle. If σ_3^{cv} is set to a very high value relative to σ_{ci}, the model condition approaches an associated-flow state.

1.6.8.3 Implementation Procedure

The equations presented above are implemented using two iterative solvers: a fast Newton's method and a slower bisection method. For Newton's method, one difficulty with the failure criterion (Eq. (1.249)) is that real values for F do not exist if $\sigma_3 < -s\sigma_{ci}/m_b$. During an iteration process, this condition is likely to be encountered, so it is necessary that the expression for F, and its first derivatives, be continuous everywhere in stress space. This is fulfilled by adapting the composite expression

$$\text{if } \sigma_3 \geq -\frac{s\sigma_{ci}}{m_b} \text{ then } F = \sigma_1^f - \sigma_3^f - \sigma_{ci}\left\{m_b\frac{\sigma_3^f}{\sigma_{ci}} + s\right\}^a = 0 \tag{1.255}$$

$$\text{if } \sigma_3 < -\frac{s\sigma_{ci}}{m_b} \text{ then } F = \sigma_1^f - \sigma_3^f + \sigma_{ci}\left\{m_b\frac{\sigma_3^f}{\sigma_{ci}} + s\right\}^a = 0 \tag{1.256}$$

To initialize the iteration for Newton's method, a starting value for Δe_3^p is taken as the absolute maximum of all the strain increment components. This value, denoted by Δe_1, is inserted into Eq. (1.248), together with the value for γ found from the flow-rule equations, and the resulting stress values inserted into Eqs. (1.255) and (1.256). The resulting value of F is denoted by F_1. Taking the original value of F as F_0 (and the corresponding plastic strain increment of zero as Δe_0), we can estimate a new value of the plastic strain increment using

$$\Delta e_2 = \frac{F_1\Delta e_0 - F_0\Delta e_1}{F_1 - F_0} \tag{1.257}$$

From this we find a new value of F (call it F_2) and, if it is sufficiently close to zero, the iteration stops. Otherwise, we set $F_0 = F_1$, $F_1 = F_2$, $\Delta e_0 = \Delta e_1$ and $\Delta e_1 = \Delta e_2$, and apply Eq. (1.257) again.

Tests have shown that for high confining stresses, the Newton scheme converges in one step; at low confining stresses, up to ten steps are necessary. (The limit built into the Newton scheme is presently set at 15.)

In tensile conditions, the Newton solver occasionally has problems converging. In this case, a bisection solver (with a slower convergence rate than the Newton solver) is used. High and low values for Δe_3^p are selected and substituted into Eq. (1.248); one results in $F < 0$ and the other results in $F > 0$ in Eq. (1.249). The bisection method searches between these two limits to find the value of Δe_3^p that results in $F = 0$ in Eq. (1.249).

1.6.8.4 Material Softening

In the Hoek-Brown model, the material properties σ_{ci}, m_b, s and a are assumed to remain constant, by default. Material softening, after the onset of plastic yield, can be simulated by specifying that these mechanical properties change (i.e., reduce the overall material strength) according to a softening parameter. The softening parameter selected for the Hoek-Brown-PAC model is the plastic confining strain component, e_3^p. The choice of e_3^p is based on physical grounds. For yield near the unconfined state, the damage in brittle rock is mainly by splitting (not by shearing), with crack normals oriented in the σ_3 direction. The parameter e_3^p is expected to correlate with the microcrack damage in the σ_3 direction.

The value of e_3^p is calculated by summing the strain increment values for Δe_3^p calculated by Eq. (1.257). Softening behavior is provided by specifying tables that relate each of the properties σ_{ci}, m_b, s and a to e_3^p. Each table contains pairs of values: one for the e_3^p value, and one for the corresponding property value. It is assumed that the property varies linearly between two consecutive parameter entries in the table.

A multiplier, μ (denoted as **table-multiplier**), can also be specified to relate the softening behavior to the confining stress, σ_3. The relation between μ and σ_3 is also given in the form of a table. (See Cundall et al. (2003) for an application of softening parameters.)

1.6.8.5 Triaxial Compression Test

Triaxial compression tests are performed on models composed of Hoek-Brown-PAC material in *UDEC*, to verify the stress and strain paths that develop. The triaxial load conditions are illustrated in Figure 1.31. The triaxial tests are performed on a sample of Hoek-Brown material with properties of $m_b = 5$, $s = 1$, $a = 0.5$, $\sigma_{ci} = 1.0$ and $\sigma_3^{cv} = 1.5$, and with elastic properties of $E = 100$ and $\nu = 0.35$. Compression loading tests are performed under two loading conditions: $\sigma_3/\sigma_{ci} = 0$ and 1.0. The analytical solutions for stress and strain during compression loading are presented by the plots shown in Figures 1.32 and 1.33.

A single-zone model is constructed in *UDEC* to simulate the triaxial loading tests. The *UDEC* results are compared to the analytical solutions in Figures 1.34 through 1.37. The solutions compare within 1%.

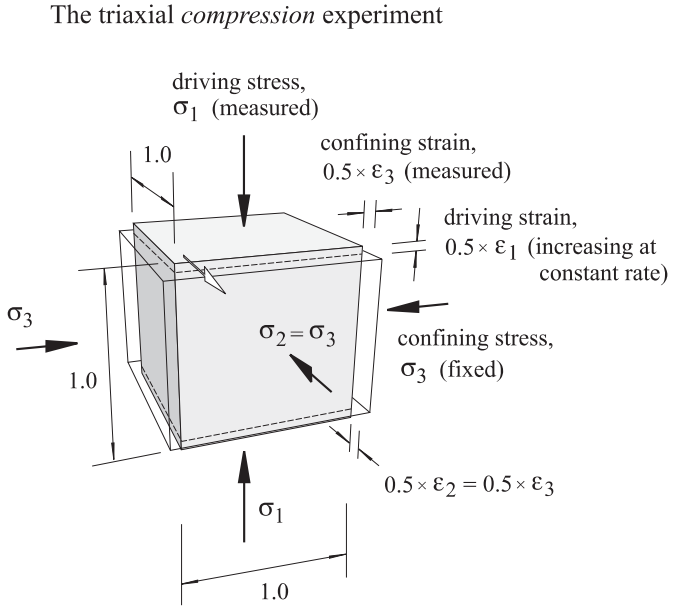

Figure 1.31 Triaxial compression tests – loading conditions

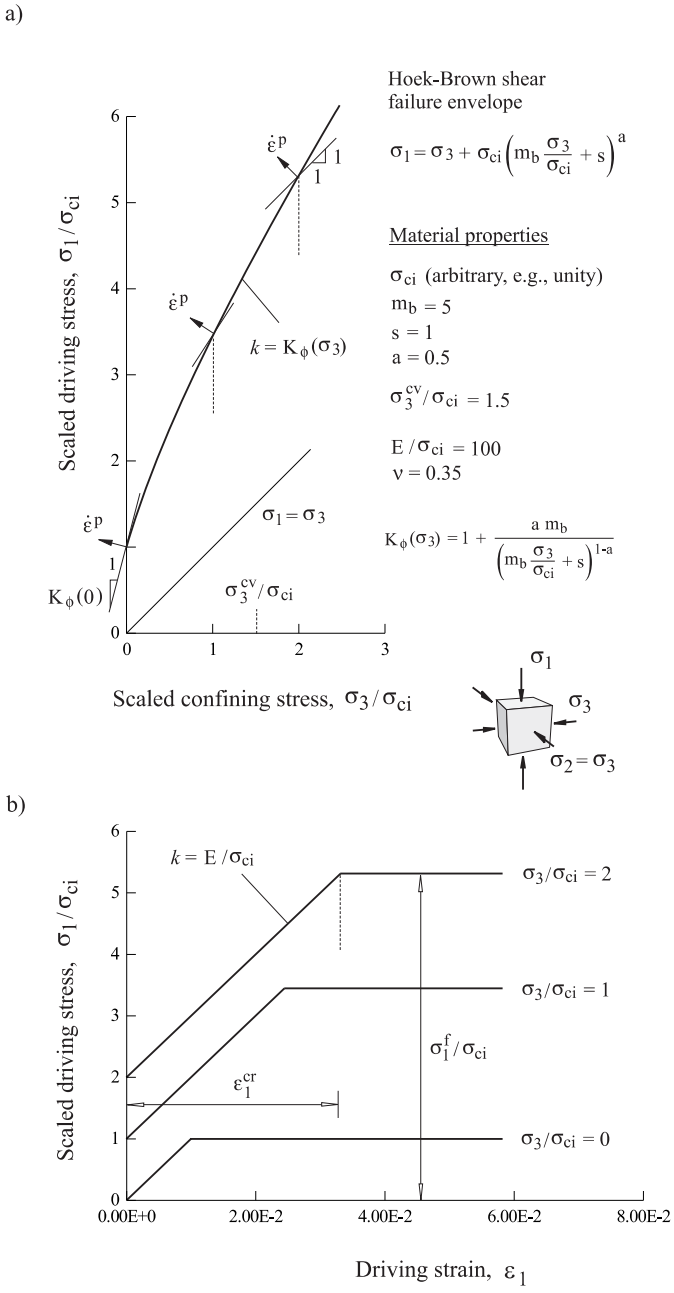

Figure 1.32 Triaxial compression tests – a) Hoek-Brown failure envelope; b) stress-strain plots

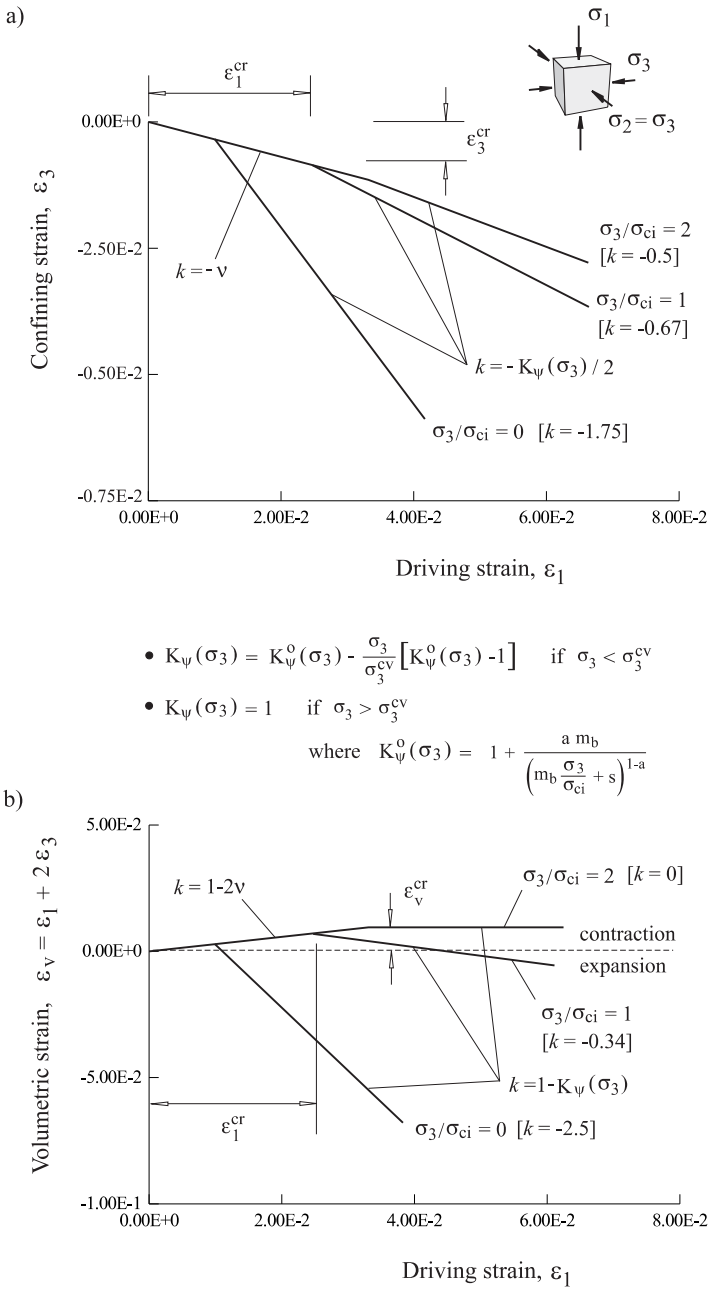

Figure 1.33 Triaxial compression tests – a) confining (lateral) strain versus axial strain; b) volumetric strain versus axial strain

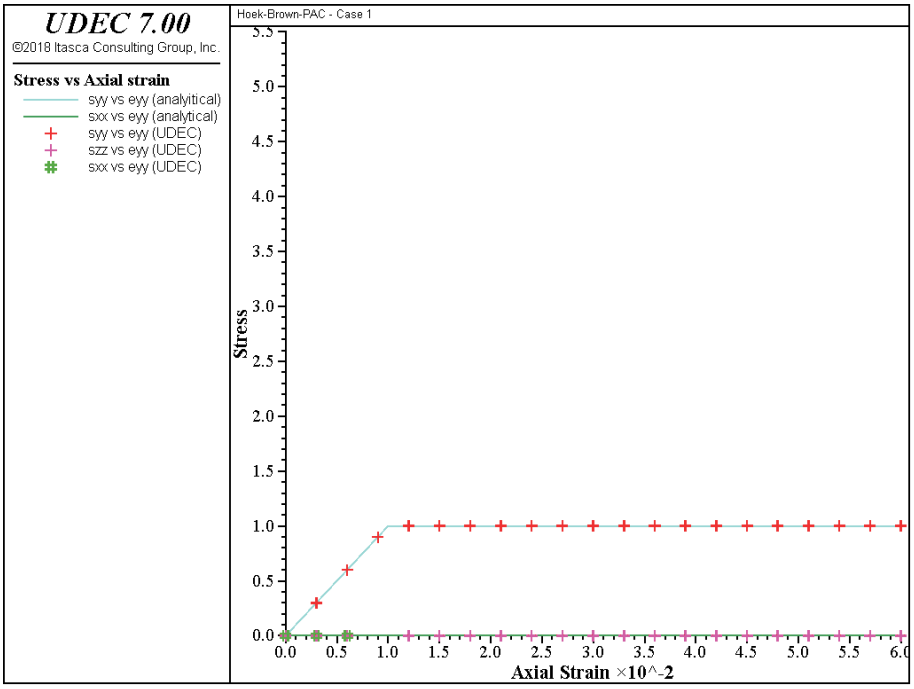

Figure 1.34 Triaxial compression test – stress versus axial strain (σ_3/σ_{ci} = 0)

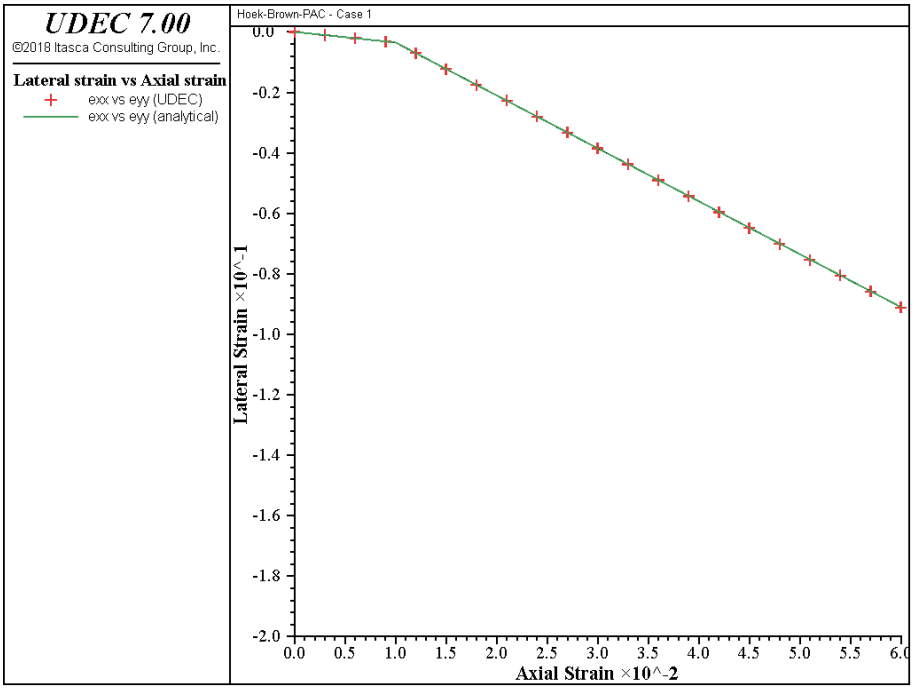

Figure 1.35 Triaxial compression test – lateral strain versus axial strain (σ_3/σ_{ci} = 0)

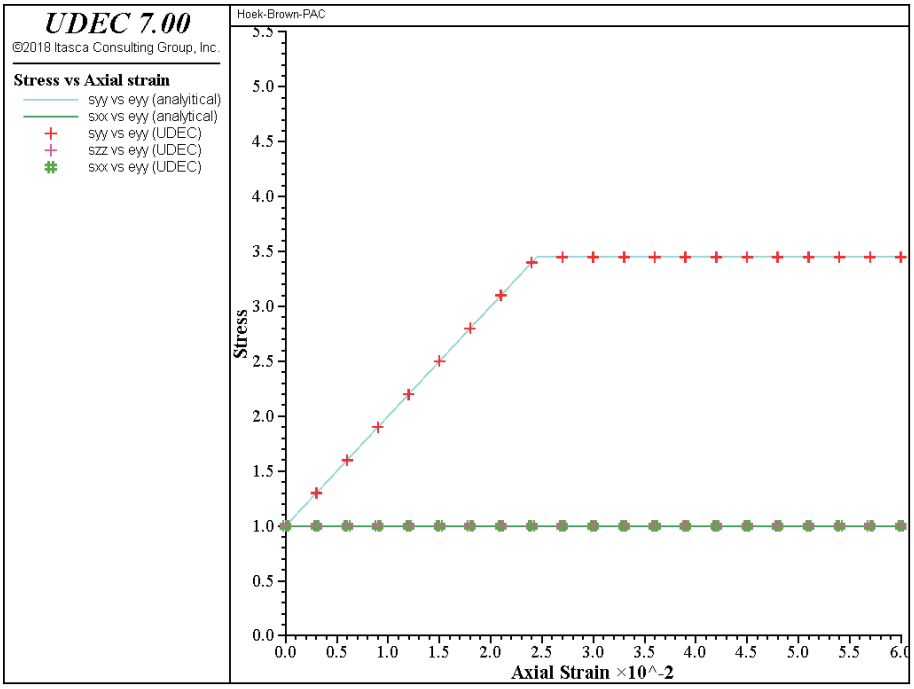

Figure 1.36 Triaxial compression test – stress versus axial strain (σ_3/σ_{ci} = 1.0)

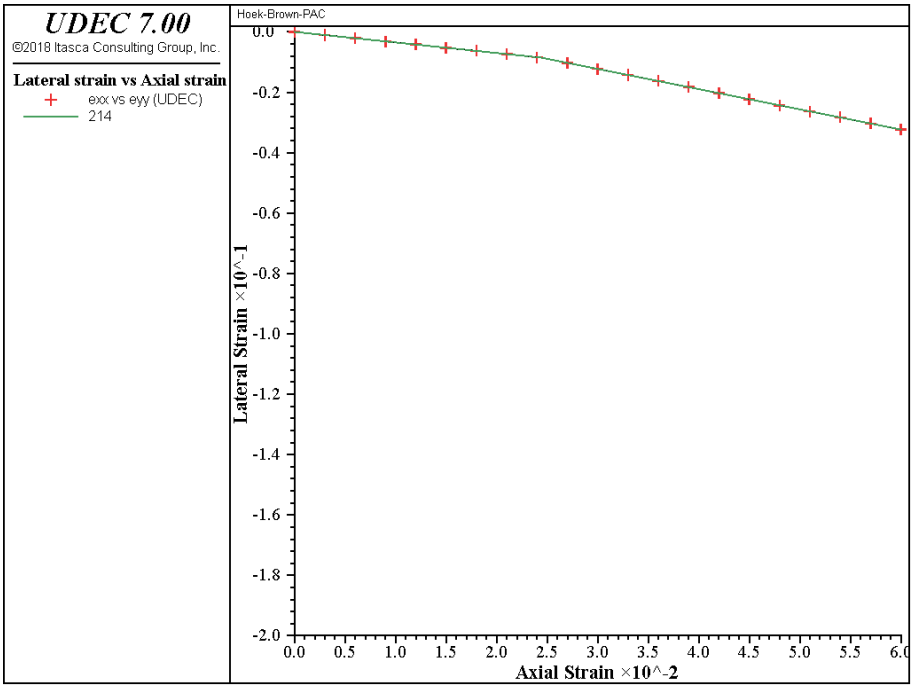

Figure 1.37 Triaxial compression test – lateral strain versus axial strain (σ_3/σ_{ci} = 1.0)

Example 1.6 Triaxial tests on a Hoek-Brown-PAC material

```
model new
;file 'Hoek_Brown_pac_1.dat
model title 'Hoek-Brown-PAC - Case 1'
fish define _variables
;
; --- To reconstruct the compression analytical curves: ---
  _sig_conf = 0.0
  _max_eyy = -6.0e-2 ;<-- maximum 'driving' strain (contraction negative)
;
; Plastic properties
  _sig_ci = 1.0 ; <-- enter UCS as positive always
  _mb = 5.0
  _s = 1.0
  _a = 0.5
  _sig3_cv = 1.5 ; <-- enter UCS as positive always
;
  _sig_tm2 = - _s*_sig_ci/_mb
;
; Elastic properties
  _young = 100
  _poiss = 0.35
  _bulk = _young/3.0/(1-2*_poiss)
  _shear = _young/2.0/(1+_poiss)
;
; Loading
  _cyc = 20000 ; <-- number of steps in which load is to be applied
  _delta_u = _max_eyy * 1.0
  _y_vel = 0.5*_delta_u / _cyc
  _minus_y_vel = -_y_vel
;
end
@_variables
block config axisymmetry
block  smallstrain
block tolerance corner-round-length 1E-3
block tolerance minimum-edge-length 2E-3
block create polygon 0 0 0 1 1 1 1 0
block zone gen quad 2.0
block zone group 'mat1'
block zone cmodel assign hoek-brown-pac density 1 shear @_shear ...
  bulk @_bulk constant-sci @_sig_ci constant-mb @_mb constant-s @_s ...
  constant-a @_a stress-confining-prescribed @_sig3_cv range group 'mat1'
block edge apply stress @_sig_conf 0.0 0.0 ...
```

```
  range pos-x 0.9861 1.0188 pos-y -2.04E-2 1.0142
block gridpoint apply velocity-y -7.6e-5 ...
  range pos-x -1.105E-2 1.011 pos-y 0.9877 1.0064
block gridpoint apply velocity-y 7.6e-5 ...
  range pos-x -1.572E-2 1.0266 pos-y -1.105E-2 1.544E-2
block insitu  stress @_sig_conf 0.0 @_sig_conf stress-ZZ @_sig_conf
fish define _record_variables
;
  _disp_0 = 0.5*(block.gp.disp.x(block.gp.near(0,0)) + ...
                 block.gp.disp.x(block.gp.near(0,1)))
  _disp_1 = 0.5*(block.gp.disp.x(block.gp.near(1,0)) + ...
                 block.gp.disp.x(block.gp.near(1,1)))
  _eps_xx = -(_disp_0 - _disp_1)/1.0
;
  _disp_0 = 0.5*(block.gp.disp.y(block.gp.near(0,0)) +...
                 block.gp.disp.y(block.gp.near(1,0)))
  _disp_1 = 0.5*(block.gp.disp.y(block.gp.near(0,1)) + ...
                 block.gp.disp.y(block.gp.near(1,1)))
  _eps_yy = -(_disp_0 - _disp_1)/1.0
;
  zi = block.zone(block.head)
  _count = 0
  _sig_zz = 0.0
  _sig_xx = 0.0
  _sig_yy = 0.0
  loop while zi # 0
     _sig_zz = _sig_zz + block.zone.stress.zz(zi)
     _sig_xx = _sig_xx + block.zone.stress.xx(zi)
     _sig_yy = _sig_yy + block.zone.stress.yy(zi)
     zi = block.zone.next(zi)
     _count = _count + 1
  endloop
;
  _sig_zz = _sig_zz /_count
  _sig_xx = _sig_xx /_count
  _sig_yy = _sig_yy /_count
  _record_variables = 1.0
;
end
fish history @_record_variables
history interval 1000
fish history @_eps_xx
fish history @_eps_yy
fish history @_eps_yy
fish history @_sig_xx
fish history @_sig_yy
```

```
fish history @_sig_zz
block cycle 20000
;
; Copy histories to tables
;
hist export 2 table 11
hist export 3 table 12
hist export 4 table 13
hist export 5 table 21
hist export 6 table 22
hist export 7 table 23
;
fish define _copy_histories_to_tables
; Table 111 contains syy   stress vs axial strain diagram
; Table 112 contains sxx   stress vs axial strain diagram
; Table 113 contains szz   stress vs axial strain diagram
; Table 114 contains lateral strain vs axial strain diagram
  _n = table.size(11)
  loop i (1,_n)
;  _sig_yy vs _eps_yy
    table.x(111,i) = -table.y(12,i)/_sig_ci
    table.y(111,i) = -table.y(22,i)/_sig_ci
;  _sig_xx vs _eps_yy
    table.x(112,i) = -table.y(12,i)/_sig_ci
    table.y(112,i) = -table.y(21,i)/_sig_ci
;  _sig_zz vs _eps_yy
   table.x(113,i) = -table.y(12,i)/_sig_ci
   table.y(113,i) = -table.y(23,i)/_sig_ci
;  _eps_xx vs _eps_yy
   table.x(114,i) = -table.y(12,i)
   table.y(114,i) = -table.y(11,i)
;
  end_loop
;
end
@_copy_histories_to_tables
;
; Compute analytical solution
;
fish define _analytical_solution
;
; Stress-strain diagram
;
  _sig1F = _sig_conf-_sig_ci*(-_mb*_sig_conf/_sig_ci+_s)^_a
  _S_s1e1_Elast = _young
  _eps1CR = (_sig1F-_sig_conf)/_S_s1e1_Elast
```

```
  _eps1MAX = _max_eyy
;
; Table 211 contains syy   stress vs axial strain diagram
; Table 212 contains sxx   stress vs axial strain diagram
; Table 214 contains lateral strain vs axial strain diagram
;
  table.x(211,1) = 0.0
  table.x(211,2) = -_eps1CR/_sig_ci
  table.x(211,3) = -_eps1MAX/_sig_ci
  table.y(211,1) = -_sig_conf/_sig_ci
  table.y(211,2) = -_sig1F/_sig_ci
  table.y(211,3) = -_sig1F/_sig_ci
;
  table.x(212,1) = 0.0
  table.x(212,2) = -_eps1CR/_sig_ci
  table.x(212,3) = -_eps1MAX/_sig_ci
  table.y(212,1) = -_sig_conf/_sig_ci
  table.y(212,2) = -_sig_conf/_sig_ci
  table.y(212,3) = -_sig_conf/_sig_ci
;
; Strain-strain diagram
;
  _S_e3e1_Elast = -_poiss
  _eps3CR = _eps1CR*_S_e3e1_Elast
  _Kpsi_0 = 1 + _a*_mb/(-_mb*_sig_conf/_sig_ci+_s)^(1-_a)
;
  if -_sig_conf > _sig3_cv
    _Kpsi = 1.0
  else
    _Kpsi = _Kpsi_0 + _sig_conf/_sig3_cv * (_Kpsi_0-1)
  end_if
  _S_e3e1_Plast = -_Kpsi / 2.0
  _eps3MAX = _eps3CR + (_eps1MAX-_eps1CR)*_S_e3e1_Plast
;
  table.x(214,1) = 0.0
  table.x(214,2) = -_eps1CR/_sig_ci
  table.x(214,3) = -_eps1MAX/_sig_ci
  table.y(214,1) = 0.0
  table.y(214,2) = -_eps3CR/_sig_ci
  table.y(214,3) = -_eps3MAX/_sig_ci
;
end
@_analytical_solution
table 212 label 'sxx vs eyy (analytical)'
table 211 label 'syy vs eyy (analyitical)'
table 111 label 'syy vs eyy (UDEC)'
```

```
table 112 label 'sxx vs eyy (UDEC)'
table 113 label 'szz vs eyy (UDEC)'
table 114 label 'exx vs eyy (UDEC)'
table 214 label 'exx vs eyy (analytical)'
model save 'HB_1.sav'
return
```

1.6.8.6 **block zone cmodel** *Command and Property Keywords*

Hoek-Brown-PAC – **block zone cmodel assign hoek-brown-pac**

(1)	**bu**lk	elastic bulk modulus, K
(2)	**cons**tant-**a**	Hoek-Brown parameter, a
(3)	**cons**tant-**mb**	Hoek-Brown parameter, m_b
(4)	**cons**tant-**s**	Hoek-Brown parameter, s
(5)	**cons**tant-**sci**	Hoek-Brown parameter, σ_{ci}
(6)	**dens**ity	mass density, ρ
(7)	**nu**mber-**it**erations	number of iterations*
(8)	**ta**ble-**a**	number of table relating a to e_3^p
(9)	**ta**ble-**mb**	number of table relating m_b to e_3^p
(10)	**ta**ble-**mu**ltiplier	number of table relating a multiplier to σ_3
(11)	**ta**ble-**s**	number of table relating s to e_3^p
(12)	**tab**le-**sci**	number of table relating σ_{ci} to e_3^p
(13)	**sh**ear	elastic shear modulus, G
(14)	**stra**in-**3-pl**astic	accumulated plastic strain, e_3^p
(15)	**stre**ss-**co**nfining-**pr**escribed	Hoek-Brown parameter, σ_3^{cv}

The following property can be printed, plotted or accessed via *FISH*.

(1)	**sta**te	plastic state

*The Hoek-Brown-PAC model makes three attempts to bring a stress point to the yield surface:

1) A fast Newton solver is tried.

2) If 1) does not converge, the stress point is checked to see whether it falls below the apex of the Hoek-Brown envelope (i.e., does it cross the $\sigma_1 = \sigma_3$ line). If this is the case, then the stress point is set to the apex.

3) If 1) and 2) do not work, a bisection method is used to find the stress point on the yield surface.

The **number-iteration** property reflects the attempts made to bring a stress point to the yield surface. Each zone contains a number of triangular subzones that are sent in sequence to the constitutive model. When the first subzone is received by the Hoek-Brown-PAC model, the Hoek-Brown-PAC model sets **number-iteration** to 0. If case 1 works, **number-iteration** is set to max(**number-iteration**, number of iterations required by the Newton solver). If case 2 is encountered, **hb_ind** is set to max(**number-iteration**, 1000). If case 3 is encountered, **number-iteration** is set to max(**number-iteration**, 1000 + iterations required by the bisection algorithm). If none of the cases work, then **number-iteration** is set to 9999.

1.6.9 Hoek-Brown Model

A modified version of the hardening/softening Hoek-Brown model, described in Section 1.6.8, is available as an alternative formulation. The Hoek-Brown model provides a representation for yielding that accounts for the changing failure condition. This model works well at higher confining stress states, but can produce excessive dilation at low confinement or under tensile-stress conditions. The alternative version, described in this section, is modified to include a tensile yield criterion, and also to allow the user to specify a dilation angle as an input parameter and manually control the level of dilation that develops.

The modified Hoek-Brown model is derived directly from the Mohr-Coulomb model and, like the Mohr-Coulomb model, can be used to perform factor-of-safety calculations using the **block factor-of-safety** command. The formulation and an example exercise are given below.

1.6.9.1 Formulation and Implementation

The Hoek-Brown criterion is used for plastic yielding when the minor principal stress, σ_3, is compressive. The criterion is based on a nonlinear relation between major and minor principal stresses, σ_1 and σ_3, as shown previously in Eq. (1.242), and repeated here:

$$\sigma_1 = \sigma_3 + \sigma_{ci}\left\{m_b \frac{\sigma_3}{\sigma_{ci}} + s\right\}^a \tag{1.258}$$

where σ_{ci} is the unconfined compressive strength of the intact rock, and m_b, s and a are material constants that can be related to the Geological Strength Index and rock damage (Hoek et al. 2002).

The Hoek-Brown envelope is extended for σ_3 tensile by a combination of the Mohr-Coulomb envelope (tangent to Hoek-Brown at $\sigma_3 = 0$) and a tensile cut-off at $\sigma_3 = -s\sigma_{ci}/m_b$.

The numerical implementation of the Hoek-Brown model uses a linear approximation, whereby the nonlinear failure surface is continuously approximated by the Mohr-Coulomb tangent, at the current stress level, σ_3. The current tangent Mohr-Coulomb criterion is

$$\sigma_1 = \sigma_3 N_{\phi_c} + 2c_c\sqrt{N_{\phi_c}} \tag{1.259}$$

where

$$N_{\phi_c} = \frac{1+\sin\phi_c}{1-\sin\phi_c} = \tan^2\left(\frac{\phi_c}{2} + 45^\circ\right) \tag{1.260}$$

The current (apparent) value of cohesion, c_c, and friction, ϕ_c, are calculated using

$$\phi_c = 2\tan^{-1}\sqrt{N_{\phi_c}} - 90^\circ \tag{1.261}$$

$$c_c = \frac{\sigma_c^{ucs}}{2\sqrt{N_{\phi_c}}} \tag{1.262}$$

where

$$N_{\phi_c} = 1 + am_b\left(m_b\frac{\sigma_3}{\sigma_{ci}} + s\right)^{a-1} \tag{1.263}$$

$$\sigma_c^{ucs} = \sigma_3(1 - N_{\phi_c}) + \sigma_{ci}\left(m_b\frac{\sigma_3}{\sigma_{ci}} + s\right)^{a} \tag{1.264}$$

The Mohr-Coulomb envelope extension in the region of tensile σ_3 is accounted for in the logic by considering the following cap in Eqs. (1.263) and (1.264) (recall that compressive stress is positive):

$$\sigma_3 = \max(\sigma_3, 0) \tag{1.265}$$

The tensile yield logic is the same as the one used for the strain-softening model; it is described in Section 1.6.4.2.

The plastic strain increment for shear yielding is defined using the current Mohr-Coulomb flow rule:

$$\Delta e_{ij}^p = \Delta e^p \frac{\partial g}{\partial \sigma_{ij}} - \frac{1}{3}\Delta e_{vol}^p \delta_{ij} \qquad i = 1, 3 \tag{1.266}$$

where Δe^p is the plastic flow increment intensity, g is the plastic potential function, and

$$\Delta e_{vol}^p = \Delta e^p\left(\frac{\partial g}{\partial \sigma_{11}} + \frac{\partial g}{\partial \sigma_{22}} + \frac{\partial g}{\partial \sigma_{33}}\right) \tag{1.267}$$

The plastic potential function is

$$g = \sigma_1 - \sigma_3 N_{\psi_c} \tag{1.268}$$

where ψ_c is the current value of dilation and

$$N_{\psi_c} = \frac{1 + \sin \psi_c}{1 - \sin \psi_c} \tag{1.269}$$

The direction of plastic flow ($\frac{\partial g}{\partial \sigma_{ij}}$ in Eq. (1.266)) is expressed using the plastic potential function. The plastic flow increment intensity, Δe^p, is derived from the current tangent Mohr-Coulomb yield criterion, Eq. (1.259). There are three choices of flow rule for the model:

1. Input a dilation angle (ψ_c is a constant value) specified by property keywords **constant-dilation** and **flag-dilation** = 0.
2. Specify associated plastic flow (ψ_c is set equal to ϕ_c) by setting **flag-dilation** = -1.
3. Set dilation as a fraction of the friction angle (ψ_c is set to a constant times ϕ_c); **flag-dilation** is a positive fraction.

Strain hardening/softening behavior can be prescribed for the Hoek-Brown properties m_b, s, a and σ_{ci}. The input is via tables, and in terms of an evolution parameter. There are two choices for evolution parameter: plastic shear strain (property keyword **flag-evolution** is set to 1), or plastic strain in the direction of the least compressive principal stress, σ_3 (property keyword **flag-evolution** is set to 0). The evolution parameter can be monitored via the property **strain-plastic**.

A simple regularization technique can be selected to address the issue of grid dependency on softening behavior. To activate this technique, the grid zone size used to calibrate model properties with experimental data is assigned to the property **length-calibration**. This property is the calibration length. The input softening rate is then adjusted automatically to account for a different zone size used in the full *UDEC* model. Note that this technique is experimental and should be used with caution.

1.6.9.2 Triaxial Compression Test

The triaxial compression tests performed in Section 1.6.8.5 for the Hoek-Brown model described in Section 1.6.8 are repeated for the modified Hoek-Brown model. Two compression loading tests are performed: one test at zero confining stress, $\sigma_3/\sigma_{ci} = 0$; and the other test at high confining stress, $\sigma_3/\sigma_{ci} = 1$.

The data file shown in Example 1.6 is used for these tests, with the Hoek-Brown model and properties replaced by the modified Hoek-Brown model and properties. For the zero confining stress case, we specify an associated flow rule; this is done with the command **PROPERTY flag-dilation = -1**. The following commands are specified for this case.

```
block zone cmodel assign hoek-brown group 'biaxial test sample'
block zone prop bulk _bulk shear _shear
block zone prop const-sci=_sig_ci const-m=_mb const-s=_s hba=_a
block zone prop flag-dilation -1
```

For the higher confining stress case, we need to specify a dilation angle that is consistent with the limiting constant-volume stress, $\sigma_3^{cv} = 1.5$, chosen for this test in Section 1.6.8.5. We linearly interpolate a value for dilation corresponding to the current confining stress level of $\sigma_3 = 1$, relative to a nonassociated zero dilation at $\sigma_3^{cv} = 1.5$. The current dilation, ψ_c, is then taken to be a fraction of the current friction angle, ϕ_c, using the linear interpolation

$$\frac{\psi_c}{\phi_c} = 1 - \frac{\sigma_3}{\sigma_3^{cv}} = 0.333 \tag{1.270}$$

The following commands are used to apply the modified Hoek-Brown model for this case.

```
_sig_conf = -1.0 ; confining stress
```

and

```
block zone cmodel assign hoek-brown group 'biaxial test sample'
block zone prop bulk _bulk shear _shear
block zone prop const-sci=_sig_ci const-m=_mb const-s=_s hba=_a
block zone prop flag-dilation 0.333
```

The *UDEC* results for the zero confining stress case are compared to the analytical solution (from Section 1.6.8.5) in Figures 1.38 and 1.39, and the results for the high confining stress case are compared in Figures 1.40 and 1.41.

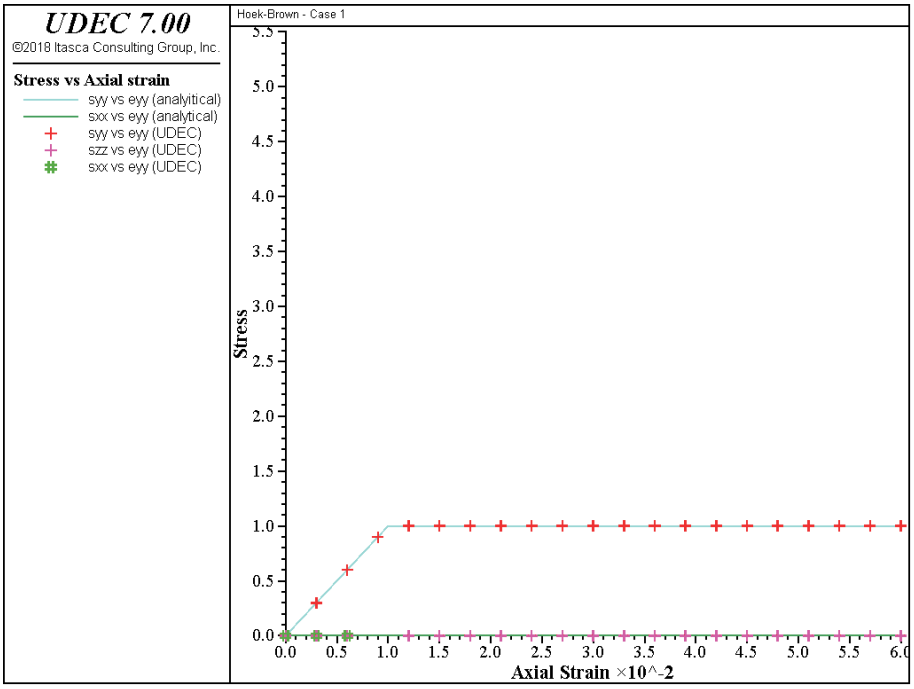

Figure 1.38 Triaxial compression test – stress versus axial strain (σ_3/σ_{ci} = 0) – modified Hoek-Brown model

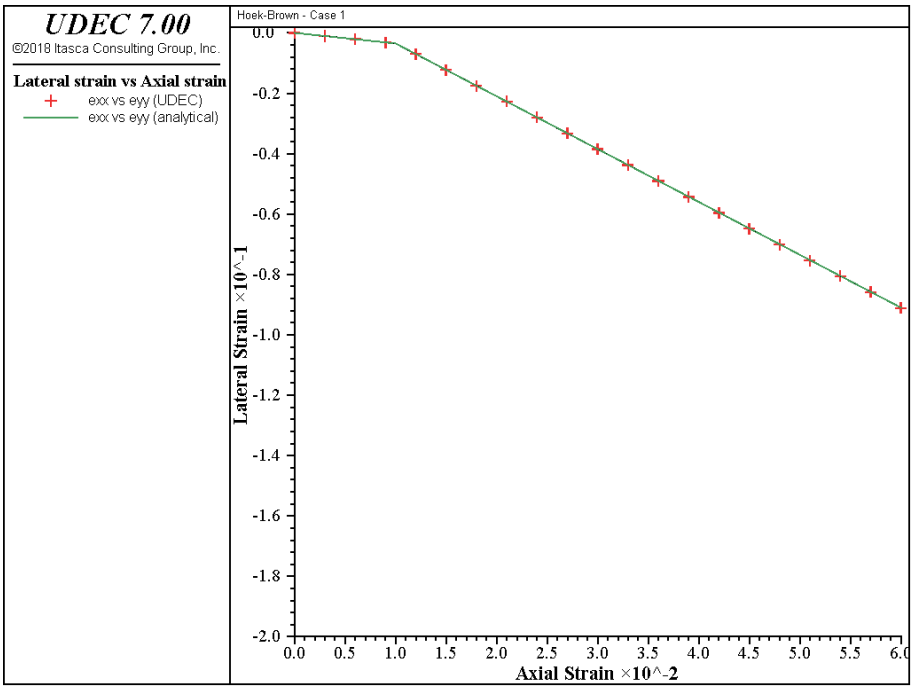

Figure 1.39 Triaxial compression test – lateral strain versus axial strain (σ_3/σ_{ci} = 0) – modified Hoek-Brown model

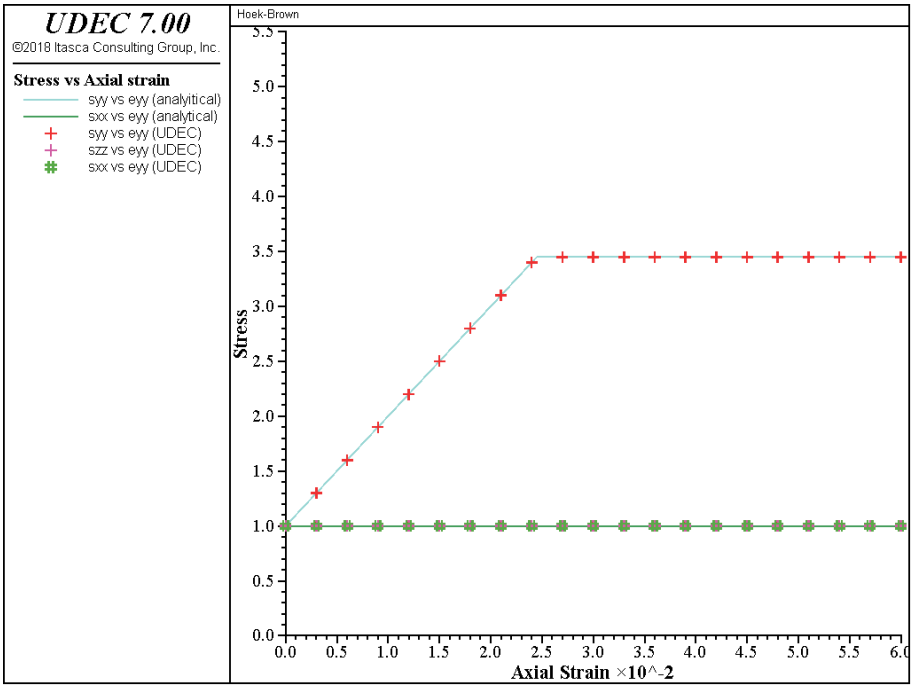

Figure 1.40 Triaxial compression test – stress versus axial strain (σ_3/σ_{ci} = 1.0) – modified Hoek-Brown model

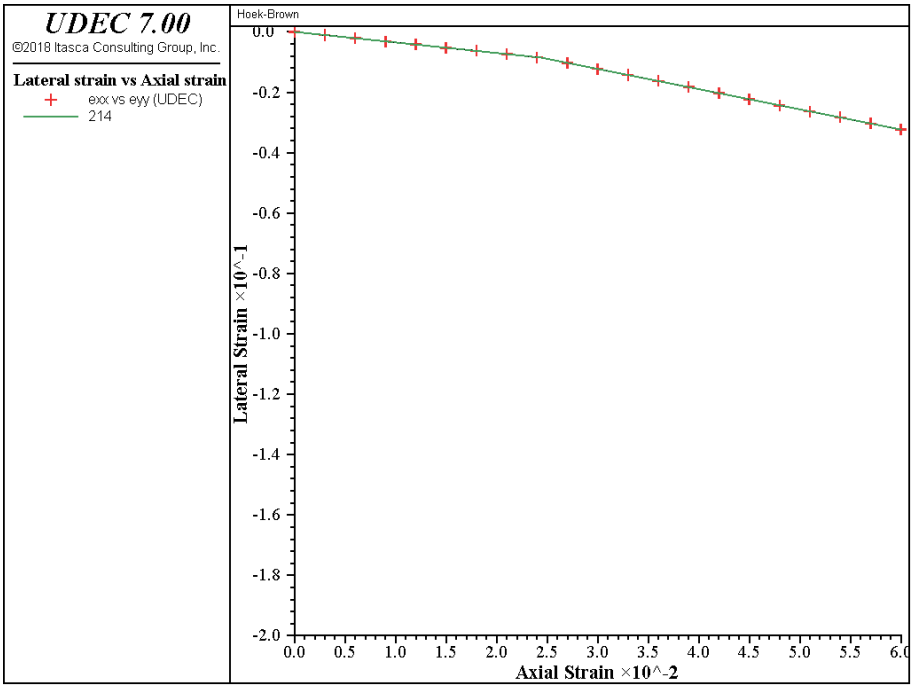

Figure 1.41 Triaxial compression test – lateral strain versus axial strain (σ_3/σ_{ci} = 1.0) – modified Hoek-Brown model

1.6.9.3 **block zone cmodel** *Command and Property Keywords*

Hoek-Brown – **block zone cmodel assign hoek-brown**

(1) **bu**lk elastic bulk modulus, K

(2) **cons**tant-**a** Hoek-Brown parameter, a

(3) **cons**tant-**mb** Hoek-Brown parameter, m_b

(4) **cons**tant-**di**lation dilation angle, ψ_c (specified if **flag-dilation** = 0)

(5) **cons**tant-**s** Hoek-Brown parameter, s

(6) **cons**tant-**sci** Hoek-Brown parameter, σ_{ci}

(7) **dens**ity mass density, ρ

(8) **fl**ag-**di**lation = 0 to input a constant dilation angle specified by **constant-dilation**
= −1 to specify associated plastic flow; $\psi_c = \phi_c$
= ***val*** where ***val*** is a fraction of friction angle, ϕ_c (ψ_c = ***val*** × ϕ_c)

(9) **fl**ag-**ev**olution = 0 for evolution parameter set to plastic strain in direction of least compressive principal stress
= 1 for evolution parameter set to plastic shear strain

(10) **fl**ag-**f**os = 0 for **block factor-of-safety** solution controlled by shear strength
= 1 for **block factor-of-safety** solution controlled by unconfined compressive strength

(11) **le**ngth-**ca**libration calibration length to calibrate model properties to account for zone size

(12) **ta**ble-**a** number of table relating a to the evolution parameter

(13) **ta**ble-**mb** number of table relating m_b to the evolution parameter

(14) **sh**ear elastic shear modulus, G

(15) **table-s** number of table relating s to the evolution parameter

(16) **ta**ble-**sci** number of table relating σ_{ci} to the evolution parameter

(17) **ta**ble-**ten**sion number of table relating tension, t, to the evolution parameter

(18) **ten**sion tension cutoff, t

The following properties can be printed, plotted or accessed via *FISH*.

(1)	**cu**rrent-**a**	current value of a
(2)	**cu**rrent-**co**hesion	current value of cohesion, c_c
(3)	**cu**rrent-**di**lation	current value of dilation angle, ψ_c *
(4)	**cu**rrent-**fri**ction	current value of friction angle, ϕ_c
(5)	**cu**rrent-**mb**	current value of m_b
(6)	**cu**rrent-**s**	current value of s
(7)	**cu**rrent-**sci**	current value of σ_{ci}
(8)	**sta**te	plastic state
(9)	**stra**in-**pl**astic	plastic strain in direction of least compressive principal stress (if **flag-evolution** = 0) plastic shear strain (if **flag-evolution** = 1)

* If **flag-dilation** = 0, **dilation** = min(**constant-dilation**, ψ_c). Thus, **dilation** may not always be equal to the specified value of **constant-dilation**.

1.6.10 Cap-Yield (formerly Cysoil) Model

The double-yield model (see Section 1.6.6) is a shear and volumetric hardening/softening model for the simulation of soil behavior. One flexible feature of the model is the capability for adding user-defined hardening/softening laws, which are then communicated to the model by means of tables. As mentioned by Davis and Selvadurai (2002), the general concept of hardening is very useful whenever there is a need for model responses that are more detailed than is possible with perfect plasticity. In particular, a closed yield surface would be almost useless without volumetric (cap) hardening.

The motivation for closing the yield surface by a cap on the mean stress axis is to permit plastic behavior in response to an isotropic stress increase. This plasticity effect accounts for grain crushing and rearrangement, and is particular to soils. In the double-yield model, the cap is a plane, normal to the mean stress axis in stress space. The impact of this particular shape on the coefficient of lateral earth pressure, K_0, as predicted by the model in uniaxial compression tests, has been considered by some users to be somewhat restrictive. The cap-yield model is a modification of the double-yield model that addresses this issue by accounting for a cap with an elliptic shape in the (p', q) plane. The ratio of axes of the ellipse, α, determines the value of K_0, and is a material property for the model, which can be chosen to match a known value in uniaxial compression.

In addition, when subjected to deviatoric loading, soils usually exhibit a decrease in stiffness, accompanied by irreversible deformation. In most cases, the plot of deviatoric stress versus axial strain obtained in a drained triaxial test may be approximated by a hyperbola. This feature has been used by Duncan and Chang (1970) to formulate their well-known "hyperbolic soil" model. The hyperbolic soil model of Duncan and Chang is a nonlinear elastic model that has been shown to exhibit some drawbacks. These drawbacks include, for example, difficulty in detecting and characterizing unloading/reloading and, in specific cases, producing a nonphysical bulk-modulus value that can lead to an erroneous energy generation in the model. Because the cap-yield model is formulated in the theory of hardening plasticity, it allows for an alternative expression of the hyperbolic behavior (based on friction hardening), which is capable of addressing some of these problems.*

When tested under drained triaxial conditions, soils generally exhibit shear-induced volume changes that are strongly dependent on soil density. Typically, there is a tendency for the soil to contract under small shear strains, and to dilate under larger strains, unless it is very loose (Byrne et al. 2003). In particular, when fluid fills the pores, it is this tendency of the soil skeleton to contract and dilate that controls its liquefaction response. Also, the shear-stress/shear-strain response of loose soil may exhibit a softening response under undrained conditions. It is the existence of a peak in shear strength which may lead to instability (static liquefaction) during a monotonic load-controlled process (Boukpeti 2001). Shear-induced volume changes can be accounted for in the cap-yield model by means of a dilation hardening/softening law.

---

* A simplified version of the cap-yield model (the cap-yield-simplified model) also addresses the difficulties of the Duncan and Chang model, and is provided as an alternative to the Duncan and Chang model. See Section 1.6.11.

The cap-yield model is a strain-hardening constitutive model characterized by a frictional and cohesive Mohr-Coulomb shear envelope, and an elliptic volumetric cap with ratio of axes, defined by a shape parameter, α. The double-yield model, with its planar volumetric cap, is obtained as a special case of the cap-yield formulation by assuming a value of α that is large compared to 1, and specifying zero cohesion. The basic model is described in the following pages.

The basic cap-yield model behavior can be enhanced using three types of hardening laws: a cap-hardening law, to capture the volumetric power law behavior observed in isotropic compaction tests; a friction-hardening law, to reproduce the hyperbolic stress-strain law behavior observed in drained triaxial tests; and a compaction/dilation law to model irrecoverable volumetric strain taking place as a result of soil shearing. This customizing of the cap-yield model is discussed in Section 1.6.10.3.

1.6.10.1 Incremental Elastic Law

The elastic behavior is expressed using Hooke's law. The incremental expression of the law in terms of principal stress and strain* has the form

$$\begin{aligned}\Delta\sigma_1' &= \alpha_1 \Delta e_1^e + \alpha_2(\Delta e_2^e + \Delta e_3^e)\\ \Delta\sigma_2' &= \alpha_1 \Delta e_2^e + \alpha_2(\Delta e_1^e + \Delta e_3^e)\\ \Delta\sigma_3' &= \alpha_1 \Delta e_3^e + \alpha_2(\Delta e_1^e + \Delta e_2^e)\end{aligned} \tag{1.271}$$

where $\alpha_1 = K^e + 4G^e/3$, $\alpha_2 = K^e - 2G^e/3$, and K^e and G^e are current, tangent elastic bulk and shear modulus, respectively. Some useful relations between K^e, G^e, Young modulus, E^e, and Poisson's ratio, ν, are listed for reference:

$$K^e = \frac{E^e}{3(1-2\nu)} \qquad G^e = \frac{E^e}{2(1+\nu)}$$

$$\frac{K^e}{G^e} = \frac{2(1+\nu)}{3(1-2\nu)} \tag{1.272}$$

* Principal stress and strain components, represented by the symbol σ_i and e_i (i = 1,3), respectively, are positive in extension. Also, effective stresses are denoted by a prime. The principal effective stresses are σ_1', σ_2', σ_3' and, by convention, $\sigma_1' < \sigma_2' < \sigma_3'$ (i.e., σ_1' is the most compressive stress).

1.6.10.2 Yield and Potential Functions

Shear Yield Criterion and Flow Rule – Shear yielding is defined by a Mohr-Coulomb criterion. The yield envelope is expressed, in a form consistent with the cap formulation:

$$f^s = Mp' - q + Nc \tag{1.273}$$

where c is cohesion, $M = 6\sin\phi_m/(3 - \sin\phi_m)$ and $N = 6\cos\phi_m/(3 - \sin\phi_m)$. p' is the mean effective stress, $p' = -(\sigma_1' + \sigma_1' + \sigma_1')\,/\,3$, and q is a measure of shear stress, defined as

$$q = -[\sigma_1' + (\delta - 1)\sigma_2' - \delta\sigma_3'] \tag{1.274}$$

where $\delta = (3 + \sin\phi_m)/(3 - \sin\phi_m)$.

In the *UDEC* formulation, the mobilized friction angle, ϕ_m, and cohesion, c, are given in terms of plastic shear-strain measure, γ^p, by means of a user-defined table. If no table is provided, it is assumed that friction and cohesion are constant, and equal to the input value of the friction property and cohesion property. Also, plastic shear strain, γ^p, is measured by a hardening parameter, whose incremental form is the second invariant of the incremental plastic deviatoric strain tensor as shown below in Eq. (1.279) (also see Section 1.6.4.1).

The potential function is nonassociated, and has the form

$$g = M^* p' - q^* \tag{1.275}$$

where

$$q^* = [\sigma_1' + (\delta^* - 1)\sigma_2' - \delta^*\sigma_3'] \tag{1.276}$$

In these equations, $\delta^* = (3 + \sin\psi_m)/(3 - \sin\psi_m)$ and $M^* = 6\sin\psi_m/(3 - \sin\psi_m)$. Also, the mobilized dilatancy angle, ψ_m, is given in terms of plastic shear strain, γ^p, by means of a user-defined table. If no table is provided, it is assumed that dilation is constant, and equal to the input value of dilation property.

Volumetric Cap Criterion and Flow Rule – Yielding on the cap is associated; the criterion is

$$f^c = \frac{q^2}{\alpha^2} + p'^2 - p_c^2 \tag{1.277}$$

where α is a dimensionless parameter, defining the shape of the elliptical cap in the (p', q) plane, and p_c is cap pressure. The hardening curve relating cap pressure, p_c, to cap plastic volumetric

strain, e^p, is provided by means of a user-defined table. If no table is provided, p_c is assumed to be constant, and equal to the input value of cap pressure property.

Like the double-yield model, the cap-yield model uses a simple rule whereby the incremental elastic stiffness, K^e, is proportional to the current incremental plastic stiffness, $H = dp_c/de^p$. The factor of proportionality is a constant, R. The current value of elastic shear modulus, G^e, is derived assuming a constant Poisson's ratio, using the input upper-bound values of shear and bulk modulus.

Tensile Yield Criterion and Flow Rule – The tensile yield function is the same as that used for the Mohr-Coulomb and strain-hardening/softening models (see Sections 1.6.2.2 and 1.6.6.2)

$$f^t = \sigma^t - \sigma_3 \tag{1.278}$$

The tensile strength, σ^t, is given in terms of the plastic tensile-strain measure, e^{pt}, as defined in Section 1.6.4.1, and input by means of a user-defined table. If no table is provided, it is assumed that tensile strength is constant, and equal to the input value of the tensile strength property.

Hardening Parameters – The evolution parameters for shear, cap and tensile yielding are independent. The parameter for shear yielding, γ^p, is defined incrementally as

$$\Delta\gamma^p = \left\{ \frac{1}{2}\left(\Delta e_1^{ps} - \Delta e_m^{ps}\right)^2 + \frac{1}{2}\left(\Delta e_m^{ps}\right)^2 + \frac{1}{2}\left(\Delta e_3^{ps} - \Delta e_m^{ps}\right)^2 \right\}^{\frac{1}{2}} \tag{1.279}$$

where

$$\Delta e_m^{ps} = \frac{1}{3}\left(\Delta e_1^{ps} + \Delta e_3^{ps}\right)$$

and Δe_j^{ps}, $j = 1, 3$ are the principal plastic shear strain increments.

The evolution parameter for cap yielding is the modulus of plastic volumetric strain, e^p, and its increment is defined as (see Section 1.6.6.3)

$$\Delta e^p = |\Delta e_1^p + \Delta e_2^p + \Delta e_3^p| \tag{1.280}$$

where Δe_j^p, $j = 1, 3$ are principal plastic strain increments from yielding on the cap.

The evolution parameter for tensile yielding is the modulus of plastic tensile strain, e^{pt}. The increment of plastic tensile strain is defined as (also see Section 1.6.4.1)

$$\Delta e^{pt} = \Delta e_3^{pt} \tag{1.281}$$

where Δe_3^{pt} is the increment of tensile plastic strain in the direction of the major principal stress (recall that tensile stresses are positive).

1.6.10.3 Customizing the cap-yield Model

Cap Hardening – Soil stiffness usually increases in a nonlinear fashion as a function of isotropic pressure. A cap-hardening table is used to specify a power law behavior. In most experimental cases, soil volumetric behavior in an isotropic compaction test can be captured by a power law of the form

$$\frac{dp'}{de} = K_{ref}^{iso}\left(\frac{p'}{p_{ref}}\right)^m \tag{1.282}$$

where e is (minus) volumetric strain, K_{ref}^{iso} is the slope of the laboratory curve for p' versus e at reference effective pressure, p_{ref}, and m is a constant ($m < 1$). A typical graph, representative of this law, is sketched with a small unloading excursion in Figure 1.42.

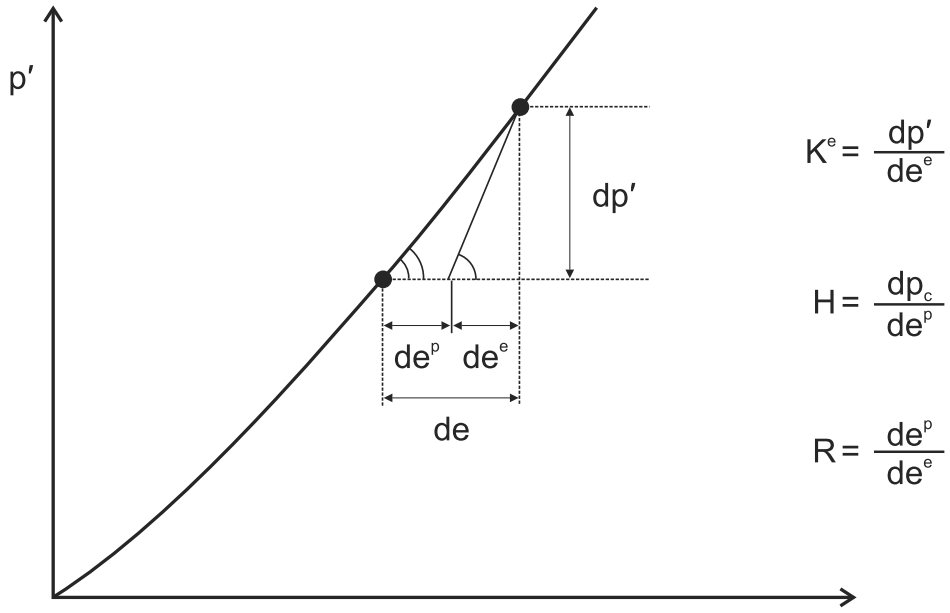

Figure 1.42 Isotropic consolidation test: pressure versus volumetric strain

For input into the cap-yield model, a relation between cap pressure, p_c, and plastic volumetric strain, e^p, is required. This relation can be obtained from the following considerations. For isotropic compression $dp' = dp_c$, and we can write

$$\frac{dp_c}{de^p} = \frac{de}{de^p}\frac{dp'}{de} \tag{1.283}$$

Now, the total strain increment has elastic and plastic contributions: $de = de^e + de^p$. Substitution of this expression for de in Eq. (1.283) gives

$$\frac{dp_c}{de^p} = \frac{de^e + de^p}{de^p}\frac{dp'}{de} \tag{1.284}$$

The cap-yield model assumes that the ratio of elastic modulus, K^e, to hardening modulus, H, is equal to a constant, $R = K^e \,/\, H$, where, by definition, $K^e = dp'/de^e$ and $H = dp_c \,/\, de^p$. For isotropic compression, $dp' = dp_c$, and we can write

$$R = \frac{de^p}{de^e} \tag{1.285}$$

Finally, using Eq. (1.285) in Eq. (1.284) gives, after some manipulation,

$$\frac{dp_c}{de^p} = \frac{1+R}{R}\frac{dp'}{de} \tag{1.286}$$

After substitution of Eq. (1.282) in Eq. (1.286), we obtain

$$\frac{dp_c}{de^p} = \frac{1+R}{R}K^{iso}_{ref}\left(\frac{p'}{p_{ref}}\right)^m \tag{1.287}$$

Integration of this expression gives, with $p_c = 0$ at $e^p = 0$,

$$p_c = p_{ref}\left[(1-m)\frac{1+R}{R}\frac{K^{iso}_{ref}}{p_{ref}}e^p\right]^{\frac{1}{1-m}} \tag{1.288}$$

This formula is used to generate the input table of p_c in terms of e^p. The law has 4 parameters: K^{iso}_{ref}, p_{ref}, m and R. Note that, since the cap-yield model assumes that $K^e = R \times dp_c/de^p$, by virtue of Eq. (1.287), the equation for the elastic bulk modulus is

$$K^e = (1 + R)K^{iso}_{ref}\left(\frac{p'}{p_{ref}}\right)^m \tag{1.289}$$

Friction Hardening – For most soils, the plot of deviatoric stress versus axial strain obtained in a drained triaxial test may be approximated by a hyperbola. The model is supplemented by a friction strain-hardening table to capture this hyperbolic behavior. For friction-hardening behavior, we adopt the following (hyperbolic) incremental law, similar to the one implemented in the UBCSAND model (Byrne et al. 2003),

$$d(\sin\phi_m) = \frac{G^p}{p'}d(\gamma^p) \tag{1.290}$$

where p' is effective pressure, and the plastic shear modulus, G^p, is given by

$$G^p = \beta G^e\left(1 - \frac{\sin\phi_m}{\sin\phi_f}R_f\right)^2 \qquad : \phi_m \le \phi_f \tag{1.291}$$

In this formula, G^e is the elastic tangent shear modulus, ϕ_f is the ultimate friction angle, R_f (the failure ratio) is a constant, smaller than 1 (0.9 in most cases), used to assign a lower bound for G^p, and β is a calibration factor.

The elastic tangent shear modulus is a function of p', and we have

$$G^e = G^e_{ref}\left(\frac{p'}{p_{ref}}\right)^m \tag{1.292}$$

where G^e_{ref} is elastic tangent shear modulus at reference effective pressure, p^{ref}, and m is a constant ($m \le 1$), taken as 1 for this discussion. After substitution of Eq. (1.292) in Eq. (1.291), the resulting expression in Eq. (1.290), and rearranging terms, we obtain

$$d(\gamma^p) = \frac{p_{ref}}{G^e_{ref}}\left(\frac{p'}{p_{ref}}\right)^{1-m}\frac{d(\sin\phi_m)}{\left(1 - \frac{\sin\phi_m}{\sin\phi_f}R_f\right)^2} \tag{1.293}$$

Using that $\phi_m = 0$ at $\gamma^p = 0$, integration of this expression gives

$$\gamma^p = \frac{p_{ref}}{G^e_{ref}}\left(\frac{p'}{p_{ref}}\right)^{1-m}\frac{\sin\phi_f}{R_f}\left[\frac{1}{1 - \frac{\sin\phi_m}{\sin\phi_f}R_f} - 1\right] \tag{1.294}$$

For $m = 1$, the hardening law simplifies to

$$\gamma^p = \frac{p_{ref}}{G^e_{ref}} \frac{\sin\phi_f}{R_f} \left[\frac{1}{1 - \frac{\sin\phi_m}{\sin\phi_f} R_f} - 1 \right] \tag{1.295}$$

This expression is used to generate the model input table of friction in terms of plastic shear strain. As demonstrated in the example below, the use of this hardening law for modeling primary loading in a triaxial test will produce a hyperbolic curve of deviatoric stress versus axial strain. The law has 5 parameters: G^e_{ref}, p_{ref}, R_f, ϕ_f and β.

Dilation Hardening – A certain amount of irrecoverable volumetric strain, e^p, is expected to take place as a result of soil shearing. Also, under small (monotonic or cyclic) shear strains, there is a tendency for the soil skeleton to contract due to grain rearrangements. For larger shear strains, the soil skeleton may dilate if the soil is dense, as a result of grains riding over each other. A dilation strain-hardening table is used to model this non-monotonic behavior. For the cap-yield model, the shear-hardening flow rule has the form

$$\dot{e}^p = \dot{\gamma}^p \sin\psi_m \tag{1.296}$$

where ψ_m is the (mobilized) dilation angle.

Several different laws are available in the literature to characterize ψ_m. For the purpose of the present illustration, we use an equation based on Rowe's stress-dilatancy theory (Rowe 1962). According to this theory, there is a constant-volume stress ratio, ϕ_{cv}, below which the material contracts (i.e., for $\phi_m < \phi_{cv}$), while for higher stress ratios (i.e., for $\phi_m > \phi_{cv}$), the material dilates. The equation has the form

$$\sin\psi_m = \frac{\sin\phi_m - \sin\phi_{cv}}{1 - \sin\phi_m \sin\phi_{cv}} \tag{1.297}$$

where

$$\sin\phi_{cv} = \frac{\sin\phi_f - \sin\psi_f}{1 - \sin\phi_f \sin\psi_f} \tag{1.298}$$

and ϕ_f and ψ_f are ultimate (known) values of friction and dilation, respectively.

A table of dilation value versus plastic shear strain is produced for input in *UDEC*, based on the last two equations and the assumed relation between ϕ_m and γ^p reported in Eq. (1.295).

1.6.10.4 Implementation Procedure

Note that the parameters involved in the selected shear and volumetric hardening laws are not all independent: they must be chosen consistent with the model assumptions. One assumption is that the ratio K^e / G^e be constant, and equal to the ratio of input upper-bound values K and G. Assuming that the reference pressure is the same in Eqs. (1.289) and (1.292), it follows that the exponent m should be the same in both laws. Also, we must have

$$\frac{K}{G} = \frac{(1+R)K^{iso}_{ref}}{G^e_{ref}} \tag{1.299}$$

Thus, the parameter R should be consistent with the choice for K^{iso}_{ref} and G^e_{ref} (assuming these were selected independently). The consistency condition gives

$$R = \frac{K}{G}\frac{G^e_{ref}}{K^{iso}_{ref}} - 1 \tag{1.300}$$

Obviously, the derived value for R should be larger than or equal to zero.

1.6.10.5 Isotropic Compression Tests

Isotropic compression tests on dense, medium and loose sand are simulated using the cap-yield model with the cap-hardening law described by Eq. (1.288), input in the form of a table. The cap-yield model properties for the tests are listed in Table 1.2.

Table 1.2 Cap-yield model properties for isotropic compr. test

Parameter	Dense	Medium	Loose
K^{iso}_{ref} (kN/m^2)	40,000	30,000	20,000
p_{ref} (kPa)	100	100	100
ν	0.2	0.2	0.2
m	0.5	0.5	0.5
R	0.66	0.66	0.66
α	1	1	1

The simulation is run in axisymmetric mode. The *UDEC* grid consists of three separate zones with unit dimensions, lined up along the symmetry axis. The initial stress state is isotropic in each zone; the magnitude of the confining stress is 10 kN/m^2. The sand is normally consolidated for the tests (the initial cap pressure is equal to 10 kN/m^2). The input values of bulk and shear modulus are set

to high values, consistent with the given Poisson's ratio, ν, listed in Table 1.2. (These input values are used as the upper bound for tangent bulk and shear elastic modulus calculated by the code.) The cap behavior is assigned using a different table for each zone, consistent with the formula (Eq. (1.288)) and the data in Table 1.2. The base of the zones is fixed in the axial (y-) direction, confining velocities of magnitude 10^{-6} m/step are applied at the top and lateral sides of the zone for a total of 2500 steps. Five unloading/reloading excursions are also included.

A plot of vertical (axial) stress versus axial strain for the test is shown for dense, medium and loose soil cases in Figure 1.43. The plot shows the power law and stiffer behavior achieved by the denser soil, as expected from the model. A plot of elastic bulk modulus versus axial strain for the test is shown in Figure 1.44. The bulk modulus is seen on the plot to remain constant during unloading/reloading; also, the value is higher for higher strain levels, consistent with the dependency of the property on plastic deformation.

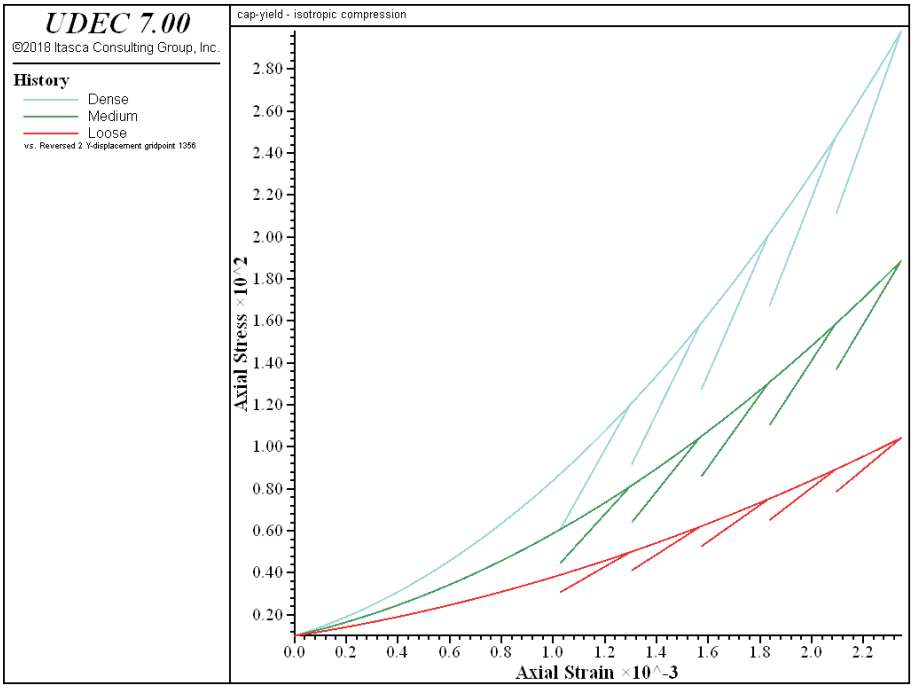

Figure 1.43 Axial stress (in kN/m^2) versus axial strain for dense, medium and loose sand

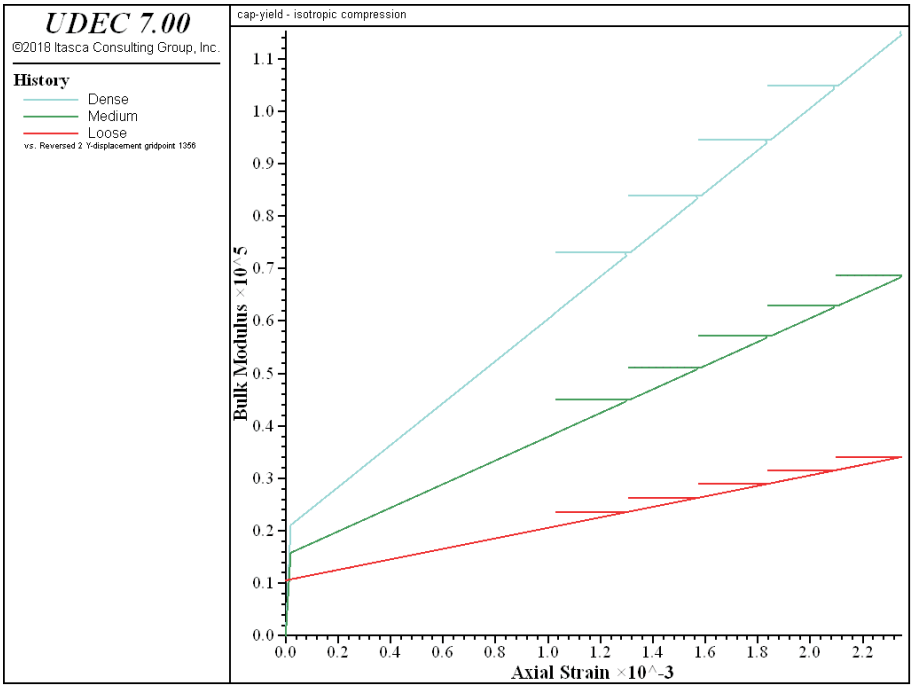

Figure 1.44 Bulk modulus (in kN/m^2) versus axial strain for dense, medium and loose sand

Example 1.7 Isotropic compression tests

```
model new
;file: cysoil_1.dat'
Model title 'cap-yield - isotropic compression'
[global pc0 = 10.0]
[global  _v1=-2e-5]
[global  _v2= 2e-6]
[global  _v3=-2e-6]
block config axisymmetry
block tolerance corner-round-length 5E-3
block tolerance minimum-edge-length 1E-2
block create polygon 0 0 0 5 1 5 1 0
block cut crack 0 1 1 1
block cut crack 0 2 1 2
block cut crack 0 3 1 3
block cut crack 0 3 1 3
block cut crack 0 4 1 4
block zone gen edge 2.0
block zone group 'mat1'
block zone cmodel assign cap-yield range group 'mat1'
block zone prop density 1E3 pressure-reference=100 poisson=.2 ...
  multiplier=.667 pressure-initial=@pc0 flag-cap=1 pressure-cap @pc0 ...
  friction 45 range group 'mat1'
block contact prop mat 1 st-n 1e5 st-s 1e5
block zone group 'Null:j2' range atblock 0.5 1.5
block zone cmodel assign null range group 'Null:j2'
block zone group 'Null:j4' range atblock 0.5 3.5
block zone cmodel assign null range group 'Null:j4'
block zone prop shear-reference 300 range pos-x 0 1 pos-y 4 5
; --- medium ---
block zone prop shear-reference 225 range pos-x 0 1 pos-y 2 3
; --- loose ---
block zone prop shear-reference 150 range pos-x 0 1 pos-y 0 1
;
block insitu  stress -10.0 0.0 -10.0 stress-ZZ -10.0
block gridpoint apply vel-x 0 vel-y 0
block gridpoint apply velocity-y @_v1 range pos-x 0 1 pos-y 0.9 1.1
block gridpoint apply velocity-y @_v1 range pos-x 0 1 pos-y 2.9 3.1
block gridpoint apply velocity-y @_v1 range pos-x 0 1 pos-y 4.9 5.1
block gridpoint apply velocity-x @_v1 range pos-x 0.9 1.1 pos-y 0 5
block insitu  stress -10.0 0.0 -10.0 stress-ZZ -10.0
;
[global _z5 = block.zone.near(0,5)]
[global _z3 = block.zone.near(0,3)]
```

```
[global _z1 = block.zone.near(0,1)]
fish define _bulk_current1
  global _bulk_current5 = block.zone.prop(_z5,'bulk')
  global _bulk_current3 = block.zone.prop(_z3,'bulk')
  global _bulk_current1 = block.zone.prop(_z1,'bulk')
end
history interval 20
;
block zone hist stress-yy 0 5
block gridpoint history displacement-y 0 5
fish history @_bulk_current5
block zone hist stress-yy 0 3
block gridpoint history displacement-y 0 3
fish history @_bulk_current3
block zone hist stress-yy 0 1
block gridpoint history displacement-y 0 1
fish history @_bulk_current1
;
fish define trip
  loop i (1,5)
    command
      bl gridpoint apply velocity-y @_v1 range pos-x 0 1 pos-y 0.9 1.1
      bl gridpoint apply velocity-y @_v1 range pos-x 0 1 pos-y 2.9 3.1
      bl gridpoint apply velocity-y @_v1 range pos-x 0 1 pos-y 4.9 5.1
      bl gridpoint apply velocity-x @_v1 range pos-x 0.9 1.1 pos-y 0 5
      bl cycle 300
      bl gridpoint apply velocity-y @_v2 range pos-x 0 1 pos-y 0.9 1.1
      bl gridpoint apply velocity-y @_v2 range pos-x 0 1 pos-y 2.9 3.1
      bl gridpoint apply velocity-y @_v2 range pos-x 0 1 pos-y 4.9 5.1
      bl gridpoint apply velocity-x @_v2 range pos-x 0.9 1.1 pos-y 0 5
      bl cycle 3000
      bl gridpoint apply velocity-y @_v3 range pos-x 0 1 pos-y 0.9 1.1
      bl gridpoint apply velocity-y @_v3 range pos-x 0 1 pos-y 2.9 3.1
      bl gridpoint apply velocity-y @_v3 range pos-x 0 1 pos-y 4.9 5.1
      bl gridpoint apply velocity-x @_v3 range pos-x 0.9 1.1 pos-y 0 5
      bl cycle 3000
    end_command
  end_loop
end
block cycle 1000
@trip
model save 'cysoil_1.sav'
```

1.6.10.6 Oedometer Tests

Oedometer test simulations are carried out for different values of the parameter α, to evaluate the impact of the cap aspect ratio on confining stress when yielding occurs on the cap. The values of α considered for the tests are 0.5, 1 and 10^{20} (i.e., a value very large compared to 1, in which case the behavior of the double-yield model is recovered).

We use the same setup and properties (apart from α) as in the previous example, except in this case the simulations are run in plane-strain, with fixed lateral boundaries to simulate oedometer test conditions. Friction is assigned a large value to prevent shear yielding. The ratio, K_0, of confining stress to vertical stress, σ_{xx} / σ_{yy}, is plotted versus axial strain for dense, medium and loose sand in two figures below: Figure 1.45 compares predictions for α = 0.5 and $\alpha = 10^{20}$ (double-yield model), and Figure 1.46 shows plots for α = 1.0 and $\alpha = 10^{20}$ (double-yield model).

The results of the oedometer simulations show that, with the given properties, a higher value of K_0 is achieved for the cap-yield model than the double-yield model. And for all tests, the lower the aspect ratio of the cap, the higher the K_0 achieved. Also, dense, medium and loose sands converge to the same ultimate K_0 value as deformation takes place, and they do so at a faster deformation rate for the cap-yield model than the double-yield model.

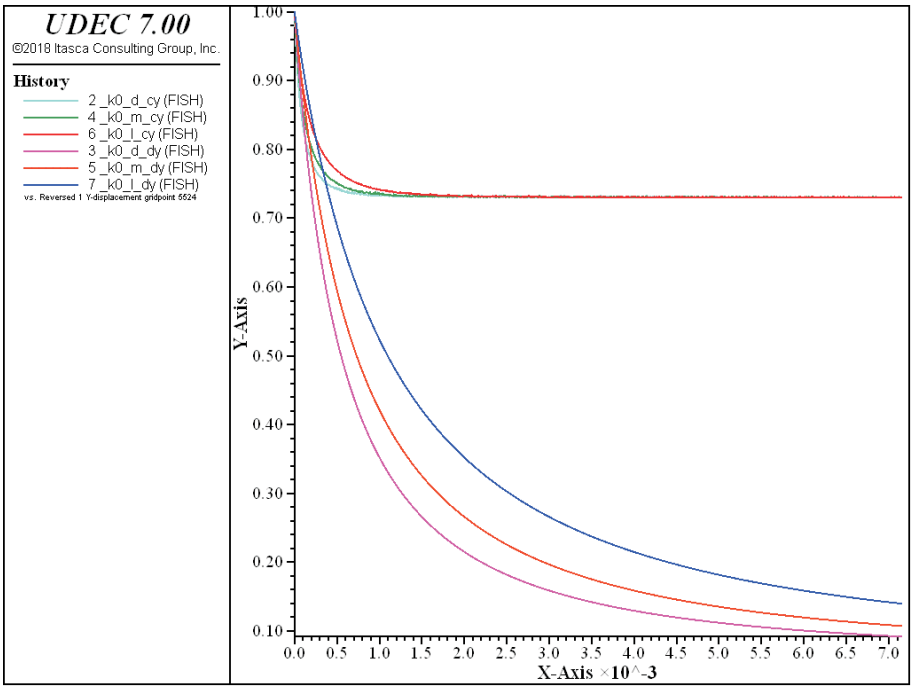

Figure 1.45 K_0 versus axial strain for dense, medium and loose sand – α = 0.5 (top) and double-yield model (bottom)

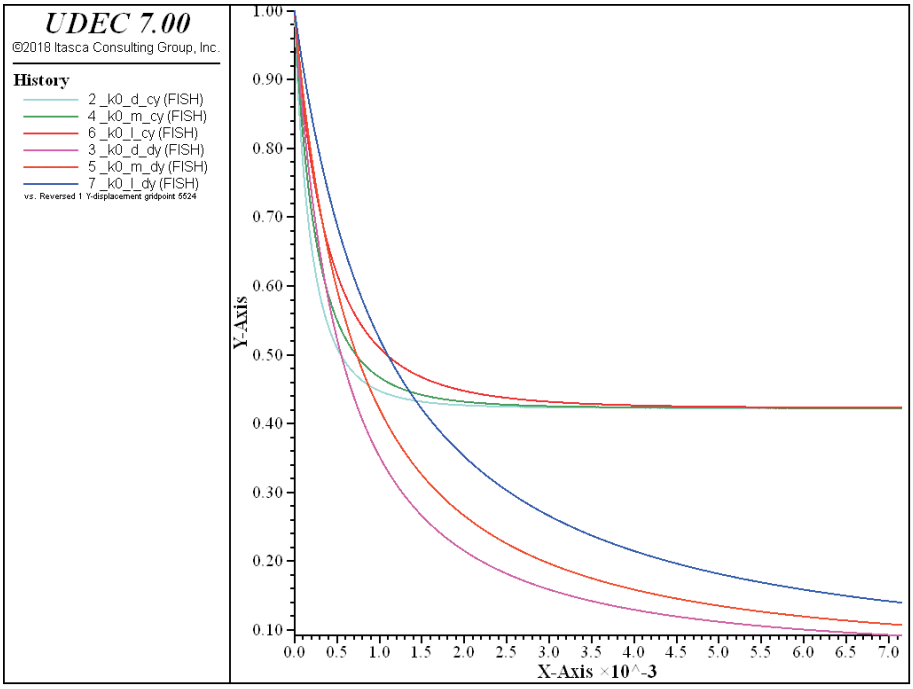

Figure 1.46 K_0 versus axial strain for dense, medium and loose sand – α = 1.0 (top) and double-yield model (bottom)

Example 1.8 Oedometer tests

```
model new
;file: cysoil_2.dat'
model title "Oedometer test - dense, medium, loose sand - CYSoil and DY"
block config
[global _pc0 = 10.0]
[global _vy = -1.83e-4]
block tolerance corner-round-length 5E-3
block tolerance minimum-edge-length 1E-2
block create polygon 0 0 0 5 3 5 3 0
block cut crack (0,1) (3,1) join
block cut crack (0,2) (3,2) join
block cut crack (0,3) (3,3) join
block cut crack (0,4) (3,4) join
block cut crack (1,0) (1,5) join
block cut crack (2,0) (2,5) join
block zone gen edge 2.0
block zone group 'gcy'
block zone group 'gdy' range pos-x 2 3 pos-y 0 5
block zone cmodel assign cap-yield  range group 'gcy'
block zone property density=1000 pressure-reference=100. poisson=0.2 ...
```

```
  multiplier=[2.0/3.0] flag-cap=1 flag-shear=1 friction=89.0  ...
  pressure-cap=@_pc0  pressure-initial=@_pc0  range group 'gcy'
block zone cmodel assign double-yield range group 'gdy'
block zone property density=1000 bulk-maximum=1.e15 ...
  shear-maximum=0.75e15 friction=89.0 pressure-cap=@_pc0 ...
  multiplier=[2.0/3.0] range group 'gdy'
block zone group 'gnull' range pos-x 0 3 pos-y 1 2
block zone group 'gnull' range pos-x 0 3 pos-y 3 4
block zone group 'gnull' range pos-x 1 2 pos-y 0 5
block zone cmodel assign null  density 1000 bu 1e8 sh .7e8 ...
  range group 'gnull'
; double-yield
call 'fish'
@cap_table(1, 300.)
block zone property strain-volumetric-plastic=@evp0 ...
  table-pressure-cap=1 range group 'gdy' position-z 4 5
@cap_table(2, 225.)
block zone property strain-volumetric-plastic=@evp0 ...
  table-pressure-cap=2 range group 'gdy' position-z 2 3
@cap_table(3, 150.)
block zone property strain-volumetric-plastic=@evp0 ...
  table-pressure-cap=3 range group 'gdy' position-z 0 1
; cap-yield-soil
zone property shear-reference 300. range group 'gcy' position-z 4 5
zone property shear-reference 225. range group 'gcy' position-z 2 3
zone property shear-reference 150. range group 'gcy' position-z 0 1
bloc con prop mat 1 st-n 1e9 st-s 1e9
block insitu  stress [-_pc0] 0.0 [-pc0] stress-ZZ [-pc0]
block gridpoint apply velocity-y 0
block gridpoint apply velocity-x 0
block gridpoint apply-interior velocity-y 0
block gridpoint apply-interior velocity-x 0

block gridpoint apply velocity-y [_vy] range pos-x 0 3 pos-y 0.9 1.1
block gridpoint apply velocity-y [_vy] range pos-x 0 3 pos-y 2.9 3.1
block gridpoint apply velocity-y [_vy] range pos-x 0 3 pos-y 4.9 5.1
block gridpoint apply-int velocity-y [_vy] range pos-x 0 3 pos-y 0.9 1.1
block gridpoint apply-int velocity-y [_vy] range pos-x 0 3 pos-y 2.9 3.1
;block gridpoint apply-int velocity-y [_vy] range pos-x 0 3 pos-y 4.9 5.1
;
@_hist_setup
history interval 100
block grid hist dis-y 0,1
fish history @_k0_d_cy
fish history @_k0_d_dy
fish history @_k0_m_cy
```

```
fish history @_k0_m_dy
fish history @_k0_l_cy
fish history @_k0_l_dy
model save 'ini'

; -- alpha = 0.5
model restore 'ini'
block zone prop alpha=0.5 range group 'gcy'
block cycle 120000
model save 'al1'
 -- alpha = 1.0
model restore 'ini'
block zone prop alpha=1.0 range group 'gcy'
block cycle 120000
ret
model save 'al2'
 -- alpha = 1.5
model restore 'ini'
block zone prop alpha=1.5 range group 'gcy'
block cycle 12000
model save 'al3'
ret
```

1.6.10.7 Drained Triaxial Tests – Constant Dilation

Triaxial tests on dense, medium and loose sand are simulated using the cap-yield model with the friction-hardening law described in Eq. (1.294) – input in the form of tables. The model properties are listed in Table 1.3. The cap pressure is assigned a value that is very large compared to the stress level reached in the simulations, in order to prevent yielding on the cap. The cap α is 1.

Two simulations are run: one without cohesion, and one with cohesion set to 100 kPa. The simulations are run in axisymmetric mode. The *UDEC* grid consists of one zone with unit dimensions. The initial stress state is isotropic, with mean pressure equal to 100 kPa. The lateral pressure is kept constant during the test, the base of the model is fixed in the axial (y-) direction, and an axial velocity of 10^{-6} m/step is applied at the top of the model for a total of 5000 steps. In addition, three unloading/reloading excursions are performed.

Table 1.3 Cap-yield model properties for triaxial test

Parameter	Dense	Medium	Loose
G^e_{ref} (kPa)	50,000	37,500	25,000
p_{ref} (kPa)	100	100	100
ν	0.2	0.2	0.2
m	1	1	1
ϕ_f (degrees)	40	35	30
ψ_f (degrees)	10	5	0
R_f	0.9	0.9	0.9
β	0.35	0.35	0.35
cohesion (kPa)	100	100	100

A plot of deviatoric stress versus axial strain for the cohesionless simulation is shown in Figure 1.47 for dense, medium and loose sand cases. The plot shows the hyperbolic behavior expected from the model, and the higher failure level achieved by the denser soil. Three unloading/reloading excursions (also shown on the figure) illustrate the model capabilities. The plot of volumetric strain versus axial strain for the cohesionless simulation is shown in Figure 1.48. The volumetric behavior is monotonic in the plot, the dilatant behavior of the dense sand is clearly shown.

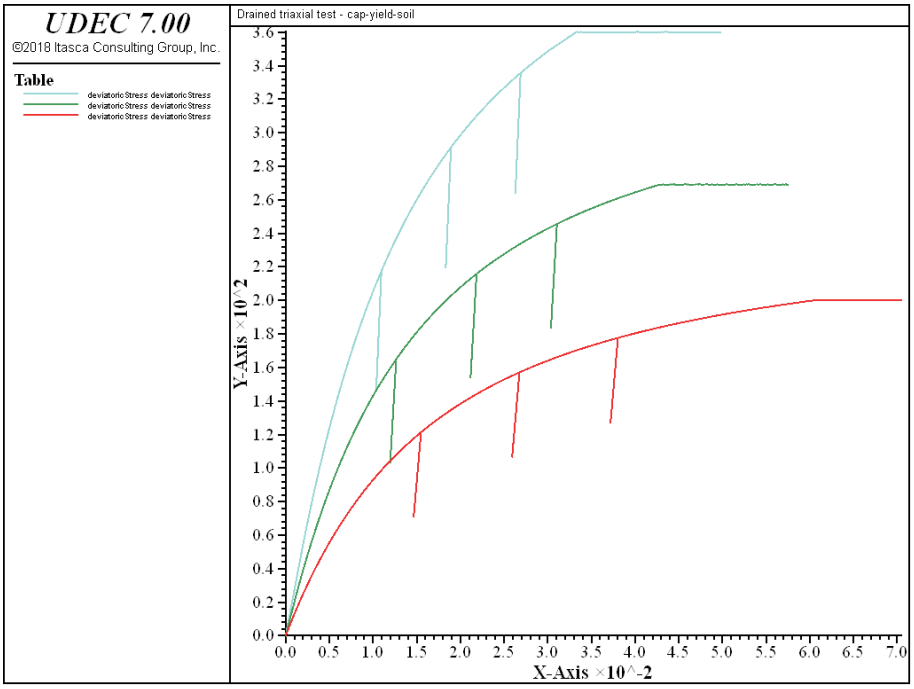

Figure 1.47 *$|\sigma_1 - \sigma_3|$ (in kN/m^2) versus axial strain for dense, medium and loose sand – constant dilation*

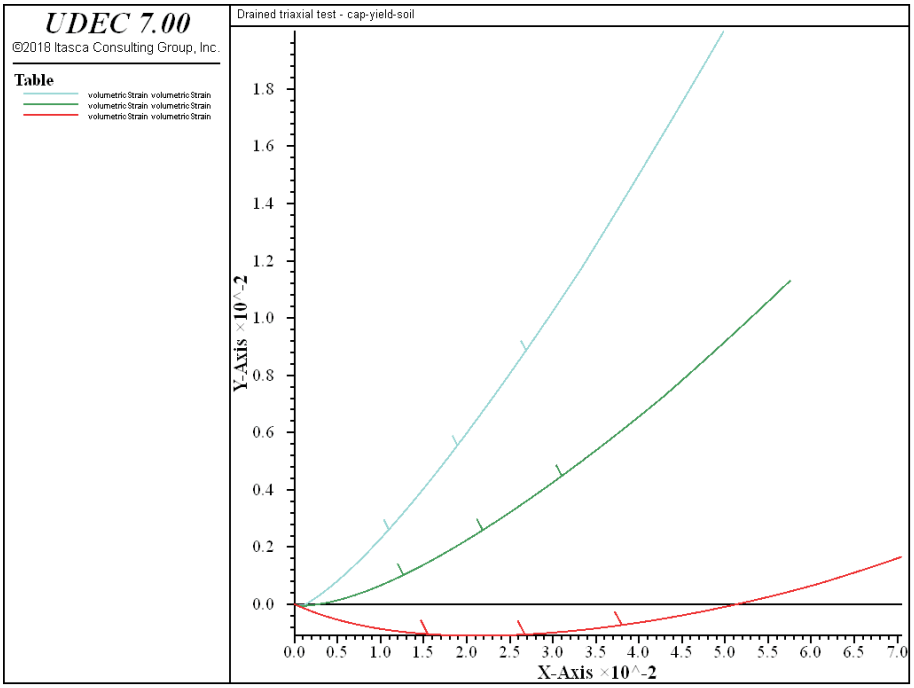

Figure 1.48 *Volumetric strain versus axial strain for dense, medium and loose sand – constant dilation*

The comparable results for the simulation with cohesion set to 100 kPa are shown in Figures 1.49 and 1.50. By specifying the same friction table and zero initial friction, the material behavior is expected to be elastic for values of maximum shear stress smaller than the cohesion value, and elastic-plastic at higher shear stress levels. This is evident in Figure 1.49. This simulation is done to illustrate the working of the cohesion logic; the friction hardening table should be adjusted to reflect more realistic behavior for a cohesive material.

Example 1.9 lists the data file for the triaxial test on dense sand. Test results for all three cases are written to tables. Plots in Figures 1.47 through 1.50, compare the three cases for cohesionless and cohesive soil.

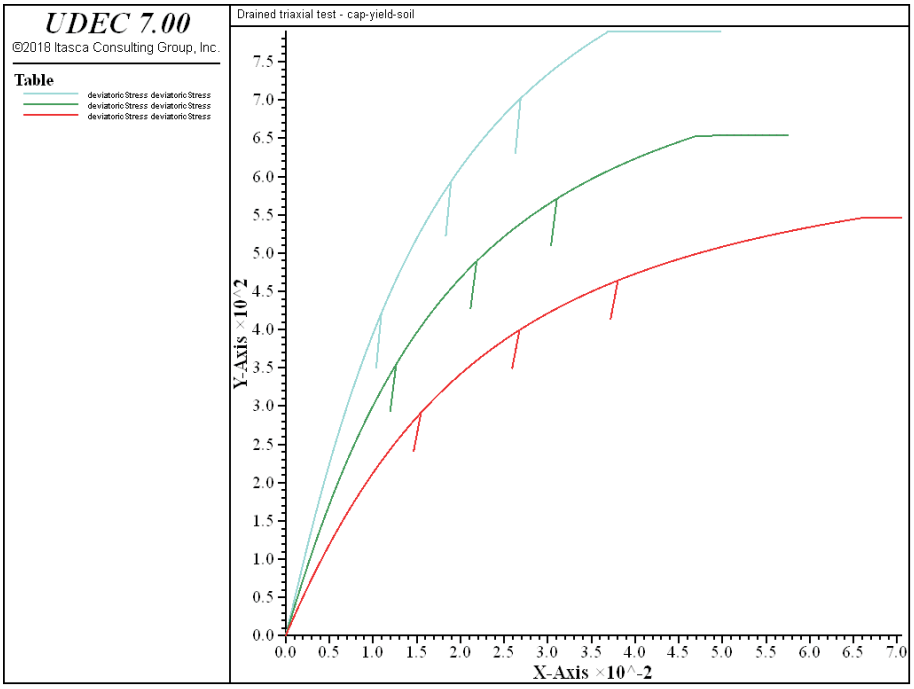

Figure 1.49 *$|\sigma_1 - \sigma_3|$ (in kN/m^2) versus axial strain for dense, medium and loose sand – constant dilation, cohesion = 100*

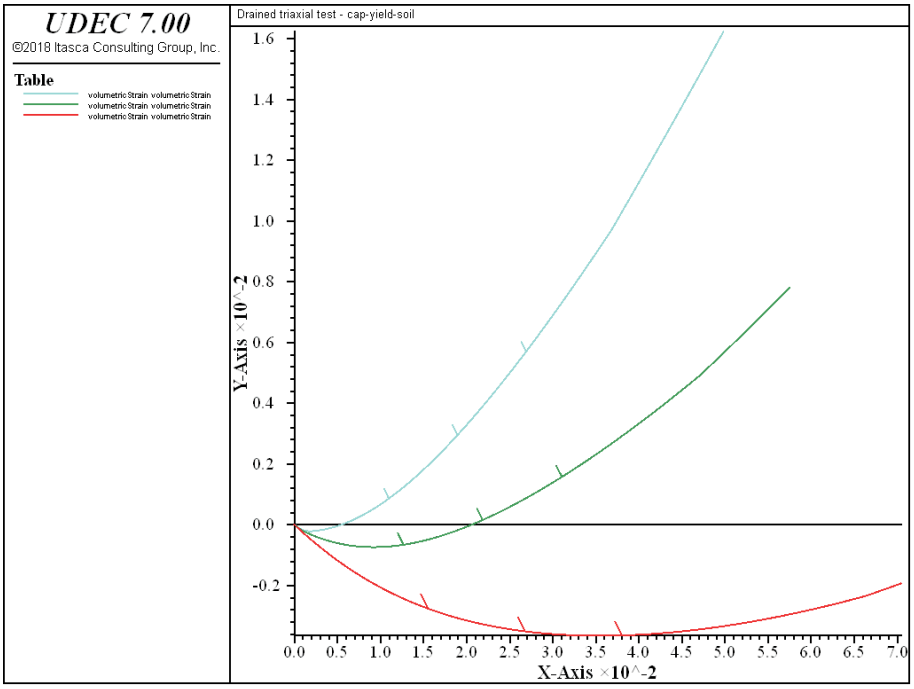

Figure 1.50 *Volumetric strain versus axial strain for dense, medium and loose sand – constant dilation, cohesion = 100*

Example 1.9 Triaxial tests (constant dilation)

```
; Drained Triaxial Tests - Constant Dilation

model new
[global _iChoice = 1]
[global _Gref = 500.]
[global _friu = 40.]
[global _dilu = 10.]
[global _coh = 0.]
call 'drained_constant.dat'


model new
[global _iChoice = 2]
[global _Gref = 375.]
[global _friu = 35.]
[global _dilu = 5.]
[global _coh = 0.]
call 'drained_constant.dat'

model new
[global _iChoice = 3]
[global _Gref = 250.]
[global _friu = 30.]
[global _dilu = 0.]
[global _coh = 0.]
call 'drained_constant.dat'

model new
model title "Drained triaxial test - cap-yield-soil"

table 'deviatoricStress1' import 'deviatoricStress1'
table 'deviatoricStress2' import 'deviatoricStress2'
table 'deviatoricStress3' import 'deviatoricStress3'
table 'volumetricStrain1' import 'volumetricStrain1'
table 'volumetricStrain2' import 'volumetricStrain2'
table 'volumetricStrain3' import 'volumetricStrain3'
ret
model new
[global _iChoice = 1]
[global _Gref = 500.]
[global _friu = 40.]
[global _dilu = 10.]
[global _coh = 100.]
```

```
call 'drained_constant.dat'


model new
[global _iChoice = 2]
[global _Gref = 375.]
[global _friu = 35.]
[global _dilu = 5.]
[global _coh = 100.]
call 'drained_constant.dat'

model new
[global _iChoice = 3]
[global _Gref = 250.]
[global _friu = 30.]
[global _dilu = 0.]
[global _coh = 100.]
call 'drained_constant.dat'

model new
model title "Drained triaxial test - cap-yield-soil"

table 'deviatoricStress1' import 'deviatoricStress1'
table 'deviatoricStress2' import 'deviatoricStress2'
table 'deviatoricStress3' import 'deviatoricStress3'
table 'volumetricStrain1' import 'volumetricStrain1'
table 'volumetricStrain2' import 'volumetricStrain2'
table 'volumetricStrain3' import 'volumetricStrain3'
```

1.6.10.8 Drained Triaxial Tests – Dilation Hardening

The triaxial test simulations with friction hardening in Section 1.6.10.7 are repeated, this time also using a dilation hardening table as described by Eq. (1.296). Initial dilation is zero, and the ultimate value of dilation is listed in Table 1.3. Example 1.10 lists the data file for the triaxial test on dense sand, including dilation hardening. The results of all three cases are compared, as before, by writing the results to tables and creating plots using the command file listed in Example 1.10.

The simulation results of deviatoric stress and volumetric strain versus axial strain are plotted in Figures 1.51 and 1.52, respectively. The non-monotonic volumetric behavior is apparent in the second plot: all soil types do compact initially, and the denser soil is shown to dilate upon further shearing.

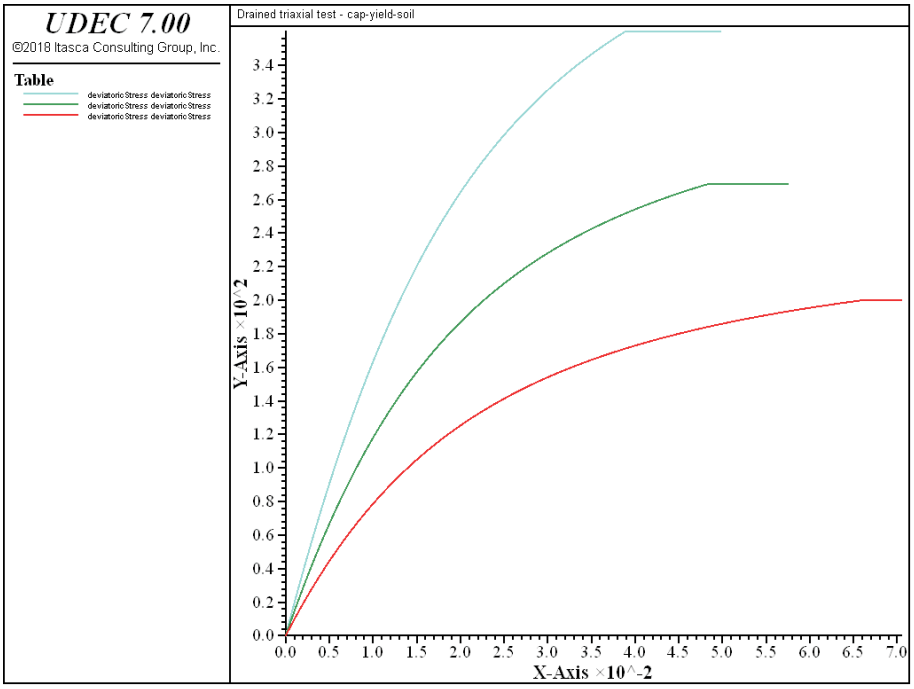

Figure 1.51 *$|\sigma_1 - \sigma_3|$ (in kN/m^2) versus axial strain for dense, medium and loose sand – dilation hardening*

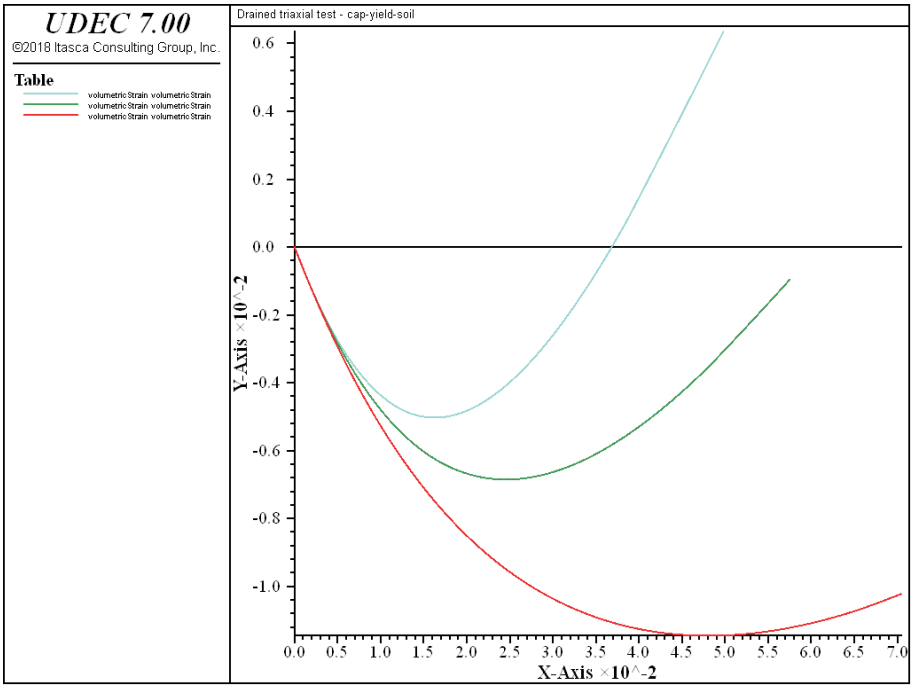

Figure 1.52 Volumetric strain versus axial strain for dense, medium and loose sand – dilation hardening

Example 1.10 Triaxial tests (dilation hardening)

```
; Drained Triaxial Tests - Dilation Hardening

model new
[global _iChoice = 1]
[global _Gref = 500.]
[global _friu = 40.]
[global _dilu = 10.]
[global _coh = 0.]
call 'Drained_Dilational.dat'

model new
[global _iChoice = 2]
[global _Gref = 375.]
[global _friu = 35.]
[global _dilu = 5.]
[global _coh = 0.]
call 'Drained_Dilational.dat'

model new
[global _iChoice = 3]
```

```
[global _Gref = 250.]
[global _friu = 30.]
[global _dilu = 0.]
[global _coh = 0.]
call 'Drained_Dilational.dat'

model new
model title "Drained triaxial test - cap-yield-soil"

table 'deviatoricStress1' import 'deviatoricStress_dh1'
table 'deviatoricStress2' import 'deviatoricStress_dh2'
table 'deviatoricStress3' import 'deviatoricStress_dh3'
table 'volumetricStrain1' import 'volumetricStrain_dh1'
table 'volumetricStrain2' import 'volumetricStrain_dh2'
table 'volumetricStrain3' import 'volumetricStrain_dh3'
ret
```

1.6.10.9 **block zone cmodel** *Command and Property Keywords*

Cap-Yield (formerly Cysoil) – **block zone cmodel assign cap-yield**

(1)	**al**pha	cap yielding surface parameter, α
(2)	**bu**lk	maximum elastic bulk modulus, K
(3)	**coh**esion	cohesion, c
(4)	**dens**ity	mass density, ρ
(5)	**di**lation	ultimate dilation angle, ψ
(6)	**di**lation-**mo**bilized	mobilized dilation angle, ψ_m
(7)	**fri**ction	ultimate friction angle, ϕ
(8)	**fri**ction-**mo**bilized	mobilized friction angle, ϕ_m
(9)	**mu**ltiplier	multiplier on current plastic cap modulus to give elastic bulk and shear moduli, R
(10)	**pr**essure-**ca**p	current intersection of volumetric yield surface (cap) with pressure (mean stress) axis, p_c
(11)	**sh**ear	maximum elastic shear modulus, G
(12)	**ta**ble-**coh**esion	number of table relating cohesion to plastic shear strain
(13)	**ta**ble-**di**lation	number of table relating mobilized dilation angle to plastic shear strain
(14)	**ta**ble-**fri**ction	number of table relating mobilized friction angle to plastic shear strain
(15)	**ta**ble-**pr**essure-**ca**p	number of table relating cap pressure, p_c, to plastic volumetric strain
(16)	**ta**ble-**ten**sion	number of table relating tensile strength to plastic tensile strain
(17)	**ten**sion	tensile strength, σ^t

The following properties can be printed, plotted or accessed via *FISH*.

(1)	**bu**lk	current elastic bulk modulus
(2)	**pr**essure-**ef**fective	mean effective pressure, p
(3)	**she**ar	current elastic shear modulus
(4)	**sta**te	plastic state
(5)	**stra**in-**sh**ear-**pl**astic	accumulated plastic shear strain, ε^{ps}
(6)	**stra**in-**ten**sion-**pl**astic	accumulated plastic tensile strain, ε^{pt}
(7)	**stra**in-**vo**lumetric-**pl**astic	accumulated plastic volumetric strain, ε^{pc}
(8)	**stre**ss-**de**viatoric	deviatoric stress, q

1.6.11 Cap-yield-simplified (formerly Chsoil) Model

As discussed previously in Section 1.6.10, when subjected to deviatoric loading, soils usually exhibit a decrease in stiffness, accompanied by irreversible deformation. The well-known Duncan and Chang model (1970) is commonly used to simulate this hyperbolic stress-strain behavior. The Duncan and Chang model is relatively easy to use but, as noted in Section 1.6.10, this model has several drawbacks. In addition, hyperbolic relations that rely on nonlinear elasticity are known to have significant limitations (Duncan et al. 1980), including (1) the relations are applicable prior to failure, but may produce unrealistic behavior of soils at and after failure; (2) the hyperbolic relations do not include volume change resulting from change in shear stress (the implied dilation relies on the Poisson's ratio), and thus may not be able to predict deformations in dilatant soils accurately, such as dense sands under low confining pressure; and (3) the relations predict an isotropic behavior in the Π plane which is not always realistic (soil strengths in triaxial compression and extension usually differ in magnitude).

A simplified version of the cap-yield model (the *cap-yield-simplified* model) is provided as an alternative to the Duncan and Chang model that does not have the drawbacks of this model. The cap-yield-simplified model is derived from the same strain hardening/softening logic that exists in the cap-yield model, and therefore can provide a realistic stress-strain relation at failure and post-failure. The cap-yoeld-simplified model provides built-in features, and does not have a volumetric cap.

There are three specific features of the cap-yield-simplified model:

1. A built-in friction hardening law that uses hyperbolic model parameters as direct input.
2. A frictional Mohr-Coulomb shear envelope.
3. Two built-in dilation laws: one is based on Rowe's stress dilatancy theory (Rowe 1962), and the other is a user-defined dilation hardening/softening law.

The unloading behavior of the cap-yield-simplified model is elastic. Reloading is elastic up to the outermost yield envelope reached previously. Note that in its present form, the cap-yield-simplified model is not intended to simulate cyclic loading.

1.6.11.1 Incremental Elastic Law

The elastic behavior of the cap-yield-simplified model is expressed using Hooke's law. The incremental expression of the law in terms of principal stress and strain has the form

$$\begin{aligned}
\Delta\sigma_1' &= \alpha_1 \Delta e_1^e + \alpha_2(\Delta e_2^e + \Delta e_3^e) \\
\Delta\sigma_2' &= \alpha_1 \Delta e_2^e + \alpha_2(\Delta e_1^e + \Delta e_3^e) \\
\Delta\sigma_3' &= \alpha_1 \Delta e_3^e + \alpha_2(\Delta e_1^e + \Delta e_2^e)
\end{aligned} \tag{1.301}$$

where $\alpha_1 = K^e + 4G^e/3$, $\alpha_2 = K^e - 2G^e/3$, and K^e and G^e are the tangent elastic bulk and shear modulus, respectively.

In the cap-yield-simplified model, the elastic shear modulus depends on the initial value of mean effective stress, p'_m. The mean effective stress is specified by the user using, for example, the expression

$$p'_m = -\frac{\sigma'_1 + \sigma'_2 + \sigma'_3}{3} \tag{1.302}$$

The variation of G^e with p'_m is represented by the equation (see, for example, Byrne et al. 2003)

$$G^e = G_{ref}\, p_{ref} \left(\frac{p'_m}{p_{ref}} \right)^n \tag{1.303}$$

The parameter p_{ref} is the reference pressure, and G_{ref} is the shear modulus number ($G_{ref} \times p_{ref}$ is the value of the tangent elastic shear modulus at reference pressure). n is a constant modulus exponent ($n \leq 1$). Also, the tangent elastic bulk modulus is described by the relation

$$K^e = K_{ref}\, p_{ref} \left(\frac{p'_m}{p_{ref}} \right)^m \tag{1.304}$$

The parameter K_{ref} is the bulk modulus number, the product ($K_{ref} \times p_{ref}$ is the value of the tangent elastic bulk modulus at reference pressure), and m is a constant modulus exponent ($m \leq 1$).

Some useful relations between K_{ref}, G_{ref}, Young's modulus number, E_{ref}, and Poisson's ratio at reference pressure, ν_{ref}, are listed for reference:

$$K_{ref} = \frac{E_{ref}}{3(1 - 2\nu_{ref})} \qquad G_{ref} = \frac{E_{ref}}{2(1 + \nu_{ref})}$$
$$\frac{K_{ref}}{G_{ref}} = \frac{2(1 + \nu_{ref})}{3(1 - 2\nu_{ref})} \tag{1.305}$$

The user can specify either E_{ref} and ν_{ref} or K_{ref} and G_{ref} as input properties for the model. If E_{ref} and ν_{ref} are specified, K_{ref} and G_{ref} are calculated internally from Eq. (1.305), and the resulting values are used with Eqs. (1.303) and (1.304). Values of Poisson's ratio are restricted to positive values smaller than 0.49. Accordingly, upper and lower bounds for K^e are specified internally as

$$\frac{2G^e}{3} < K^e < 49.66G^e \tag{1.306}$$

As noted above, the initial mean effective pressure, p'_m, must be provided as an input property for the model. (This value may be evaluated using *FISH*, and stored in the associated zone property offset.) The value of p'_m is used to calculate the tangent elastic shear and bulk moduli, according to Eqs. (1.303) and (1.304). G^e and K^e stay constant in this implementation; the moduli are not updated automatically in terms of mean effective pressure.

1.6.11.2 Shear Yield Criterion and Flow Rule

Shear yielding is defined by a Mohr-Coulomb criterion. The yield envelope is expressed as

$$f^s = \sigma'_1 - \sigma'_3 N_{\phi_m} + 2c\sqrt{N_{\phi_m}} \tag{1.307}$$

where c is the cohesion, ϕ_m is the mobilized friction angle and, by definition,

$$N_{\phi_m} = \frac{1 + \sin\phi_m}{1 - \sin\phi_m} \tag{1.308}$$

The potential function is nonassociated, and has the form

$$g = \sigma'_1 - \sigma'_3 N_{\psi_m} \tag{1.309}$$

where

$$N_{\psi_m} = \frac{1 + \sin\psi_m}{1 - \sin\psi_m} \tag{1.310}$$

and ψ_m is the mobilized dilation angle. Several different laws are available in the literature to characterize ψ_m.

By default, ψ_m can be given in terms of plastic shear strain via a user-defined table of ψ_m versus γ^p. The evolution parameter for shear yielding, γ^p, is defined incrementally by

$$\Delta\gamma^p = \sqrt{(\Delta\varepsilon_1^{dp})^2 + (\Delta\varepsilon_2^{dp})^2 + (\Delta\varepsilon_3^{dp})^2}/\sqrt{2} \tag{1.311}$$

where $\Delta\varepsilon_i^{dp}$, $i = 1, 3$ are the principal, deviatoric, plastic shear-strain increments.

The model parameter **flag-dilation** must be set to zero to activate this option. If **flag-dilation** = 0 and no table is provided, it is then assumed that dilation is equal to the input value for ultimate dilation property set with **dilation**. Note that **dilation** is not used if a dilation table is provided.

Two built-in dilation laws are also available. A law based on Rowe's dilatancy theory (Rowe 1962) is used if **flag-dilation** = 1. This is the default setting. Alternatively, a simple step function can be

used, in which ψ_m is zero for $\phi_m < \phi_{cv}$, where ϕ_{cv} is a constant specified by the user, and ψ_m is equal to the ultimate dilation value ψ_f (set by **dilation**) for values of mobilized friction larger than ψ_{cv}. The model property **flag-dilation** must be set to 2 to activate this option. The additional constraint that ψ_m cannot exceed ϕ_m (to prevent unwanted generation of energy from taking place) is enforced internally by the code.

1.6.11.3 Tensile Yield Criterion and Flow Rule

The tensile yield function is the same as that used for the cap-yield model, and is of the form

$$f^t = \sigma^t - \sigma_3 \tag{1.312}$$

The tensile strength, σ^t, is given in terms of the plastic tensile-strain measure, e^{pt}, and input by means of a user-defined table. If no table is provided, it is assumed that tensile strength is constant, and equal to the input value of the tensile strength property.

The evolution parameter for tensile yielding is the modulus of plastic tensile strain, e^{pt}. The increment of plastic tensile strain is defined as

$$\Delta e^{pt} = \Delta e_3^{pt} \tag{1.313}$$

where Δe_3^{pt} is the increment of tensile plastic strain in the direction of the major principal stress (recall that tensile stresses are positive).

1.6.11.4 Friction Hardening

For most soils, the plot of deviatoric stress versus axial strain obtained in a drained triaxial test can be approximated by a hyperbola. The cap-yield-simplified model incorporates a friction strain-hardening law to capture this behavior. In this formulation, the mobilized friction angle, ϕ_m, is given in terms of plastic shear strain measure, γ^p, by means of the following differential law, similar to the one implemented by Byrne et al. (2003) in their UBCSAND liquefaction model:

$$d(\sin\phi_m) = \frac{G^p}{p'_m} d(\gamma^p) \tag{1.314}$$

where the plastic shear modulus, G^p, is given by

$$\phi_m \leq \phi_f : G^p = G^e \left(1 - \frac{\sin\phi_m}{\sin\phi_f} R_f\right)^2 \tag{1.315}$$

In this formula, G^e is the elastic tangent shear modulus, ϕ_f is the ultimate friction angle, and R_f (the failure ratio) is a constant smaller than 1 (0.9, in most cases) used to assign a lower bound for G^p.

According to Eq. (1.303) the elastic tangent shear modulus is a function of p'_m:

$$G^e = G_{ref}\, p_{ref} \left(\frac{p'_m}{p_{ref}} \right)^n \tag{1.316}$$

After substitution of Eq. (1.316) into (1.315), the resulting expression in (1.314), and rearranging terms, we obtain

$$d(\gamma^p) = \frac{p'_m}{G^e} \frac{d(\sin\phi_m)}{\left(1 - \frac{\sin\phi_m}{\sin\phi_f} R_f\right)^2} \tag{1.317}$$

Using $\phi_m = 0$ at $\gamma^p = 0$, integration of this equation gives

$$\gamma^p = \frac{p'_m}{G^e} \frac{\sin\phi_f}{R_f} \left(\frac{1}{1 - \frac{\sin\phi_m}{\sin\phi_f} R_f} - 1 \right) \tag{1.318}$$

Solving for $\sin\phi_m$, we obtain

$$\sin\phi_m = \frac{\sin\phi_f}{R_f} \left(1 - \frac{1}{1 + \gamma^p \frac{G^e}{p'_m} \frac{R_f}{\sin\phi_f}} \right) \tag{1.319}$$

This expression is used in the cap-yield-simplified model to calibrate mobilized friction in terms of plastic shear strain. The use of this hardening law for modeling primary loading in a triaxial test produces a hyperbolic-type curve of deviatoric stress versus axial strain.

1.6.11.5 Overconsolidation

The initial state of a normally consolidated soil or an overconsolidated soil is prescribed by specifying an initial value to the friction property that is equal to or larger than the normally consolidated value, ϕ_{nc}, respectively. For normal consolidation Eqs. (1.307) and (1.308) give

$$\phi_{nc} = \arcsin \frac{\sigma'_1 - \sigma'_3}{\sigma'_1 + \sigma'_3} \tag{1.320}$$

The material behavior is considered to be elastic for stress points below the current yield envelope.

The initial value of friction must be smaller than the ultimate value, ϕ_f. (An upper bound equal to ϕ_f is set automatically by the model.) An initial value of the evolution parameter, γ^p, that is consistent with the specified initial value of mobilized friction angle is also assigned automatically.

1.6.11.6 Shear-Induced Compaction and Dilation

A certain amount of irrecoverable volumetric strain, e^p, is expected to take place as a result of soil shearing. Also, under small monotonic shear strains, there is a tendency for the soil skeleton to contract due to grain rearrangements. For larger shear strains, the soil skeleton may dilate if the soil is dense, as a result of grains riding over each other. A dilation strain-hardening law is incorporated in the logic to model this behavior.

The shear-hardening flow rule implemented in the cap-yield-simplified model has the form

$$\Delta e^p = \Delta \gamma^p \sin \psi_m \tag{1.321}$$

where Δe^p is the plastic volumetric strain increment, $\Delta \gamma^p$ is the plastic shear strain increment, and ψ_m is the (mobilized) dilation angle.

One possible way to characterize ψ_m is to adopt an equation based on Rowe's stress-dilatancy theory (Rowe 1962). According to this theory, there is a (constant-volume) friction angle, ϕ_{cv}, below which the material contracts (i.e., for $\phi_m \leq \phi_{cv}$), while for higher stress ratios (i.e., for $\phi_m > \phi_{cv}$), the material dilates. The equation has the form

$$\sin \psi_m = \frac{\sin \phi_m - \sin \phi_{cv}}{1 - \sin \phi_m \sin \phi_{cv}} \tag{1.322}$$

where

$$\sin \phi_{cv} = \frac{\sin \phi_f - \sin \psi_f}{1 - \sin \phi_f \sin \psi_f} \tag{1.323}$$

and ϕ_f and ψ_f are ultimate (known) values of friction and dilation, respectively.

Dilation is evaluated in terms of plastic shear strain based on the last two equations, and the assumed relation between ϕ_m and γ^p reported in Eq. (1.318). Rowe's dilation law is selected by setting the material property **flag-dilation** = 1 (default value). A simple dilation law also can be used, in which $\psi_m = 0$ for $\phi_m \leq \phi_{cv}$, and $\psi_m = \psi_{cv}$ for $\phi_m \geq \phi_{cv}$; the option is activated by specifying **flag-dilation** = 2. Finally, the user may choose to define an alternative dilation law by creating an input table of dilation values versus plastic shear strain. The model property **flag-dilation** must be set to zero to activate this option.

1.6.11.7 Correlation between cap-yield-simplified Properties and Duncan and Chang Properties

A parallel can be drawn, for particular cases, between properties used in the hyperbolic stress-strain relations reported in Duncan et al. (1980) for the Duncan and Chang model and the properties of the cap-yield-simplified model. The correlations depend on property input; they are listed in Tables 1.4 and 1.5.

Table 1.4 Property correlation for input of K_{ref} and G_{ref}

Model	$m = n$	No Dilation
Duncan and Chang	K_{ur},n	K_b,m
cap-yield-simplified	$\frac{9K_{ref}G_{ref}}{3K_{ref}+G_{ref}}$, n	K_{ref},m

Table 1.5 Property correlation for input of E_{ref} and ν_{ref}

Model	$m = n$	No Dilation
Duncan and Chang	K_{ur},n	K_b,m
cap-yield-simplified	E_{ref},n	$\frac{E_{ref}}{3(1-2\nu_{ref})}$, m

1.6.11.8 Calibration of the cap-yield-simplified Model to Triaxial Test Results on Nevada Sand

Results of drained triaxial tests at constant mean effective stress, p', on Nevada sand are used to provide an example of the methodology that can be used to calibrate the properties of the cap-yield-simplified model. The test results are listed in data files "40-40.log," "40-80.log" and "40-160.log," and correspond to values of the mean stress at 40 kPa, 80 kPa and 160 kPa, respectively. The relative density of the sand for these tests is 40%. The test results consist of three sets of data:

(1) deviatoric stress versus mean effective stress;

(2) deviatoric stress versus axial strain (up to 25% strain); and

(3) volumetric strain versus axial strain (up to 25% strain).

For this calibration exercise, we consider axial strains up to 5%, because strains are not expected to develop above this level for the intended (static, drained) application. The Nevada sand appears to be purely frictional in character. Also, two main features characterize the data: (1) hyperbolic behavior is observed in the plot of deviatoric stress versus axial strain, and (2) bilinear dilatant behavior is exhibited by the plot of volumetric strain versus axial strain. The cap-yield-simplified model capabilities, including friction hardening and variable dilation, are used to simulate these features.

The elastic tangent shear and bulk moduli are functions of the initial mean effective stress according to Eqs. (1.303) to (1.305). For friction hardening we use the built-in law Eq. (1.318). The dilation law is bilinear; its value is zero below the stress ratio $\phi = \phi_{cv}$, and a constant, ψ_f, above it:

$$\begin{aligned} \psi &= 0 \qquad \phi < \phi_{cv} \\ \psi &= \psi_f \qquad \phi \geq \phi_{cv} \end{aligned} \tag{1.324}$$

The failure ratio, R_f, is 0.99 for this exercise. Eight properties must be defined:

$$E_{ref}, \nu, p_{ref}, \phi_f, \psi_f, \phi_{cv}, m, n$$

Calibration of the model properties is done in two steps. First, using theoretical considerations and values recorded in the literature, we derive a first estimate for the property values. Second, we improve on the estimates by modeling the triaxial experiments numerically and matching the results obtained in the laboratory.

First Estimates – The value of ultimate friction is derived from a linear fit to plots of deviatoric stress, q, versus mean effective stress, p', obtained from the laboratory tests. The linear fit to maximum q at given p' provides a value for the maximum stress ratio, a,

$$a = \frac{q}{p'} \tag{1.325}$$

From the definition of the purely frictional Mohr-Coulomb criterion, we obtain the relation

$$\sin \phi_f = \frac{3a}{6 + a} \tag{1.326}$$

from which the ultimate friction angle, ϕ_f, can be derived. The estimated value for $D_r = 40\%$ sand is $\phi_f = 34°$.

The value of ultimate dilation angle is derived from the slope, b, of a linear fit to the laboratory curves of minus volumetric strain versus axial strain. To relate b to ψ_f, we use, as a first approximation, the expression for bilinear idealization of triaxial stress results provided by Vermeer and deBorst (1984):

$$b = \frac{2 \sin \psi_f}{1 - \sin \psi_f} \tag{1.327}$$

The first estimate for ψ_f is 8.2° for $D_r = 40\%$ sand.

To estimate the parameter ϕ_{cv} for a given D_r, we first derive the maximum value of axial strain, ε_a^*, at which the volumetric strain is negligible from the laboratory plots of volumetric strain versus axial strain at a given p'. From the knowledge of axial strain, ε_a^*, we estimate q from the laboratory plot of deviatoric stress versus axial strain at that p', and then the ratio q/p'. Three values of the ratio are available (one at each p'). The mean value of q/p' is used to calculate the corresponding friction angle using Eq. (1.326), where ϕ_f now is replaced by ϕ_{cv}, and a by the average q/p' (see Eq. (1.325)). The estimate is $\phi_{cv} = 27.7°$ for $D_r = 40\%$.

The first guess for E_{ref} is taken as 1200 for $D_r = 40\%$ at atmospheric pressure; this value is equivalent to that used in the triaxial numerical experiment for dense sand listed in Example 1.9.

The value of ν for this exercise is arbitrarily selected as 0.35. Also, we select $n = m = 0.5$. The elastic constant, E_{ref}, is estimated by matching the initial slopes of q versus axial strain curves obtained in similar triaxial tests (under constant mean stress) performed numerically and in the laboratory. These estimates may not be very accurate; more robust estimates for the elastic constants can be obtained from laboratory results of small unloading-reloading excursions. Such results were not available for this example.

Numerical Triaxial Experiments – Triaxial experiments are conducted numerically at the three levels of mean stress (40, 80 and 160 kPa) for the $D_r = 40\%$ sand. The axisymmetric geometry configuration is selected for the strain-controlled simulations. A servo control is applied to maintain the mean stress constant during the numerical experiments.

The estimates for model properties are used to conduct the numerical tests, and the test results are compared to the available laboratory data (imported into tables). The properties are adjusted (in the order listed above), and the numerical experiment is repeated until a satisfactory curve fitting is obtained.

The results of the curve fitting experiment are listed in Table 1.6.

Table 1.6 Calibration results

D_r	E_{ref}	ν	ϕ_f	ψ_f	ϕ_{cv}	m	n
40%	1800	0.35	34°	7.5°	28°	0.5	0.5

A comparison between numerical predictions using the calibrated properties and laboratory results is shown in Figures 1.53 through 1.55. Note that the soil-mechanics convention for positive stress/strain in compression is adopted in these plots. (Dilation is negative.) The comparison is quite reasonable. The data file for this comparison example is listed in Example 1.11.

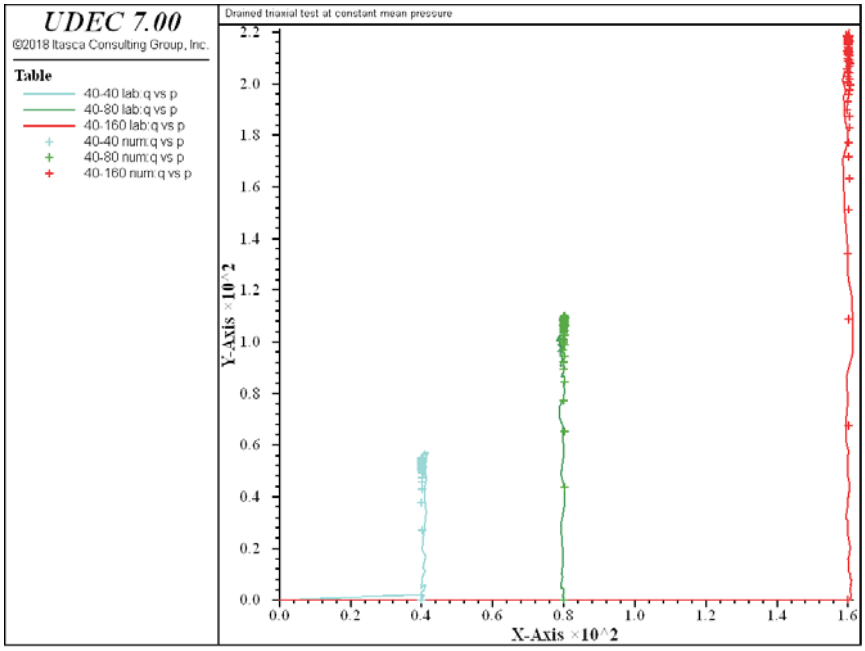

Figure 1.53 Deviatoric stress versus mean stress for D_r = 40% – comparison between laboratory (line) and numerical (cross) results

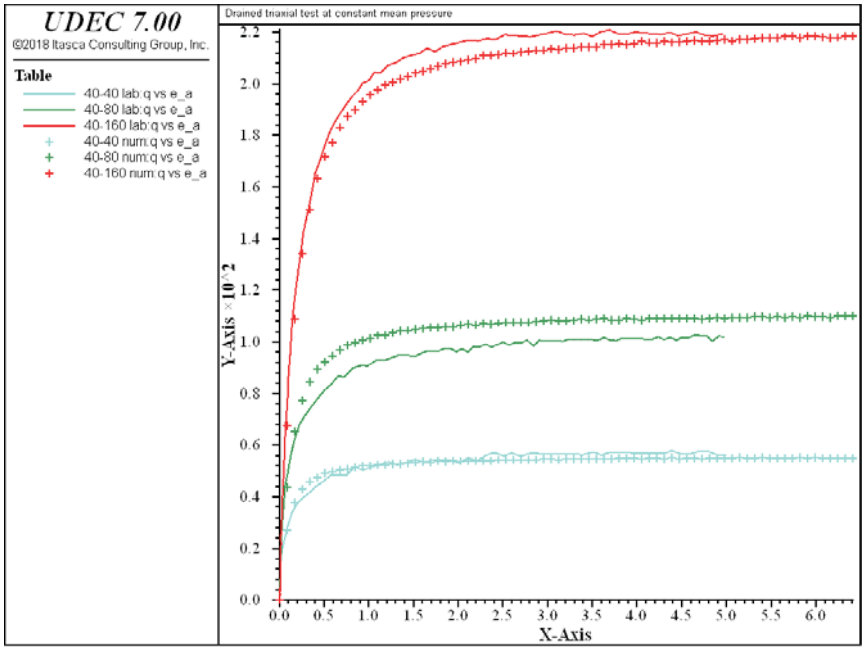

Figure 1.54 Deviatoric stress versus axial strain (in %) for D_r = 40% – comparison between laboratory (line) and numerical (cross) results

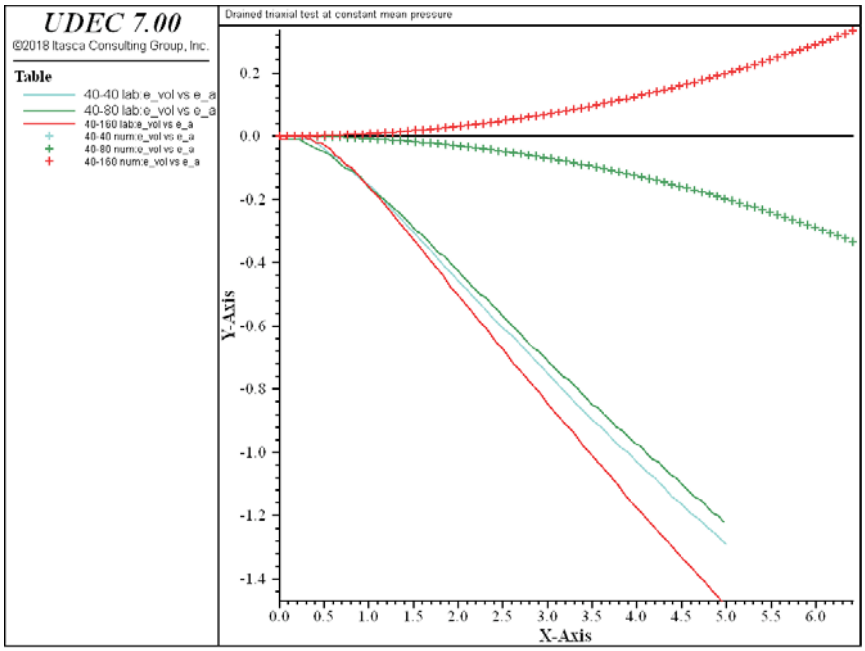

Figure 1.55 Volumetric strain (in %) versus axial strain (in %) for D_r = 40% – comparison between laboratory (line) and numerical (cross) results

Example 1.11 Drained triaxial test at constant mean pressure – Dr = 40 – Chsoil model

```
model new
;file: chsoil.dat
;
Model title 'Drained triaxial test at constant mean pressure'
; Relative density (DR) = 40%
; CHSOIL model
;
fish define setup
_nu = 0.35
_Eref = 1800.
_Pa = 100.
_m = 0.5
_n = 0.5
_friu = 34.
_dilu = 7.5
_ficv = 28.
_Rf = 0.99
_fric = 0.
_coh = 0.
_yvel = -6.7e-5
_gain = 1.
high_vel = 8.0e-5
_p0 = 40.
_nt = 2
_xvel = -_yvel/2.0
end
@setup
;
block config axisymmetry
block tolerance corner-round-length 5E-3
block tolerance minimum-edge-length 1E-2
block create polygon 0 0 0 5 1 5 1 0
block cut crack 0 1 1 1 join
block cut crack 0 2 1 2 join
block cut crack 0 3 1 3 join
block cut crack 0 4 1 4 join
block zone gen edge 1.0
block zone group 'mat1'
block zone cmodel assign cap-yield-simplified
block zone prop young-reference=1800. poisson=0.35 ...
  pressure-reference=100. failure-ratio=0.99 friction=34.0 ...
  exponent-bulk=0.5 exponent-shear=0.5 ...
  dens=1000. cohesion=0. dilation-mobilized=0. friction-mobilized=0.
```

```
block zone prop flag-dilation 2 range pos-y 0 1
block zone prop flag-dilation 3 range pos-y 2 3
block zone prop flag-dilation 4 range pos-y 4 5
block zone prop pressure-initial= 40. range pos-y 0 1
block zone prop pressure-initial= 80. range pos-y 2 3
block zone prop pressure-initial=160. range pos-y 4 5
block contact prop mat 1 st-n 1e8 st-s 1e8

block zone group 'Null' range pos-y 1 2
block zone group 'Null' range pos-y 3 4
block zone cmodel assign null range group 'Null'
;
block gridpoint apply velocity-x 0
block gridpoint apply velocity-y 0
block gridpoint apply velocity-x @_xvel range pos-x 0.99 1.01
block gridpoint apply velocity-y @_yvel range pos-x 0 1 pos-y 0.99 1.01
block gridpoint apply velocity-y @_yvel range pos-x 0 1 pos-y 2.99 3.01
block gridpoint apply velocity-y @_yvel range pos-x 0 1 pos-y 4.99 5.01
;
block insitu  stress -160.0 0.0 -160.0 stress-ZZ -160.0 ...
  range pos-x 0 1 pos-y 4 5
block insitu  stress  -80.0 0.0  -80.0 stress-ZZ  -80.0 ...
  range pos-x 0 1 pos-y 2 3
block insitu  stress  -40.0 0.0  -40.0 stress-ZZ  -40.0 ...
  range pos-x 0 1 pos-y 0 1
[global _strain=array.create(4)]
call 'z_strain.fis'
fish define _getStress
  ib = block.near(_x, _y)
  iz = block.zone(ib)
  count = 0
  _sxx = 0
  _syy = 0
  _szz = 0
  _vsi = 0
  _sxx =  block.zone.stress.xx(iz)
  _syy = block.zone.stress.yy(iz)
  _szz = block.zone.stress.zz(iz)
   z_strain
  block.zone.strain.increment(iz,_strain)
  _vsi = 2*zs_xx + zs_yy
  ;_vsi = 2*_strain(1) + _strain(4)
end
;
; --- servo for constant mean stress ---
```

```
fish define _keyPoints
  _g10 = block.gp.near(1,0)
  _g11 = block.gp.near(1,.9)
  _b_g10 = block.gp.boundary.corner(_g10)
  _b_g11 = block.gp.boundary.corner(_g11)
;
  _g12 = block.gp.near(1,2)
  _g13 = block.gp.near(1,2.9)
  _b_g12 = block.gp.boundary.corner(_g12)
  _b_g13 = block.gp.boundary.corner(_g13)
;
  _g14 = block.gp.near(1,4)
  _g15 = block.gp.near(1,4.9)
  _b_g14 = block.gp.boundary.corner(_g14)
  _b_g15 = block.gp.boundary.corner(_g15)
end
@_keyPoints

;
fish define servo_sig0
  while_stepping
  _x = 0.5
  _y = 0.5
  _getStress
  _sig=-(_sxx + _syy + _szz)/3.
  _svel=block.gp.vel.x(_g10)-_gain*(1.-_sig/40.)
  if math.abs(_svel) > high_vel then
    _svel=math.sgn(_svel)*high_vel
  end_if
  block.bou.vel.x(_b_g10) = _svel
  block.bou.vel.x(_b_g11) = _svel
;
  _x = 0.5
  _y = 2.5
  _getStress
  _sig=-(_sxx + _syy + _szz)/3.
  _svel=block.gp.vel.x(_g12)-_gain*(1.-_sig/80.)
  if math.abs(_svel) > high_vel then
    _svel=math.sgn(_svel)*high_vel
  end_if
  block.bou.vel.x(_b_g12) = _svel
  block.bou.vel.x(_b_g13) = _svel
;
  _x = 0.5
  _y = 4.5
  _getStress
```

```
  _sig = -(_sxx + _syy + _szz)/3.
  _svel = block.gp.vel.x(_g14) - _gain*(1.-_sig/160.)
  if math.abs(_svel) > high_vel then
    _svel=math.sgn(_svel)*high_vel
  end_if
  block.bou.vel.x(_b_g14) = _svel
  block.bou.vel.x(_b_g15) = _svel
end
;
fish define _q1
  _x = 0.5
  _y = 0.5
  _getStress
  _q1    = _sxx - _syy
  _p1    = -(_sxx + _syy + _szz)/3.
  eps_v1 = _vsi*100.
  eps_a1 = block.gp.disp.y(_g11)*100
;
  _x = 0.5
  _y = 2.5
  _getStress
  _q2    = _sxx - _syy
  _p2    = -(_sxx + _syy + _szz)/3.
  eps_v2 = _vsi*100.
  eps_a2 = block.gp.disp.y(_g13)*100
;
  _x = 0.5
  _y = 4.5
  _getStress
  _q3    = _sxx - _syy
  _p3    = -(_sxx + _syy + _szz)/3.
  eps_v3 = _vsi*100.
  eps_a3 = block.gp.disp.y(_g15)*100
end
;
hist int 1300
;
fish history @_q1
fish history @_p1
fish history @eps_v1
fish history @eps_a1
;
fish history @_q2
fish history @_p2
fish history @eps_v2
fish history @eps_a2
```

```
;
fish history @_q3
fish history @_p3
fish history @eps_v3
fish history @eps_a3
;
block  smallstrain on
block cycle 100000
;
fish define read_in
  array in_line(1)
  oo=file.open('40-40.log',0,1)
  loop kk (1,232)
    oo=file.read(in_line,1)
    _astr=string.token(in_line(1),1)
    _q   =string.token(in_line(1),2)
    _p   =string.token(in_line(1),3)
    _vs  =string.token(in_line(1),4)
    if _astr < 5.01 then
      table.x(11,kk)=_astr
      table.y(11,kk)=_q
      table.x(12,kk)=_astr
      table.y(12,kk)=_vs
      table.x(13,kk+1)=_p
      table.y(13,kk+1)=_q
    end_if
  end_loop
  oo=file.close
;
  oo=file.open('40-80.log',0,1)
  loop kk (1,306)
    oo=file.read(in_line,1)
    _astr=string.token(in_line(1),1)
    _vs  =string.token(in_line(1),2)
    _q   =string.token(in_line(1),3)
    _p   =string.token(in_line(1),4)
    if _astr < 5.01 then
      table.x(21,kk)=_astr
      table.y(21,kk)=_q
      table.x(22,kk)=_astr
      table.y(22,kk)=_vs
      table.x(23,kk+1)=_p
      table.y(23,kk+1)=_q
    end_if
  end_loop
  oo=file.close
```

```
;
  oo=file.open('40-160.log',0,1)
  loop kk (1,258)
    oo=file.read(in_line,1)
    _astr=string.token(in_line(1),1)
    _q   =string.token(in_line(1),2)
    _p   =string.token(in_line(1),3)
    _vs  =string.token(in_line(1),4)
    if _astr < 5.01 then
      table.x(31,kk)=_astr
      table.y(31,kk)=_q
      table.x(32,kk)=_astr
      table.y(32,kk)=_vs
      table.x(33,kk+1)=_p
      table.y(33,kk+1)=_q
    end_if
  end_loop
  oo=file.close
end
@read_in
;
fish define _copyHistory
  loop _n (1,12)
    _tabNum = 200 + _n
    command
      history export @_n table @_tabNum
    endcommand
  endloop
  _rows = table.size(201)
  loop _n (1, _rows)
    table.x(111,_n) = -table.y(204,_n)
    table.y(111,_n) = table.y(201,_n)
    table.x(112,_n) = -table.y(204,_n)
    table.y(112,_n) = table.y(203,_n)
    table.x(113,_n) = table.y(202,_n)
    table.y(113,_n) = table.y(201,_n)
;
    table.x(121,_n) = -table.y(208,_n)
    table.y(121,_n) = table.y(205,_n)
    table.x(122,_n) = -table.y(208,_n)
    table.y(122,_n) = table.y(207,_n)
    table.x(123,_n) = table.y(206,_n)
    table.y(123,_n) = table.y(205,_n)
;
    table.x(131,_n) = -table.y(212,_n)
    table.y(131,_n) = table.y(209,_n)
```

```
    table.x(132,_n) = -table.y(212,_n)
    table.y(132,_n) = table.y(211,_n)
    table.x(133,_n) = table.y(210,_n)
    table.y(133,_n) = table.y(209,_n)
;
  endloop
end
@_copyHistory

model title 'Drained triaxial test at constant mean pressure - DR = 40%'
table 11  label '40-40 lab:q vs e_a'
table 21  label '40-80 lab:q vs e_a'
table 31  label '40-160 lab:q vs e_a'
table 111 label '40-40 num:q vs e_a'
table 121 label '40-80 num:q vs e_a'
table 131 label '40-160 num:q vs e_a'
table 12  label '40-40 lab:e_vol vs e_a'
table 22  label '40-80 lab:e_vol vs e_a'
table 32  label '40-160 lab:e_vol vs e_a'
table 112 label '40-40 num:e_vol vs e_a'
table 122 label '40-80 num:e_vol vs e_a'
table 132 label '40-160 num:e_vol vs e_a'
table 13  label '40-40 lab:q vs p'
table 23  label '40-80 lab:q vs p'
table 33  label '40-160 lab:q vs p'
table 113 label '40-40 num:q vs p'
table 123 label '40-80 num:q vs p'
table 133 label '40-160 num:q vs p'
model save 'dr40.sav'
return
```

1.6.11.9 **block zone cmodel** *Command and Property Keywords*

Cap-yield-simplified (Chsoil) – **block zone cmodel assign cap-yield-simplified**

(1)	**bu**lk-**re**ference	bulk modulus number, K_{ref}
(2)	**coh**esion	cohesion, c
(3)	**dens**ity	mass density, ρ
(4)	**di**lation	ultimate dilation angle, ψ_f
(5)	**fa**ilure-**ra**tio	failure ratio, R_f
(6)	**fl**ag-**di**lation	= 0 for mobilized dilation angle, ψ_m, equal to input value, **dilation** or a function of plastic shear strain if table is input with **table-dilation** = 1 for mobilized dilation angle, ψ_m, characterized by Rowe's stress-dilatancy theory = 2 for mobilized dilation angle, $\psi_m = 0$ if $\phi_m < \phi_{cv}$, and ψ_m = ultimate dilation value, ψ_f, if $\phi_m \geq \phi_{cv}$
(7)	**fri**ction	ultimate friction angle, ϕ_f
(8)	**fri**ction-**cr**itical	constant used in dilation laws (**flag-dilation** = 1 or 2), ϕ_{cv}
(9)	**ex**ponent-**bu**lk	bulk modulus exponent, m
(10)	**ex**ponent-**sh**ear	shear modulus exponent, n
(11)	**po**isson	Poisson's ratio, ν
(12)	**pr**essure-**in**itial	initial effective pressure, p'_m
(13)	**pr**essure-**re**ference	reference pressure, p_{ref}
(14)	**sh**ear-**re**ference	shear modulus number, G_{ref}
(15)	**ta**ble-**coh**esion	number of table relating cohesion, c, to plastic shear strain
(16)	**ta**ble-**di**lation	number of table relating mobilized dilation angle to plastic shear strain
(17)	**ta**ble-**ten**sion	number of table relating mobilized tensile strength to plastic tensile strain
(18)	**ten**sion	tensile strength, σ^t
(19)	**yo**ung-**re**ference	Young's modulus number, E_{ref}

The following properties can be printed, plotted or accessed via *FISH*.

(1)	**bu**lk-**mo**bilized	mobilized elastic bulk modulus, K^e
(2)	**di**lation-**mo**bilized	mobilized dilation angle, ψ_m
(3)	**fri**ction	mobilized friction angle, ϕ_m
(4)	**sh**ear-**mo**bilized	mobilized elastic shear modulus, G^e
(5)	**stra**in-**sh**ear-**pl**astic	accumulated plastic shear strain, ε^{ps}
(6)	**stra**in-**vo**lumetric-**pl**astic	accumulated plastic volumetric strain, ε^{pc}

1.7 References

Amadei, B. ***The Influence of Rock Anisotropy on Measurement of Stresses In Situ***. Ph.D. Thesis, University of California, Berkeley (January 1982).

Boukpeti, N. ***Modeling Static Liquefaction in Granular Deposits***. Ph.D. Thesis, University of Minnesota (2001).

Britto, A. M., and M. J. Gunn. ***Critical State Soil Mechanics via Finite Elements***. Chichester U.K.: Ellis Horwood Ltd. (1987).

Byrne, P. M., S. S. Park and M. Beaty. "Seismic Liquefaction: Centrifuge and Numerical Modeling," in ***FLAC and Numerical Modeling in Geomechanics – 2003 (Proceedings of the 3rd International FLAC Symposium, Sudbury, Ontario, Canada, October 2003)***, pp. 321-331. R. Brummer et al., eds. Lisse: A. A. Balkema (2003).

Carter, T. G., J. L. Carvalho and G. Swan. "Towards the Practical Application of Ground Reaction Curves," in ***Innovative Mine Design for the 21st Century (Proceedings of the International Congress on Mine Design, Kingston, Ontario, Canada, August 1993)***, pp. 151-171. W. F. Bawden and J. F. Archibald, eds. Rotterdam: A. A. Balkema (1993).

Chen, W. F., and D. J. Han. ***Plasticity for Structural Engineers***. New York: Springer-Verlag (1988).

Cundall, P., C. Carranza-Torres and R. Hart. "A New Constitutive Model Based on the Hoek-Brown Criterion," in ***FLAC and Numerical Modeling in Geomechanics – 2003 (Proceedings of the 3rd International FLAC Symposium, Sudbury, Ontario, Canada, October 2003)***, pp. 17-25. R. Brummer et al., eds. Lisse: Balkema (2003).

Davis, R. O., and A. P. S. Selvadurai. ***Plasticity and Geomechanics***. Cambridge (2002).

Drescher, A. ***Analytical Methods in Bin-Load Analysis***. Amsterdam: Elsevier (1991).

Duncan, J. M., et al. "Strength, Stress-Strain and Bulk Modulus Parameters for Finite Element Analyses of Stresses and Movements in Soil Masses," University of California, Berkeley, College of Engineering, Report No. UCB/GT/80-01 (1980).

Duncan, J. M., and C-Y. Chang. "Nonlinear Analysis of Stress and Strain in Soils," *Soil Mechanics*, ***96***(SM5), 1629-1653 (1970).

Hoek, E., and E. T. Brown. "Practical Estimates of Rock Mass Strength," *Int. J. Rock Mech. Min. Sci.*, ***34***(8), 1165-1186 (1998).

Hoek, E., and E. T. Brown. ***Underground Excavations in Rock***. London: IMM (1980).

Hoek, E., C. Carranza-Torres and B. Corkum. "Hoek-Brown Failure Criterion – 2002 Edition," in ***Proceedings of NARMS-TAC 2002, 5th North American Rock Mechanics Symposium and 17th Tunnelling Association of Canada Conference (Toronto, Canada – July 7 to 10, 2002***), Vol. 1., pp. 267-271. R. Hammah et al., eds. Toronto: University of Toronto Press (2002).

Lekhnitskii, S. G. ***Theory of Elasticity of an Anisotropic Body***. Moscow: Mir Publishers (1981).

Pan, X. D., and J. A. Hudson. "A Simplified Three Dimensional Hoek-Brown Yield Criterion," in ***Rock Mechanics and Power Plants (Proceedings of the ISRM Symp.)***, pp. 95-103. M. Romana, ed. Rotterdam: A. A. Balkema (1988).

Roscoe K. H., and J. B. Burland. "On the Generalised Stress-Strain Behavior of 'Wet Clay'," in ***Engineering Plasticity***, pp. 535-609. J. Heyman and F. A. Leckie, eds. Cambridge: Cambridge University Press (1968).

Rowe, P. W. "The Stress-Dilatancy Relation for Static Equilibrium of an Assembly of Particles in Contact," *Proc. Roy. Soc. A.*, ***269***, 500-527 (1962).

Shah, S. ***A Study of the Behaviour of Jointed Rock Masses***. Ph.D. Thesis, University of Toronto (1992).

Vermeer, P. A., and R. deBorst. "Non-Associated Plasticity for Soils, Concrete and Rock," *Heron*, ***29***(3), 3-64 (1984).

Wood, D. M. ***Soil Behaviour and Critical State Soil Mechanics***. Cambridge: Cambridge University Press (1990).